Frog Trophic And Morphological Diversity: Phylogenetic And Spatial Patterns

by

Joanna G. Larson

A dissertation submitted in partial fulfillment
of the requirements for the degree of
Doctor of Philosophy
(Ecology and Evolutionary Biology)
in The University of Michigan
2020

Doctoral Committee:

Associate Professor Daniel L. Rabosky, Chair
Assistant Professor Alison Davis Rabosky
Professor Meghan A. Duffy
Assistant Professor Selena Y. Smith

Joanna G. Larson

jglarson@umich.edu

ORCID iD: 0000-0002-1401-7837

ACKNOWLEDGEMENTS

I would like to thank everyone in the EEB office, especially Cindy Carl, Michael Ehnis, Kati Ellis, Linda Garcia, Gail Kuhnlein, and Robbin Murrell, for patiently helping me navigate the bureaucratic aspects of graduate school. Ben Hess facilitated and simplified the normally stressful and complicated process of importing specimens for which I am extremely grateful. I would like to thank Greg Schneider for helping to transport thousands of specimens between RMC and Ruthven and his unfailing enthusiasm for herpetology.

I would like to thank my committee members, Meg Duffy, Alison Davis Rabosky, and Selena Smith, for their support and advice over the years. They also acted as incredible role models for me as mentors, teachers, and researchers. I am deeply grateful to Dan Rabosky for his support, patience, and willingness to let me take a risk on frog vomit.

Raquel Marchan Rivadeneira kindly had innumerable conversations with me about molecular protocols and I would not have been able to do this work without her expertise and support. Taehwan Lee, Tom Duda, and Tim James allowed my students and me to use their microscope and camera setups to examine and photograph endless frog vomit samples.

I am very grateful to my sources of funding: UM EEB Block Grants, UM EEB summer support, UMMZ Edward C. Walker Scholarship, Edwin C. Hinsdale UMMZ Scholarship, UMMZ C. F. Walker Grant, ES George Reserve Scholarship, Rackham Pre-Candidate Research Grant, Rackham Candidate Research Grant, Rackham International Research Grant, Rackham

Predoctoral Fellowship, Society for the Study of Evolution, NSF GRFP, NSF DDIG, Alison Davis Rabosky, and Dan Rabosky, including support from his Packard Fellowship.

I would like to acknowledge my many Peruvian collaborators who spent many rainy and bug-filled nights with me in the forest to catch frogs. In particular, my research would be greatly diminished without the considerable help from Ciara Sanchez Paredes, Consuelo Alarcon Rodriguez, Valia Herrera, and Jordan Milla Villegas.

I would like to thank my labmates, past and present, for their support, inspiration, and help in the field: Peter Cerda, Jonathan Chang, Gabriel Costa, Jenna Crowe-Riddell, Hayley Crowell, John David Curlis, Maggie Grundler, Mike Grundler, Mike Harvey, Iris Holmes, Talia Yuki Moore, Imani Russell, Briana Sealey, Sonal Singhal, Pascal Title, Rudi von May, Taylor West, and Erin Westeen.

I would also like to thank the EEB community of graduate students and post docs, who have filled this journey with fun and friendship. Anat Belasen has been the best life coach and role model that I could have asked for. Clara Shaw has never stopped believing me and her intelligence and empathy have always inspired me to be a better person. Bree Doering was there for that first attempt at making a frog vomit, which was a comical failure. Her moral support and ability to make me laugh helped me persevere then and for the past five years. Katy Morgan bravely volunteered to help me in the field, which led to us expanding our list of odd places that we have stayed and shared field adventures.

My family has always supported and encouraged me and my love of frogs, for which I am deeply thankful and incredibly lucky.

TABLE OF CONTENTS

LIST OF FIGURES

LIST OF TABLES

ABSTRACT

Dimensions of biodiversity such as morphology, species richness, and trophic ecology vary widely across the tree of life and geographic space, however we do not yet fully understand the processes that produce this variation, nor the relationships between these processes. My dissertation uses phylogenetic comparative methods and large scale morphological and diet datasets to test hypotheses about the mechanisms that generate variation across frogs. In Chapter 2, I quantify the tempo of morphological evolution and speciation across frogs and test whether these rates are positively correlated as is predicted from several conceptual models of evolutionary radiation. For estimation of frog morphological evolutionary rates, I utilize measurements of phenotypic traits related to diet, locomotion, and habitat that I took from museum specimens. I find that morphological evolutionary rates and speciation rates are decoupled in frogs. In Chapter 3, I test the classic hypotheses that increases in community species richness will be accompanied by an expansion of utilized niche space, greater packing of species within a static volume of niche space, or a combination of the two patterns. Using morphology as a proxy for ecological traits, I find that the volume of utilized morphological space expands and packing of species increases as frog species richness rises from the temperate zone to the tropics. In contrast to the patterns seen in birds, the majority of species richness increase is attributable to morphospace expansion rather than packing. In Chapter 4, I evaluate the impact of the taxonomic level to which prey items are identified on conclusions about dietary specialization and interspecific diet similarity of frogs. I also test how understanding of dietary

diversity and similarity shifts depending on whether phylogenetic or taxonomic metrics of diet are used. To address these questions, I use high-resolution diet information generated using DNA metabarcoding for 22 species of sympatric frogs from a lowland tropical community. I find that hundreds of samples are required to capture the full breadth of prey species consumed by a frog species in environments with diverse resource bases. Use of order-level prey identification for taxonomy-based metrics in combination with metrics based on the phylogenetic relationships between prey items provide a reliable and nuanced picture of resource utilization with more moderate sampling. In Chapter 5, I examine the impact of evolutionary history on present-day diets in frogs, specifically testing whether frog diets conform to the Deep Time Hypothesis or Adaptive Radiation Hypothesis, which make contrasting predictions about the relationship between phylogeny and ecological divergence. For this study, I leverage diet information generated with DNA metabarcoding for 111 frog species from 10 taxonomic families to test several key predictions of these models in a phylogenetic comparative framework. I propose a new hypothesis to explain the results, whereby trophic ecology across frogs is characterized by generalized diets, high interspecific overlap, and limited specialization despite the amount of evolutionary time spanned by the clade. Overall my dissertation reveals that patterns of trophic ecology and morphological diversity in frogs, one of the most species rich clades of terrestrial vertebrates, fundamentally differ from those observed in other vertebrate clades.

CHAPTER 1

Introduction

Describing patterns of diversity and understanding the mechanisms that generate them is one of the driving themes of evolutionary biology. In particular, there is a long standing fascination with the greater number of species in the tropics compared to temperate regions, a pattern referred to as the latitudinal diversity gradient (LDG). There are few taxonomic clades that do not conform to this spatial distribution of species and it is assumed that a common mechanism must underlay this pattern, although no comprehensive explanation has yet emerged (Mittelbach et al. 2007). It is predicted that various other dimensions of biodiversity will show consistent patterns along the latitudinal gradient (Macarthur 1965; Pianka 1966). Elucidating these covarying patterns of biodiversity can increase the power to identify the causal factors that generate and maintain such patterns.

In my dissertation, I explore how aspects of frog diversity are spatially and phylogenetically distributed. Frogs are a globally distributed radiation of vertebrates, currently found on every continent except Antarctica. There are over 7,000 species described with a steady rate of species descriptions published every year. Although the higher-level taxonomy of anurans remains debated, it is clear that species richness is unevenly distributed between families, regardless of taxonomic framework. The drivers of this asymmetrical species richness between clades of frogs remain undetermined.

An area of frog ecology that is particularly understudied is diet. This lack of understanding stems from the challenges related to acquiring this data because frogs, with few exceptions, are invertivores, meaning that they primarily eat invertebrates (Wells 2007). Identification of invertebrates at varying stages of digestion is challenging, even for entomologists, resulting in a limited number of detailed frog dietary studies. Despite the challenges, several herpetologists have produced impressively detailed studies of frog trophic ecology (Toft 1981; Toft 1985; Caldwell and Vitt 1999; Parmelee 1999). However, these studies only identified prey items to family or order level, which has the potential to constrain understanding of diet breadth and interspecific partitioning (Greene and Jaksić 1983; Kartzinel et al. 2015). The recent advances in high-throughput sequencing have greatly advanced our understanding of diet in many other clades that have suffered from similar challenges as frogs (Burgar et al. 2014; Kartzinel et al. 2015; McInnes et al. 2017), but molecular analysis of diet samples has not yet been applied to a study of frog trophic ecology.

Chapters 4 and 5 of my dissertation focus on advancing our understanding of frog diets based on stomach contents that I analyzed using metabarcoding. To acquire taxonomic breadth in my sampling, I conducted fieldwork in multiple locations. My three field sites in Michigan, USA, were temperate forest locations. In North Carolina, USA, I worked in a unique ecosystem of pine forest on sandy soil that hosts high frog species diversity. I also worked at four field sites in Peru, three of which were lowland Amazonian rainforests and the fourth was located in the foothills of the Andes Mountains. For Chapter 5, I was able to include samples from the Cerrado of Brazil courtesy of collaborators to further broaden the species richness in our study.

A serious constraint on investigating patterns of biodiversity across large taxonomic or geographic scales is often availability of data. Advances in sequencing technology and

computing power has facilitated generation of big data sets and large phylogenies, which can be leveraged to study macroevolutionary and macroecological questions while accounting for potential effects of phylogeny. However, there are still some data types, such as morphological measurements from museum specimens, that remain time-consuming to collect, but can be highly relevant for understanding patterns of and the processes that shape morphological variation. Other data types, such as dietary data, can be more rapidly analyzed with sequencing approaches, but acquisition of samples is a limiting step. For my dissertation, I created large-scale morphological and dietary datasets to address previously unstudied areas of frog diversity. These datasets also represent a major contribution to the scientific community and they can be leveraged to address further questions related to frog diversity beyond the topics that I present below.

SUMMARY OF CHAPTERS

Chapter 2: Are rates of speciation and morphological evolution coupled across extant frogs?

Variability in rates of diversification and morphological evolution has been documented across the tree of life (Eastman et al. 2011; Igea et al. 2017). Several hypotheses stemming from evolutionary theory predict that these two rates should be correlated, either directly or indirectly (West-Eberhard 1983; Futuyma 1987; Pigliucci 2008). We estimate the tempo of phenotypic evolutionary rates and speciation rates across frogs using morphological data for 757 species and assess the relationship between the rates using phylogenetic comparative methods. We found that body size evolutionary rates and speciation rates are very heterogeneous across frogs, whereas body shape evolutionary rates are relatively consistent. Estimates of phenotypic evolutionary rate are correlated across the axes of shape and size, indicating that frogs with relatively fast rates of

change in one dimension of morphology will also have relatively fast rates for all aspects of morphology. Overall, we find a positive correlation between morphological evolutionary rates and speciation rates, but these are marginally or not statistically significant. This ambiguous relationship was unresolved by the use of an independent and more comprehensive dataset on body size, so further work is required to understand the relationship between morphological evolution and speciation in frogs.

Chapter 3: Expansion and packing of frog morphospace along the New World latitudinal diversity gradient revealed by functional traits

The species richness of frogs in the Western Hemisphere increases by an order of magnitude between high latitude communities and low latitude tropical ones and is a classic example of the latitudinal diversity gradient. This is a well-documented pattern, but whether it is accompanied by changes in the volume of ecological niche space or the density of species within it has not previously been determined. With morphological traits that are tied to diet, habitat, and locomotion for 434 species, we evaluate how the structure of morphospace in frog assemblages changes in relation to species richness. We find that the volume of morphospace used by frog assemblages increases linearly with species richness and that morphodensity also increases. A key finding of this chapter is that morphovolume is the more dominant pattern as species richness increases, as opposed to packing as has been repeatedly documented in birds (Pigot et al. 2016; Pellissier and Kissling 2018; Schumm et al. 2019). This finding that most species richness increase is accompanied by an expansion of morphovolume rather than adding additional species to the volume occupied by a lower richness assemblage is consistent whether we compare assemblages within the temperate and tropical biomes or across biomes. The

consistency of the pattern within biomes, as well as along the latitudinal diversity gradient suggests that it is not driven by the accumulation of taxonomic families in the tropics that are not present in temperate assemblages.

Chapter 4: Evaluation of taxonomic and phylogenetic descriptors of diet diversity and dissimilarity in a community of tropical frogs

Diet is one of the central dimensions of a species' ecology, but its complexity has made it challenging to quantify and study. Results and conclusions about trophic resource use and partitioning can be dependent on the classification scheme applied to prey items (Greene and Jaksić 1983; Kartzinel et al. 2015). As high-throughput metabarcoding of dietary samples makes it feasible to generate high-resolution large dietary datasets, the question of how to quantify diet breadth and overlap has become increasingly relevant. We evaluate how understanding of frog diet breadth and similarity changes based on whether prey items are identified to species or order level and also how these taxonomic metrics compare to ones that account for the phylogenetic relationships between prey items. Our study system is 22 sympatric frog species from a lowland Amazonian forest in southeastern Peru. Despite having upwards of 40 dietary observations for several species, our sampling was not sufficient to estimate the number of prey species consumed by any frog species. The implication of this is that use of species level prey identification is not a practical approach for studying frog diets in a system like lowland Amazonian forests that have high resource base diversity. Instead, taxonomic metrics that use order or phylogenetic metrics provide more accessible and reliable approaches to understand dietary diversity and similarity with moderate sampling depth. These two approaches are

complementary and capture different dimensions of dietary diversity, as evidenced by some species showing taxonomically generalized, but phylogenetically specializated diets.

Chapter 5: The impacts of evolutionary history on frog diets

The evolution of trophic ecology varies in tempo and mode across major vertebrate clades. It can rapidly and dramatically diverge, as is seen in some adaptive radiations (Lovette et al. 2002; Seehausen 2006), or show phylogenetic inertia such that evolutionary history is a strong predictor of diet (Vitt et al. 2003; Grundler and Rabosky 2014). The evolution of diet across frogs has not previously been examined and it remains unknown whether trophic ecology is conserved or labile within frogs. We used metabarcoding to analyze stomach contents collected from nine fieldsites in the USA, Peru and Brazil and generate high-resolution diet profiles of 1,266 frog individuals from 111 species**.** With this data, we find that phylogenetic and taxonomic dietary diversity do not significantly differ between families. We also test whether frog diets fit the Deep Time Hypothesis that predicts present-day diets should reflect ecological divergences that occurred in the deep history of the clade (Vitt and Pianka 2005). Unlike other major radiations, such as squamates (Vitt and Pianka 2005; Colston et al. 2010), we do not find evidence to suggest that there are significant shifts in diet within the deep history of frogs. Indeed, aside from variation in ant consumption, frogs are remarkably homogeneous in their diets and there is little evidence of trophic innovation in deep or recent history. We propose a new framework, the Phylogenetically Widespread Hyper-Generalism Hypothesis, to describe frog trophic ecology that is characterized by generalized diets, high interspecific overlap, and limited specialization despite the amount of evolutionary time spanned by the clade.

REFERENCES

Burgar, J. M., D. C. Murray, M. D. Craig, J. Haile, J. Houston, V. Stokes, and M. Bunce. 2014. Who's for dinner? High-throughput sequencing reveals bat dietary differentiation in a biodiversity hotspot where prey taxonomy is largely undescribed. Molecular Ecology 23:3605–3617.

Caldwell, J. P., and L. J. Vitt. 1999. Dietary asymmetry in leaf litter frogs and lizards in a transitional northern Amazonian rain forest. Oikos 84:383–397.

Colston, T. J., G. C. Costa, and L. J. Vitt. 2010. Snake diets and the deep history hypothesis. Biological Journal of the Linnean Society 101:476–486.

Eastman, J. M., M. E. Alfaro, P. Joyce, A. L. Hipp, and L. J. Harmon. 2011. A novel comparative method for identifying shifts in the rate of character evolution on trees. Evolution 65:3578–3589.

Futuyma, D. J. 1987. On the Role of Species in Anagenesis. American Naturalist 130:465–473.

Greene, H. W., and F. M. Jaksić. 1983. Food-Niche Relationships among Sympatric Predators : Effects of Level of Prey Identification. Oikos 40:151–154.

Grundler, M. C., and D. L. Rabosky. 2014. Trophic divergence despite morphological convergence in a continental radiation of snakes. Proceedings of the Royal Society B: Biological Sciences 281:20140413.

Igea, J., E. F. Miller, A. S. T. Papadopulos, and A. J. Tanentzap. 2017. Seed size and its rate of evolution correlate with species diversification across angiosperms. PLoS Biology 15:1–16.

Kartzinel, T. R., P. A. Chen, T. C. Coverdale, D. L. Erickson, W. J. Kress, M. L. Kuzmina, D. I. Rubenstein, et al. 2015. DNA metabarcoding illuminates dietary niche partitioning by African large herbivores. Proceedings of the National Academy of Science 112:8019–8024.

Lovette, I. J., E. Bermingham, and R. E. Ricklefs. 2002. Clade-specific morphological diversification and adaptive radiation in Hawaiian songbirds. Proceedings of the Royal Society B: Biological Sciences 269:37–42.

Macarthur, R. H. 1965. Patterns of Species Diversity. Biological Reviews 40:510–533.

McInnes, J. C., R. Alderman, M.-A. Lea, B. Raymond, B. E. Deagle, R. A. Phillips, A. Stanworth, et al. 2017. High occurrence of jellyfish predation by black-browed and Campbell albatross identified by DNA metabarcoding. Molecular Ecology 26:4831–4845.

Mittelbach, G. G., D. W. Schemske, H. V Cornell, A. P. Allen, J. M. Brown, M. B. Bush, S. P. Harrison, et al. 2007. Evolution and the latitudinal diversity gradient: speciation, extinction and biogeography. Ecology letters 10:315–31.

Parmelee, J. R. 1999. Trophic Ecology of a Tropical Anuran Assemblage. Scientific Papers Natural History Museum the University of Kansas 11:1–59.

Pellissier, V., and W. D. Kissling. 2018. Niche packing and expansion account for species richness – productivity relationships in global bird assemblages. Global Ecolog and Biogeography 27:604–615.

Pianka, E. R. 1966. Latitudinal Gradients in Species Diversity : A Review of Concepts. American Naturalist 100:33–46.

Pigliucci, M. 2008. Is evolvability evolvable? Nature Reviews Genetics 9:75–82.

Pigot, A. L., C. H. Trisos, J. A. Tobias, and A. L. Pigot. 2016. Functional traits reveal the expansion and packing of ecological niche space underlying an elevational diversity gradient in passerine birds.

Schumm, M., A. E. White, K. Supriya, and T. D. Price. 2019. Ecological limits as the driver of bird species richness patterns along the east Himalayan elevational gradient. American Naturalist.

Seehausen, O. 2006. African cichlid fish : a model system in adaptive radiation research. Proceedings of the Royal Society B: Biological Sciences 273:1987–1998.

Toft, C. A. 1981. Feeding Ecology of Panamanian Litter Anurans : Patterns in Diet and Foraging Mode. Journal of Herpetology 15:139–144.

Toft, C. A. 1985. Resource Partitioning in Amphibians and Reptiles 1985:1–21.

Vitt, L. J., and E. R. Pianka. 2005. Deep history impacts present-day ecology and biodiversity. Proceedings of the National Academy of Science 102:7877–7881.

Vitt, L. J., E. R. Pianka, W. E. Cooper, and K. Schwenk. 2003. History and the Global Ecology of Squamate Reptiles. American Naturalist 162:44–60.

Wells, K. D. 2007. The ecology and behavior of amphibians. University of Chicago Press, Chicago, IL.

West-Eberhard, M. J. 1983. Sexual Selection, Social Competition, and Speciation. Quarterly Review of Biology 58:155–183.

CHAPTER 2

Are Rates Of Speciation And Morphological Evolution Coupled Across Extant Frogs?

with Abraham Weiner and Daniel L. Rabosky

ABSTRACT

An enduring question in biology is why species richness and morphological diversity are unevenly distributed across the tree of life. Several conceptual models predict that rates of speciation and phenotypic evolution should be coupled, but support for these predictions has been mixed. Here, we characterize the tempo of morphological evolution across frogs using morphological data for 757 species and test whether morphological evolution is correlated with speciation rate. We explored the relationships between speciation and overall size, as well as several measures of shape. We inferred minimal rate variation for all shape variables and did not detect any significant association between these rates and speciation. Estimated rates of species diversification and size evolution show considerable among-lineage variation, but are either weakly coupled or uncorrelated. Further work is required to understand the relationship between speciation and phenotypic evolution across this vertebrate radiation.

INTRODUCTION

Rates of diversification and phenotypic evolution are known to vary widely across the tree of life (Eastman et al. 2011; Igea et al. 2017) and identifying the mechanisms for this rate

variation and their role in shaping extant diversity is a central focus of macroevolutionary research. Evolutionary theory suggests that these two rates should be coupled for a number of reasons (Table 2.1), including the idea that an intrinsic capability for fast morphological evolution could drive lineage diversification. If species richness is limited by strong ecological controls, lineages with higher "evolvability" or "versatility" and therefore a greater ability to explore and utilize ecological space will more rapidly diversify (Vermeij 1970; Liem and Osse 1975; Pigliucci 2008). Morphological change in traits related to sexual signaling might also drive speciation. Sexual selection has long been considered a potential driver of speciation (Darwin 1871) since divergence in secondary sexual traits can results in pre-mating reproductive isolation through assortative mating (Mayr 1942; Lande 1981; Lande 1982; West-Eberhard 1983). Clades with high intrinsic morphological lability have the potential to more rapidly respond to sexual selection, which could result in higher speciation rates if the phenotypic response to the selective pressure influences mate choice. Underlying both of these classes of models is the direct association of speciation with morphological divergence and this can result in coupling of rates.

A coupling of rates could also result from a different direction of causality, such as speciation driving morphological evolution (Table 2.1). Under punctuated equilibrium (Eldredge and Gould 1972; Futuyma 1987), morphological change is concentrated during speciation events, even if not causally associated with the speciation itself. Therefore, a lineage that experiences higher rates of speciation will also have higher rates of phenotypic evolution relative to lineages with less speciation. This direction of causality can also arise if clades differ in rate of speciation through sexual selection, since clades with faster speciation will also have faster accumulation of phenotypic divergence in associated signaling characters (Futuyma 1987).

Despite these theoretical reasons to expect a coupling of rates of speciation and phenotypic evolution, results from empirical studies have been mixed. Positive correlations have been detected in *Carduelis* finches (Cardoso and Mota 2008), cetaceans (Gillet et al. 2019), ray-finned fishes (Rabosky et al. 2013), estrildid finches (Gomes et al. 2016), passerines (Mason et al. 2016), angiosperms (Igea et al. 2017), and tanagers (Price-Waldman et al. 2020), but not in elapid snakes (Lee et al. 2016), ferns (Testo and Sundue 2018), birds (Crouch and Ricklefs 2019) or Australian scincid lizards (Rabosky et al. 2014a). The discordance between these studies could indicate that patterns differ between clades or it could reflect that each study examined different phenotypic traits that vary in their reflection of ecological interactions or role in sexual selection. Additionally, the type of phenotypic trait under consideration is highly diverse across these studies, ranging from morphological traits such as body size to secondary sexual traits such as ornamental plumage, and these differences could also explain the lack of consistency in results.

Here, we examine whether rates of size and shape evolution are correlated with rates of speciation across frogs, a global radiation with over 7,000 currently described species (AmphibiaWeb 2020). This species diversity is unevenly distributed amongst taxonomic families with some, such as Rhinophrynidae and Ascaphidae having only one or two species, respectively, while others like Bufonidae and Craugastoridae each have upwards of 500 species. We estimate per-lineage rates of speciation and per-lineage rates of evolution for morphological traits and use phylogenetic comparative methods to test for trait-dependent speciation. Our analyses provide a window into whether and how phenotypic diversification might contribute to species richness across a major vertebrate radiation

METHODS

We collected morphological data from 757 species of frogs from 47 families (Table S2.1). Where possible, we measured multiple individuals per taxon; each species is represented by a median of three adult individuals (range: 1- 9; mode: 3). Our focal trait set consists of 11 linear external morphological traits: snout-vent length, head width, head length, internarial distance, interorbital distance, eye length, eye to naris distance, naris to snout distance, antebrachial length, femur length, and tibiofibula length. We chose these measurements because they could be readily measured from preserved specimens with high repeatability, and because we expect them to correlate with multiple aspects of anuran ecology. Specifically, these measurements are relevant to locomotion (Zug 1972; Gomes et al. 2009; Lires et al. 2016), microhabitat usage (Gomes et al. 2009; Moen et al. 2013; Moen et al. 2016), and diet (Emerson 1985; Parmelee 1999; Duellman 2005; Moen and Wiens 2009).

For each trait, we calculated the arithmetic species mean. Then by species, we took the geometric mean of the 11 traits and used this value as a shape-independent metric of size (Mosimann 1970). We used this size variable to standardize all other measurements to create isometric variables of shape (Mosimann 1970; Grundler and Rabosky 2014). With the correlation matrix of the log-transformed shape variables, we reduced dimensionality by performing a principal components analysis (PC) with axes scaled to unit variance. Trait loadings for the first four axes, which account for 74% of the variance in the data, are reported in Table S2.2. We interpret these PC axes as descriptors of shape (hereafter referred to as shape variables) and use them and the size variable to test the correlation between morphology and speciation.

For the size variable and each of the four shape variables, we used the program Bayesian Analysis of Macroevolutionary Mixtures (BAMM) (Rabosky et al. 2013; Rabosky 2014) to

simulate a posterior distribution of macroevolutionary rate shift configurations using 100 million generations of MCMC sampling with priors determined by the setBAMMpriors function in the R package *BAMMtools* v. 2.1.6 (Rabosky et al. 2014b). BAMM trait analyses were performed on a 757-tip phylogeny obtained by pruning a time-calibrated molecular phylogeny (Jetz and Pyron 2018) down to the species for which we have morphological data. We also used BAMM to reconstruct speciation rates across the full 3,449 tip molecular phylogeny (Jetz and Pyron 2018), again using the setBAMMpriors function to select priors and 100 million generations of MCMC sampling. We accounted for incomplete sampling by including family-level sampling fractions that we calculated using the taxonomy and family-level species richness available at AmphibiaWeb on 22 January 2020 (AmphibiaWeb 2020).

We tested for correlations between speciation rates and each of the 5 traits (Table 2.2) using two methods; these methods differ in how speciation rates are estimated and how significance is assessed. The first method, Structured Rate Permutations on Phylogenies (STRAPP) (Rabosky and Huang 2016) compares the BAMM speciation rates at the tips of the tree (hereafter referred to as λ_{BAMM}) to the corresponding phenotypic evolutionary tip rates; significance of the relationships is then examined through structured permutations of evolutionary rate regimes across the phylogeny. For each variable, we performed 1000 permutations and calculated a two-tailed Spearman's correlation coefficient (r_s). The second approach, ES-sim, uses "tip" speciation rates estimated using the DR statistic to test for trait-dependent speciation (Harvey and Rabosky 2018). The DR statistic (hereafter referred to as λ_{DR}; Redding and Mooers 2006), provides an estimate of the per-lineage speciation rate for each taxon in the phylogeny (Jetz et al. 2012; Belmaker and Jetz 2015; Quintero and Jetz 2018; Title and Rabosky 2019). Significance is assessed by simulating trait evolution under a Brownian motion

model and comparing the observed Pearson correlation (r) to the null distribution (Harvey and Rabosky 2018). These two methods are complementary since STRAPP can have low power if there are not many large rate shift events across the tree and λ_{DR} is more sensitive to variation in small rate regimes (Rabosky and Huang 2016; Maliet et al. 2019), although error in λ_{BAMM} estimates generally appears to be lower than those in λ_{DR} (Title and Rabosky 2019).

λ_{DR} can be biased by incomplete sampling (Harvey and Rabosky 2018), so we computed the average λ_{DR} for each taxon across a set of trees from the posterior distribution of a published 6,380 tip frog phylogeny (Jetz and Pyron 2018). These 100 trees were generated by stochastic polytomy resolution that placed species for which genetic data was not available onto the molecular backbone phylogeny, which we use as a phylogenetic framework of our BAMM analyses and tests of trait-dependent speciation (Jetz and Pyron 2018). As mentioned above, this molecular phylogeny contains 3,449 species, meaning that 54% of the species included in the larger tree are represented by genetic data.

As an additional check on our primary assessment of the relationship between size and speciation rates, we obtained a secondary, independent dataset on size by extracting maximum snout-vent length (SVL) data from the AmphiBIO database (Oliveira et al. 2017). We retained information only for species represented in the molecular phylogeny (Jetz and Pyron 2018) because trees constructed with stochastic polytomy resolution may not be appropriate for inferring phenotypic evolution (Rabosky 2015). The overlap between taxa present in the molecular phylogeny and SVL dataset from AmphiBIO was 2,733 species (Table S2.1). BAMM was used to estimate evolution rates of log-transformed SVL values using the same procedures described above. The relationship between these inferred rates and speciation rates was tested using STRAPP and ES-sim.

RESULTS

Rates of phenotypic evolution

The first four axes of the principal components analysis explained 74% of the variation within the morphological dataset (Table S2.2). The intersection between the geometric size variable and SVL datasets was 697 species. For these species, the values of the geometric size variable and maximum SVL were tightly correlated (r = 0.87) and the computed evolution rates of the two traits were moderately correlated (r = 0.58; Figure 2.1).

We found considerable among-lineage variation in the rate of change for the geometric size variable and SVL with inferred mean rate shift counts of 49 and 193, respectively (Table 2.2; Figures 2.2). Rates of evolution for the four shape variables show less rate heterogeneity with rate shift counts of 20, 16, 9, and 22, respectively (Figure S2.1). Species-specific rates of phenotypic evolution for these individual PC axes (shape variables) were moderately positively correlated (Figure 2.1), meaning that, in general, species with fast evolution on one independent axis of shape will also display fast rates on the other axes. The species-specific rate of change for the geometric size variable was weakly to moderately correlated with the shape variable rates of evolution (Figure 2.1), indicating a tendency for species with fast rates of size evolution to also have fast shape evolution.

Speciation rates across the phylogeny

For speciation-extinction analyses, the posterior mean number of rate regimes inferred with BAMM on the 3,449 tip molecular backbone was 27. We then mapped this posterior distribution of rate shifts to the subtrees containing only the 757 taxa in the morphological

dataset. Considering these subtrees containing the species in the morphological dataset, BAMM estimated a posterior mean of 20 rate regimes (Table 2.2; Figure 2.2). For these 757 species, tip-specific rates of speciation as estimated using BAMM (λ_{BAMM}) are moderately correlated with λ_{DR} (Figures 2.3 and S2.2; r = 0.50). While λ_{BAMM} and λ_{DR} indicate the presence of substantial speciation rate variation across the frog phylogeny, the estimates differ in how this variation is partitioned between and within taxonomic families (Figure 2.3). In general, there is little variance in λ_{BAMM} within families, whereas there is noticeable variation in λ_{DR} within and between families.

Tests of trait-dependent speciation

We tested for trait-dependent speciation using STRAPP and ES-sim and did not find a significant correlation between any of the trait evolutionary rates and speciation rates with either method (Table 2.3). However, we found an overall trend towards a positive correlation (Figures 2.1, 2.4, and S2.3) between all estimated rates with some correlations approaching statistical significance. ES-sim assessed the correlation between λ_{DR} and evolutionary rates of PC1 and PC4 as marginally significant with P values of 0.05 and Pearson correlation coefficients of 0.28. The STRAPP results for the geometric size variable were also marginally significant ($r_s = 0.37$; $p = 0.05$; Figure 2.4). Results from STRAPP and ES-sim tests with the SVL dataset were very similar to results generated using the geometric size variable (Table 2.3; Figure 2.4): ES-sim did not detect evidence of a significant correlation between SVL evolutionary rates and λ_{DR} ($p = 0.33$) and STRAPP produced results that were marginally non-significant ($p = 0.08$).

DISCUSSION

We examined the relationship between morphological evolution and speciation rate across the global radiation of frogs and detected high among-lineage variation in rates of speciation and size evolution. Contrary to theoretical expectations, our analyses did not find robust support for a coupling of speciation rates with rates of size or shape evolution. However, we could not strongly reject this hypothesis for several of our morphological variables and our results imply that further work is required to determine the relationship between these rates.

We did not find a robustly significant correlation between either geometric size or maximum SVL evolution with speciation rates, but we did detect a trend towards a positive correlation between both of these measures of body size and BAMM-estimated speciation rates that was nearly significant. Since we found that maximum SVL and the geometric size variable are tightly correlated and therefore equivalent metrics of body size for our purposes, we were able to re-examine this relationship with greatly improved sampling. Interestingly, this did not resolve the question, again resulting in a marginally positive correlation ($p = 0.08$), meaning that we cannot conclude that these two rates are correlated nor can we definitively discard the hypothesis that they are linked. It is unclear whether additional sampling would provide a less ambiguous answer to whether these rates are coupled, given that tripling our sampling did not materially alter our results towards a clearly significant correlation or an unambiguous decoupling of rates.

The relationship between rates of shape evolution and speciation rates is also unclear. Like with geometric size and SVL, neither STRAPP nor ES-sim detected statistically significant evidence of trait-dependent speciation for any shape variable rate evolution. However, the

consistent positive pairwise correlation between these rates that were frequently marginally non-significant do not allow us to conclusively reject the hypothesis that these two rates are linked.

Our results are also constrained by the suite of morphological characters that we chose to measure. Even though the traits that we examined are relevant to locomotion (Zug 1972; Gomes et al. 2009; Lires et al. 2016), microhabitat usage (Gomes et al. 2009; Moen et al. 2013; Moen et al. 2016), and diet (Emerson 1985; Parmelee 1999; Duellman 2005; Moen and Wiens 2009) in frogs, they might not adequately capture information about ecological resource usage or how it differs between species. Inclusion of additional traits in descriptors of shape or analysis of single traits other than size may find that morphological lability is correlated with speciation rates across the frog radiation. Trait types other than morphological traits also merit consideration in future studies of the relationship between phenotypic evolution and speciation rates in frogs. Our study did not include any traits considered to be secondary sexual traits in frogs, but the association between mating call evolution and diversification warrants testing, especially given that these two rates are correlated in passerine birds (Mason et al. 2016).

While our study utilized large morphological and phylogenetic datasets, it is still limited by several factors. Firstly, our findings could be sensitive to sampling since our morphological dataset lacked information on shape for approximately 90% of frog species (AmphibiaWeb 2020). However, we did find strong concordance in results using our dataset and the larger maximum SVL dataset that has information for approximately 38% of frog species (AmphibiaWeb 2020). Our morphological dataset was geographically biased with 57% of the 757 species from the Western Hemisphere. Despite this, we have taxonomically broad sampling, albeit with variable sampling effort per family (Table S2.1). This broad taxonomic scope might, however, obscure patterns at smaller scales. For example, size and shape evolution could be

correlated with speciation within certain clades, but not in others, so that such a pattern would not be detected when integrating across all frogs. Measurement error could also weaken or obscure the true signal of a relationship. We expect this to be a greater concern in the question of shape evolution in relation to speciation rates, given the concordance in results between the two independent datasets on body size.

In summary, our study uncovered substantial among-lineage rate heterogeneity of size evolution in frogs, but a surprising consistency of shape evolution rates. We did not detect any coupling of shape evolution and speciation rates, but we are unable to strongly reject the hypothesis that rates of size evolution and speciation are positively linked. Additional investigation is needed to clarify this relationship and determine the factors that underlie variation in rates of phenotypic evolution and speciation in frogs.

ACKNOWLEDGEMENTS

We thank Greg Schneider for access to specimens (University of Michigan Museum of Zoology) and Monica West, Erich Eberhard, and Yoshio Wagner for helping collect data. BAMM analyses were performed on the High Performance Computing Cluster that is maintained by the National Center for Genome Analysis Support at Indiana University. JGL was supported by a NSF GRFP and a University of Michigan Rackham Predoctoral Fellowship.

DATA AVAILABILITY

Raw morphological measurements used in this study are available on Deep Blue Data, https://doi.org/10.7302/abtx-c461

REFERENCES

AmphibiaWeb. 2020. <https://amphibiaweb.org> University of California, Berkeley, CA, USA. Accessed 22 Jan 2020.

Belmaker, J., and W. Jetz. 2015. Relative roles of ecological and energetic constraints, diversification rates and region history on global species richness gradients. Ecology Letters 18:563–571.

Cardoso, G. C., and P. G. Mota. 2008. Rapid origin of sexual isolation and character divergence in a cline. Evolution 62:753–762.

Crouch, N. M. A., and R. E. Ricklefs. 2019. Speciation rate is independent of the rate of evolution of morphological size , shape , and absolute morphological specialization in a large clade of birds. American Naturalist 193:E78–E91.

Darwin, C. 1871. The descent of man, and selection in relation to sex. (John Murray, ed.). London.

Duellman, W. E. 2005. Cusco Amazonico. Comstock Pub. Associates, Ithaca, NY.

Eastman, J. M., M. E. Alfaro, P. Joyce, A. L. Hipp, and L. J. Harmon. 2011. A novel comparative method for identifying shifts in the rate of character evolution on trees. Evolution 65:3578–3589.

Eldredge, N., and S. S. Gould. 1972. Punctuated equilibria: an alternative to phyletic gradualism. In T. J. M. Schopf, ed., Models in paleobiology (pp. 182–215). Freeman Cooper, San Francisco.

Emerson, S. B. 1985. Skull Shape in Frogs : Correlations with Diet. Herpetologica 41:177–188.

Futuyma, D. J. 1987. On the Role of Species in Anagenesis. American Naturalist 130:465–473.

Gillet, A., B. Frédérich, and E. Parmentier. 2019. Divergent evolutionary morphology of the axial skeleton as a potential key innovation in modern cetaceans. Proceedings of the Royal Society B: Biological Sciences 286:20191771.

Gomes, A. C. R., M. D. Sorenson, and C. Cardoso. 2016. Speciation is associated with changing ornamentation rather than stronger sexual selection. Evolution 70:2823–2838.

Gomes, F. R., E. L. Rezende, M. B. Grizante, and C. A. Navas. 2009. The evolution of jumping performance in anurans : morphological correlates and ecological implications. European Society for Evolutionary Biology 22:1088–1097.

Grundler, M. C., and D. L. Rabosky. 2014. Trophic divergence despite morphological

convergence in a continental radiation of snakes. Proceedings of the Royal Society B: Biological Sciences 281:20140413.

Harvey, M. G., and D. L. Rabosky. 2018. Continuous traits and speciation rates : Alternatives to dependent diversification models. Methods in Ecology and Evolution 9:984–993.

Igea, J., E. F. Miller, A. S. T. Papadopulos, and A. J. Tanentzap. 2017. Seed size and its rate of evolution correlate with species diversification across angiosperms. PLoS Biology 15:1–16.

Jetz, W., and R. A. Pyron. 2018. The interplay of past diversification and evolutionary evolutionary isolation with present imperilment across the amphibian tree of life. Nature Ecology & Evolution 2:850–858.

Jetz, W., G. H. Thomas, J. B. Joy, K. Hartmann, and A. O. Mooers. 2012. The global diversity of birds in space and time. Nature 491:444–448.

Lande, R. 1981. Models of speciation by sexual selection on polygenic traits. Proceedings of the National Academy of Science 78:3721–3725.

Lande, R. 1982. Rapid origin of sexual isolation and character divergence in a cline. Evolution 36:548–550.

Lee, M. S. Y., K. L. Sanders, B. King, and A. Palci. 2016. Diversification rates and phenotypic evolution in venomous snakes (Elapidae). Royal Society Open Science 3:150277.

Liem, K. F., and J. W. M. Osse. 1975. Biological Versatility, Evolution, and Food Resource Exploitation in African Cichlid Fishes. American Zoologist 15:427–454.

Lires, A. I., I. M. Soto, and R. O. Gómez. 2016. Walk before you jump : new insights on early frog locomotion from the oldest known salientian. Paleobiology 42:612–623.

Maliet, O., F. Hartig, and H. Morlon. 2019. A model with many small shifts for estimating species-specific diversification rates. Nature Ecology & Evolution 3:1086–1092.

Mason, N. A., K. J. Burns, J. A. Tobias, S. Claramunt, N. Seddon, and E. P. Derryberry. 2016. Song evolution, speciation, and vocal learning in passerine birds. Evolution 71:786–796.

Mayr, E. 1942. Systematics and the Origin of Species. Columbia University Press, New York.

Moen, D. S., D. J. Irschick, and J. Wiens. 2013. Evolutionary conservatism and convergence both lead to striking similarity in ecology, morphology and performance across continents in frogs. Proceedings of the Royal Society B: Biological Sciences 280:20132156.

Moen, D. S., H. Morlon, and J. J. Wiens. 2016. Testing convergence versus history: convergence

dominates phenotypic evolution for over 150 million years in frogs. Systematic Biology 65:146–160.

Moen, D. S., and J. J. Wiens. 2009. Phylogenetic evidence for competitively driven divergence: Body-size evolution in caribbean treefrogs (Hylidae: Osteopilus). Evolution 63:195–214.

Mosimann, J. E. 1970. Size Allometry : Size and Shape Variables with Characterizations of the Lognormal and Generalized Gamma Distributions. Journal of the American Statistical Association 65:930–945.

Oliveira, B. F., V. A. São-Pedro, G. Santos-Barrera, C. Penone, and G. C. Costa. 2017. AmphiBIO, a global database for amphibian ecological traits. Scientific Data 4:170123.

Parmelee, J. R. 1999. Trophic Ecology of a Tropical Anuran Assemblage. Scientific Papers Natural History Museum the University of Kansas 11:1–59.

Pigliucci, M. 2008. Is evolvability evolvable? Nature Reviews Genetics 9:75–82.

Price-Waldman, R. M., A. J. Shultz, and K. J. Burns. 2020. Speciation rates are correlated with changes in plumage color complexity in the largest family of songbirds. Evolution 74:1155–1169.

Quintero, I., and W. Jetz. 2018. Global elevational diversity and diversification of birds. Nature 555:246–250.

Rabosky, D. L. 2014. Automatic Detection of Key Innovations , Rate Shifts , and Diversity-Dependence on Phylogenetic Trees. PLoS o 9:e89543.

Rabosky, D. L. 2015. No substitute for real data : A cautionary note on the use of phylogenies from birth – death polytomy resolvers for downstream comparative analyses. Evolution 69:3207–3216.

Rabosky, D. L., S. C. Donnellan, M. G. Grundler, and I. J. Lovette. 2014a. Analysis and visualization of complex macroevolutionary dynamics : an example from Australian scincid lizards. Systematic Biology 63:610–627.

Rabosky, D. L., M. Grundler, C. Anderson, P. Title, J. J. Shi, J. W. Brown, H. Huang, et al. 2014b. BAMMtools: An R package for the analysis of evolutionary dynamics on phylogenetic trees. Methods in Ecology and Evolution 5:701–707.

Rabosky, D. L., and H. Huang. 2016. A Robust Semi-Parametric Test for Detecting Trait-Dependent Diversification. Systematic biology 65:181–193.

Rabosky, D. L., F. Santini, J. Eastman, S. a Smith, B. Sidlauskas, J. Chang, and M. E. Alfaro. 2013. Rates of speciation and morphological evolution are correlated across the largest vertebrate radiation. Nature communications 4:1–8.

Redding, D. W., and A. Ø. Mooers. 2006. Incorporating Evolutionary Measures into Conservation Prioritization. Conservation Biology 20:1670–1678.

Testo, W. L., and M. A. Sundue. 2018. Are rates of species diversification and body size evolution coupled in the ferns ? American Journal of Botany 105:525–535.

Title, P. O., and D. L. Rabosky. 2019. Tip rates , phylogenies and diversification : What are we estimating , and how good are the estimates ? Methods in Ecology and Evolution 2019:821–834.

Vermeij, G. J. 1970. Adaptation, versatility, and evolution. Systematic biology 22:466–477.

West-Eberhard, M. J. 1983. Sexual Selection, Social Competition, and Speciation. Quarterly Review of Biology 58:155–183.

Zug, G. R. 1972. Anuran Locomotion : Structure and Function . I . Preliminary Observations on Relation between Jumping and Osteometrics of Appendicular and Postaxial Skeleton. Copeia 1972:613–624.

Table 2.1: Theoretical mechanisms that predict a positive correlation between phenotypic evolutionary rates and speciation rates. Arrow denotes direction of causality.

Mechanism	Direction of causality	References
Clades with high rates of morphological change are better able to explore ecological opportunities during adaptive radiations and will speciate more if the ability to exploit novel ecological opportunities is a limiting control on speciation	P è S DIRECT causality	Vermeij 1970; Liem and Osse 1975; Pigliucci 2008
Lineages that more rapidly evolve and diverge in phenotypic traits involved in sexual signals will speciate faster through assortative mating	P è S DIRECT causality	Mayr 1942; Lande 1981; Lande 1982; West-Eberhard 1983
Punctuated equilibrium or speciational trait evolution in which phenotypic change is concentrated during speciation events	S è P DIRECT or INDIRECT causality	Eldredge and Gould 1972; Futuyma 1987
Speciation via sexual selection preserves phenotypic variation in sexual signaling traits that was previously population-level variation	S è P INDIRECT causality	Futuyma 1987

Table 2.2: Summary information about BAMM analyses. Reported are the posterior mean number of rate regimes with upper and lower 95% confidence intervals reported in brackets, and the number of rate shifts with the highest posterior probability. The molecular phylogeny of Jetz and Pyron (2018) was the phylogenetic framework for all analyses. Speciation-extinction dynamics were inferred across the full 3,449 tip molecular phylogeny. Also presented are the rate regime characteristics for the pruned molecular phylogeny of the focal 757 species. SVL evolution rates were inferred with a dataset of 2,733 species. All other phenotypic analyses inferred rates across the focal 757 species.

	Mean number of rate regimes	**Number of rate shifts**
BAMM diversification		
Full molecular phylogeny	27.00 [26.82, 27.19]	26
Pruned molecular phylogeny	21.38 [21.26, 21.50]	19
BAMM phenotypic evolution		
SVL	193.93 [192.92, 194.93]	186
Geometric size	49.89 [49.62, 50.16]	46
PC1	20.86 [20.68, 21.04]	17
PC2	16.12 [15.95, 16.30]	14
PC3	9.85 [9.72, 9.99]	6
PC4	22.17 [21.98, 22.36]	19

Table 2.3: Results from tests of trait-dependent speciation. Two-tailed *p*-values and Spearman's (r_s) or Pearson's (r) correlation coefficients are reported for STRAPP and ES-sim, respectively. All traits were logged prior to STRAPP or ES-sim tests.

Trait	**STRAPP**		**ES-sim**	
	p-value	r_s	*p*-value	r
Geometric size variable evolution rate	0.05	0.37	0.40	0.15
SVL evolutionary rate	0.08	0.35	0.33	0.12
PC1 evolutionary rate	0.30	0.23	0.05	0.28
PC2 evolutionary rate	0.17	0.27	0.11	0.25
PC3 evolutionary rate	0.56	.07	0.41	0.13
PC4 evolutionary rate	0.73	.04	0.05	0.28

Figure 2.1: Correlogram showing the relationships between morphological variable evolutionary rates and speciation rates. All rates were log-transformed. Correlations between speciation rates and morphological evolutionary rates as presented in Table 2.2. Pearson correlation coefficients between morphological evolutionary rates and λ_{DR} result from ES-sim analyses. Values for the relationship between the mean tip phenotypic rates and λ_{BAMM} are the mean Spearman correlation from STRAPP (Rabosky and Huang 2016) analyses across samples from the posterior of trees The relationship between all other rates were quantified with Pearson correlation coefficients. Above diagonal are graphical representations of these correlations with color and eccentricity of ellipse reflects magnitude of correlation. Orientation of ellipse represents the direction of correlation.

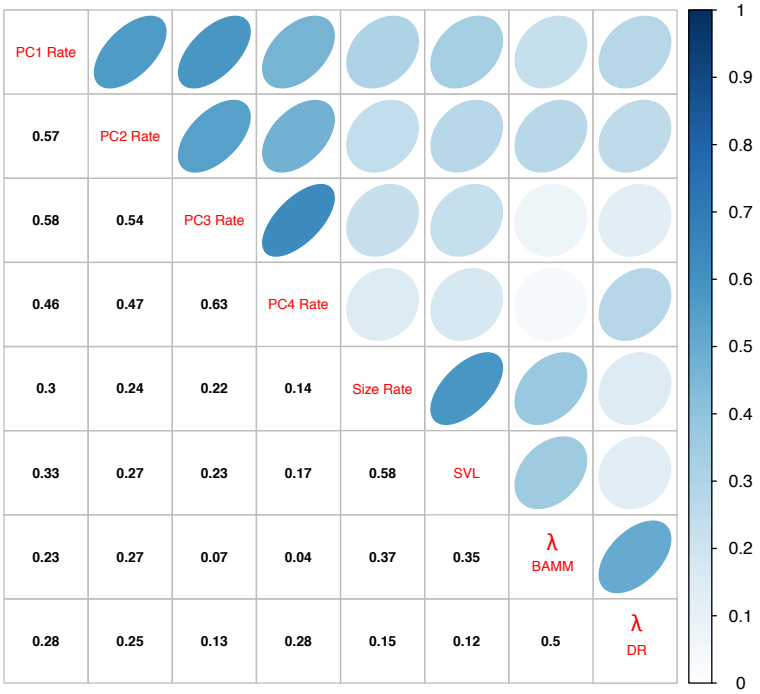

Figure 2.2: Phylorate plots of BAMM-estimated instantaneous rates of body size evolution (top) and speciation (bottom) across frogs, showing that both rates vary widely across the tree. Rates were calculated as the mean of the marginal posterior density of rates. Major families of frogs are labeled. 1: Ascaphidae and Leiopelmatidae; 2: Bombinatoridae and Alytidae; 3: Scaphiopodidae; 4: Pelodytidae and Megophryidae; 5: Ceratophryidae; 6: Hylodidae; 7: Alsodidae; 8: Sooglossidae; 9: Arthroleptidae; 10: Conrauidae; 11: Pyxicephalidae; 12: Ceratobatrachidae and Nyctibatrachidae; 13: Ranixalidae and Dicroglossidae. Molecular phylogeny pruned from Jetz and Pyron (2018). Rates were log-transformed before colors were assigned. Color ramp extends from slower rates in blue to faster rates in red.

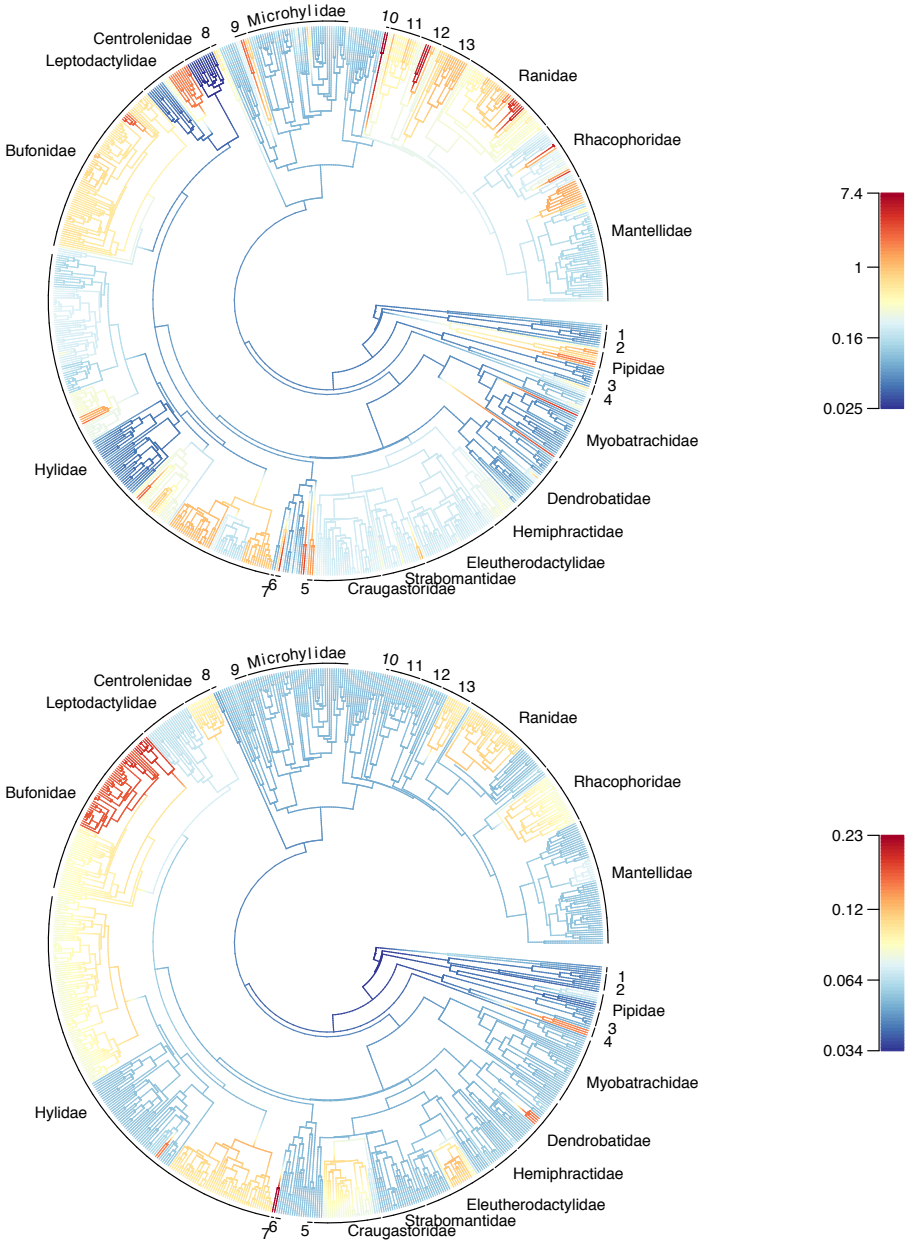

Figure 2.3: Speciation rates estimated with BAMM (λ_{BAMM}) and the DR (λ_{DR}) statistic for the 757 focal species plotted by family. Rates are log-transformed.

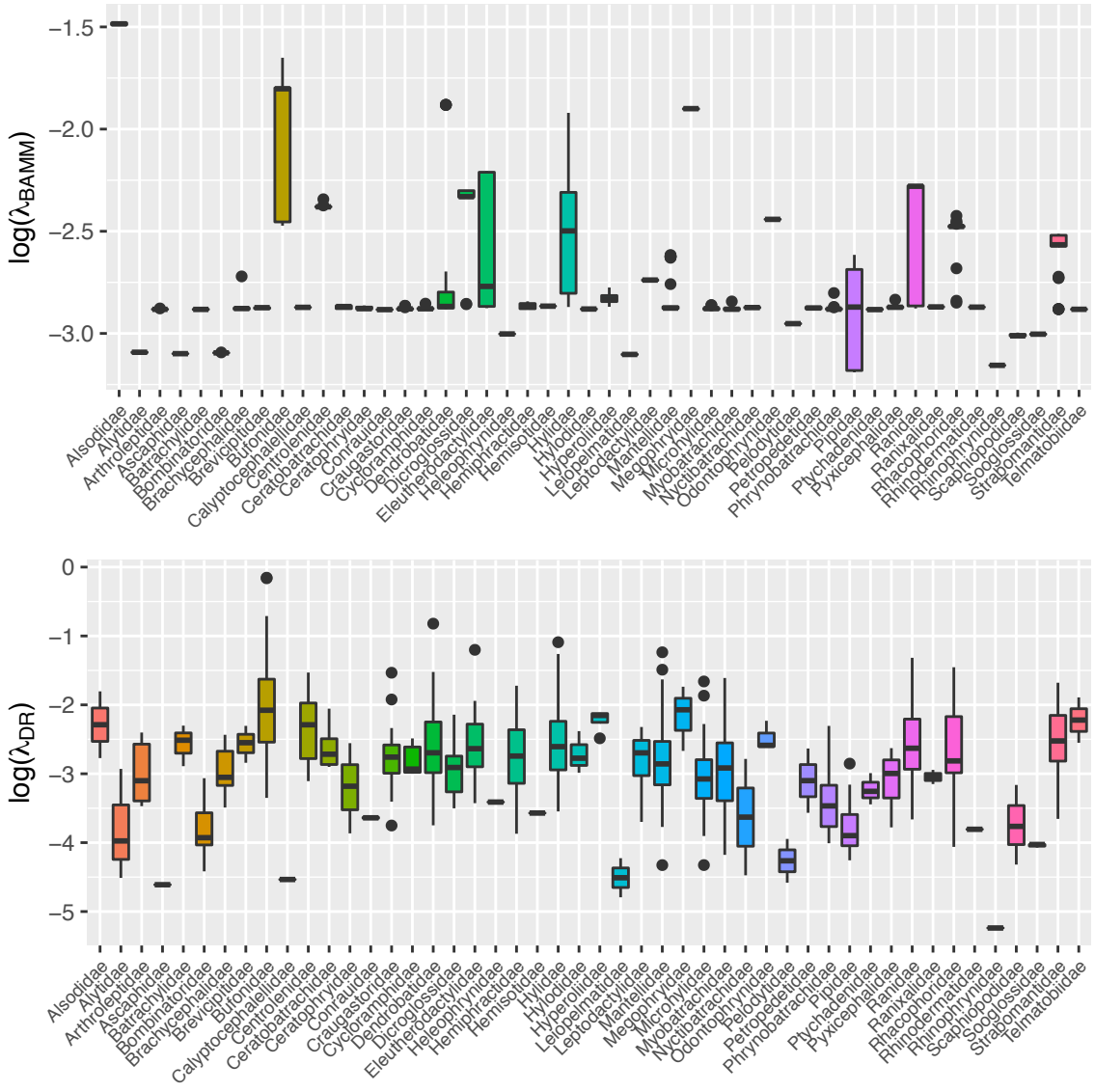

Figure 2.4: Rates of size and SVL evolution against λ_{BAMM} (top) and λ_{DR} (bottom) for the 757 focal species. All rates are log-transformed. Phenotypic and speciation rates estimated with BAMM are mean tip rates.

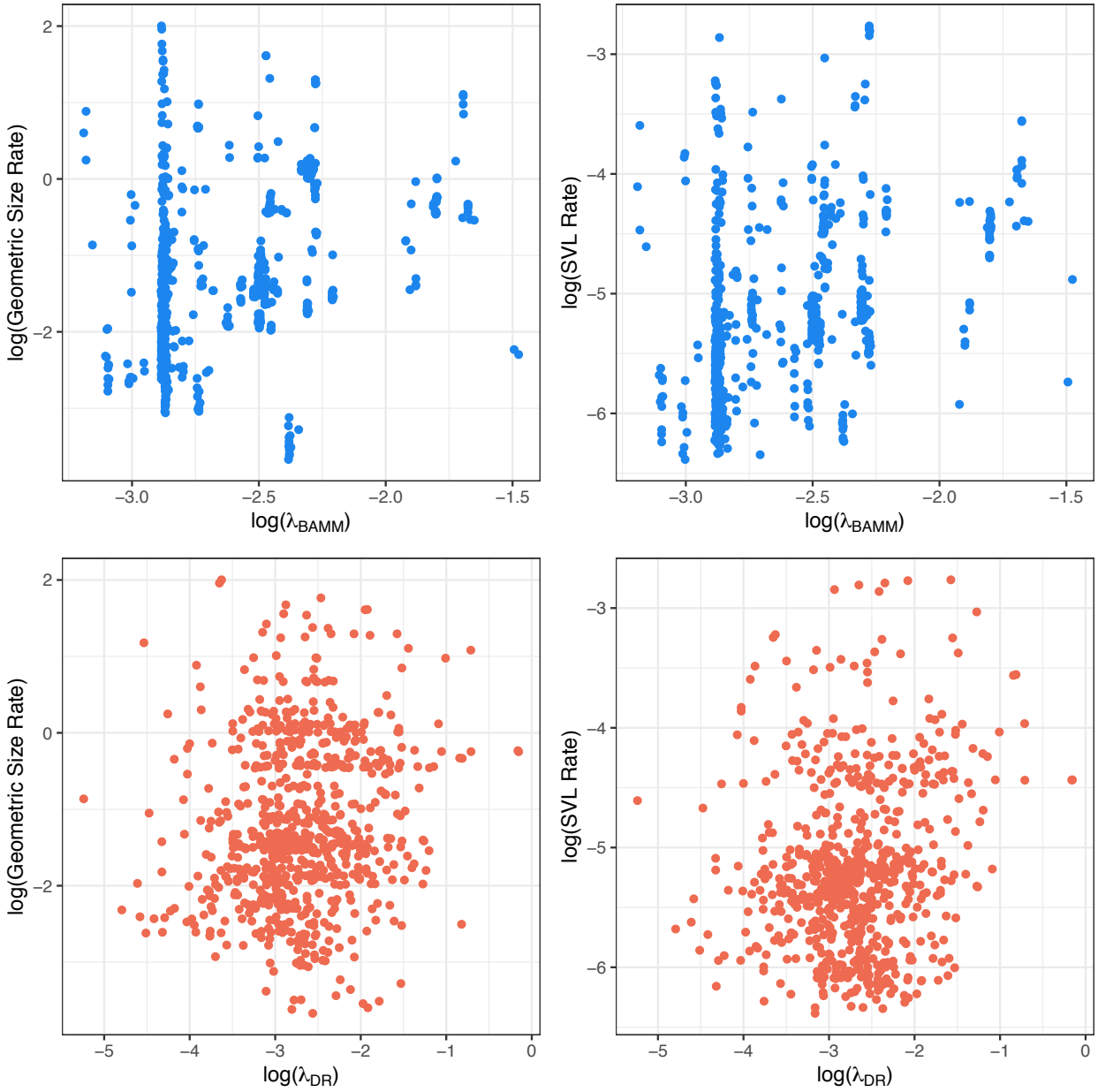

Table S2.1: Taxonomic sampling information for morphological evolutionary rate estimation. All frog families recognized by AmphibiaWeb, number of species per family included in the morphological dataset used to calculate the geometric size variable and shape variables, the proportion of each family sampled, number of species per family included in the analysis of maximum SVL evolution using data from AmphiBIO (Oliveira et al. 2017) and the proportion of each family sampled. Sampling fractions were calculated by using family-level species richness obtained from AmphibiaWeb on 22 January 2020.

Family	Family Richness	Species sampled	Sampling fraction	AmphBIO	Sampling fraction
Allophrynidae	3	0	0.00	2	0.67
Alsodidae	26	2	0.08	15	0.58
Alytidae	11	3	0.27	9	0.82
Arthroleptidae	153	6	0.04	65	0.42
Ascaphidae	2	1	0.50	2	1.00
Batrachylidae	13	3	0.23	4	0.31
Bombinatoridae	10	5	0.50	8	0.80
Brachycephalidae	74	6	0.08	26	0.35
Brevicipitidae	35	3	0.09	19	0.54
Bufonidae	628	80	0.13	209	0.33
Calyptocephalellidae	5	1	0.20	3	0.60
Centrolenidae	161	13	0.08	67	0.42
Ceratobatrachidae	101	8	0.08	14	0.14
Ceratophryidae	12	3	0.25	5	0.42
Ceuthomantidae	4	0	0.00	1	0.25
Conrauidae	6	2	0.33	4	0.67
Craugastoridae	127	20	0.16	33	0.26
Cycloramphidae	36	5	0.14	9	0.25
Dendrobatidae	323	27	0.08	150	0.46
Dicroglossidae	214	12	0.06	95	0.44
Eleutherodactylidae	225	28	0.12	157	0.70
Heleophrynidae	6	1	0.17	3	0.50
Hemiphractidae	118	13	0.11	63	0.53
Hemisotidae	9	1	0.11	1	0.11
Hylidae	1003	187	0.19	446	0.44
Hylodidae	47	3	0.06	10	0.21
Hyperoliidae	232	4	0.02	73	0.31
Leiopelmatidae	4	2	0.50	4	1.00
Leptodactylidae	217	22	0.10	79	0.36
Mantellidae	229	56	0.24	151	0.66
Megophryidae	242	3	0.01	79	0.33
Micrixalidae	24	0	0.00	1	0.04
Microhylidae	678	45	0.07	196	0.29

Myobatrachidae	134	30	0.22	73	0.54
Nasikabatrachidae	2	0	0.00	1	0.50
Nyctibatrachidae	39	2	0.05	16	0.41
Odontobatrachidae	5	0	0.00	0	0.00
Odontophrynidae	50	3	0.06	17	0.34
Pelobatidae	6	0	0.00	4	0.67
Pelodytidae	5	2	0.40	3	0.60
Petropedetidae	13	2	0.15	11	0.85
Phrynobatrachidae	94	13	0.14	49	0.52
Pipidae	41	8	0.20	17	0.41
Ptychadenidae	59	3	0.05	17	0.29
Pyxicephalidae	87	12	0.14	43	0.49
Ranidae	411	44	0.11	204	0.50
Ranixalidae	18	2	0.11	6	0.33
Rhacophoridae	425	27	0.06	92	0.22
Rhinodermatidae	3	1	0.33	2	0.67
Rhinophrynidae	1	1	1.00	1	1.00
Scaphiopodidae	7	7	1.00	7	1.00
Sooglossidae	4	3	0.75	4	1.00
Strabomantidae	715	30	0.04	145	0.20
Telmatobiidae	62	2	0.03	18	0.29

Table S2.2: Loadings of the eleven log-transformed morphological traits for the first four principal component (PC) axes.

	PC1	PC2	PC3	PC4
Snout to vent length	0.41	0.13	-0.11	0.37
Head width	0.32	0.41	0.02	-0.11
Head length	0.25	0.06	-0.22	-0.65
Internarial width	-0.49	0.04	0.03	0.21
Interorbital width	-0.08	0.18	0.61	0.14
Eye length	-0.11	0.24	-0.24	-0.32
Eye to naris length	0.03	-0.07	0.55	-0.40
Naris to snout length	-0.36	-0.13	-0.44	0.02
Antebrachial length	0.39	0.21	-0.12	0.32
Femur length	0.31	-0.51	-0.02	0.09
Tibio fibula	0.17	-0.63	0.06	-0.05
Proportion of Variance	**0.30**	**0.17**	**0.16**	**0.11**
Cumulative Proportion	**0.30**	**0.47**	**0.63**	**0.74**

Figure S2.1: Density plots for per-lineage tip rates of evolutionary change for the first four PC axes that we use as variables of shape. Rates were computed using BAMM and are plotted on a log-scale. Phylorate plot inserts show instantaneous rates of evolutionary change calculated as the mean of the marginal posterior density of rates.

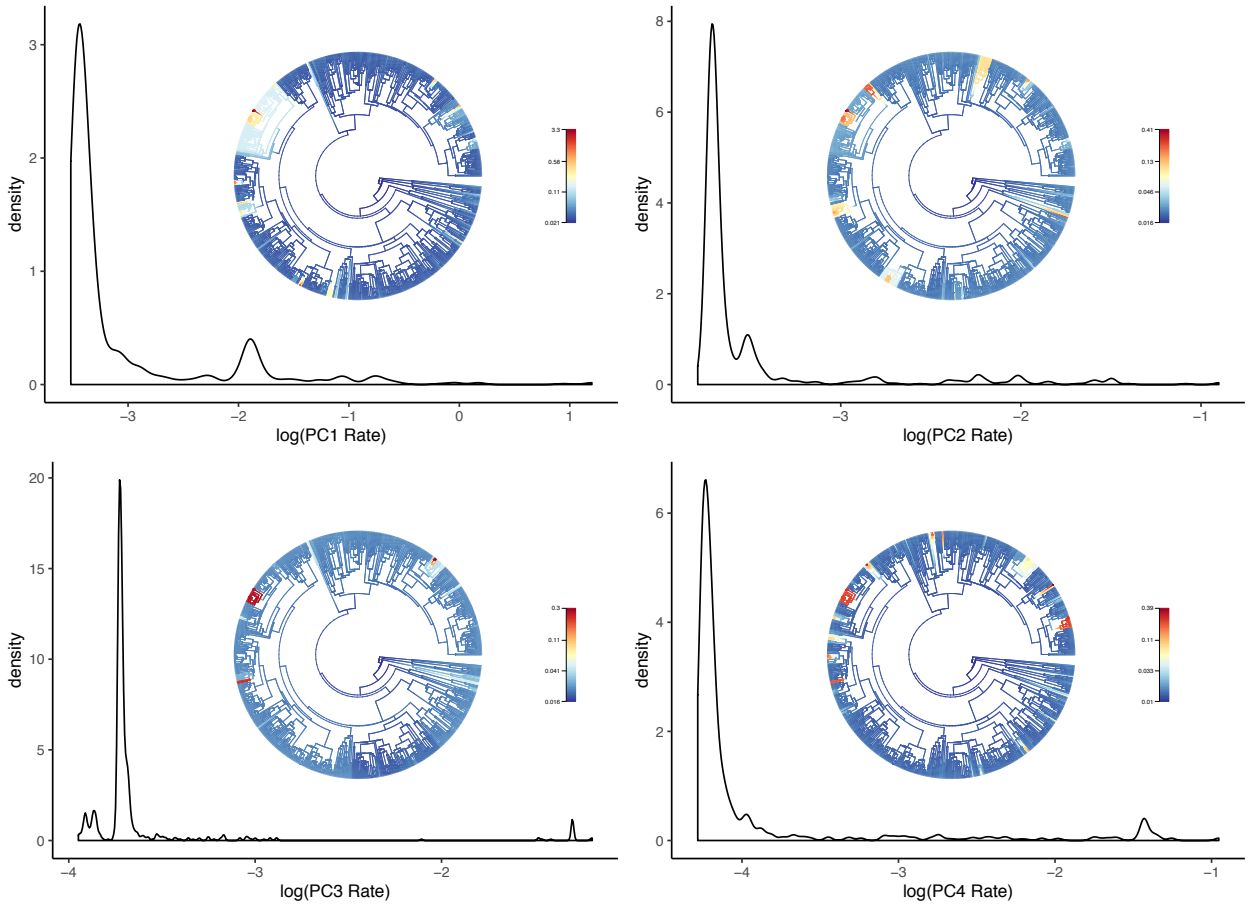

Figure S2.2: Scatterplot and marginal density plots of speciation rates estimated with BAMM and DR statistic, both on a log scale, for the 757 frog species in the morphological dataset.

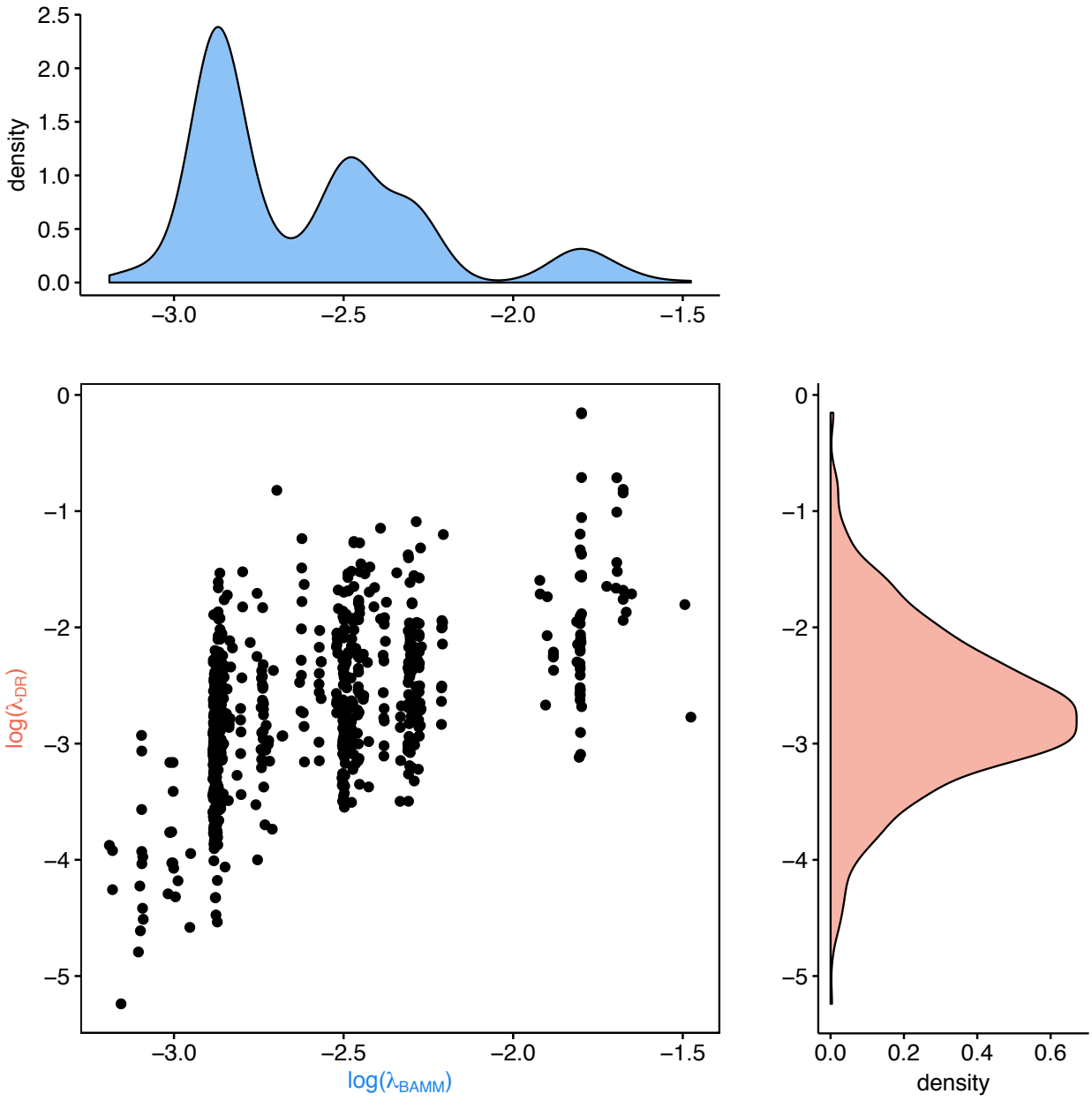

Figure S2.3: Scatterplots of speciation rates against rates of shape variable evolution for the 757 frog species in the morphological dataset.

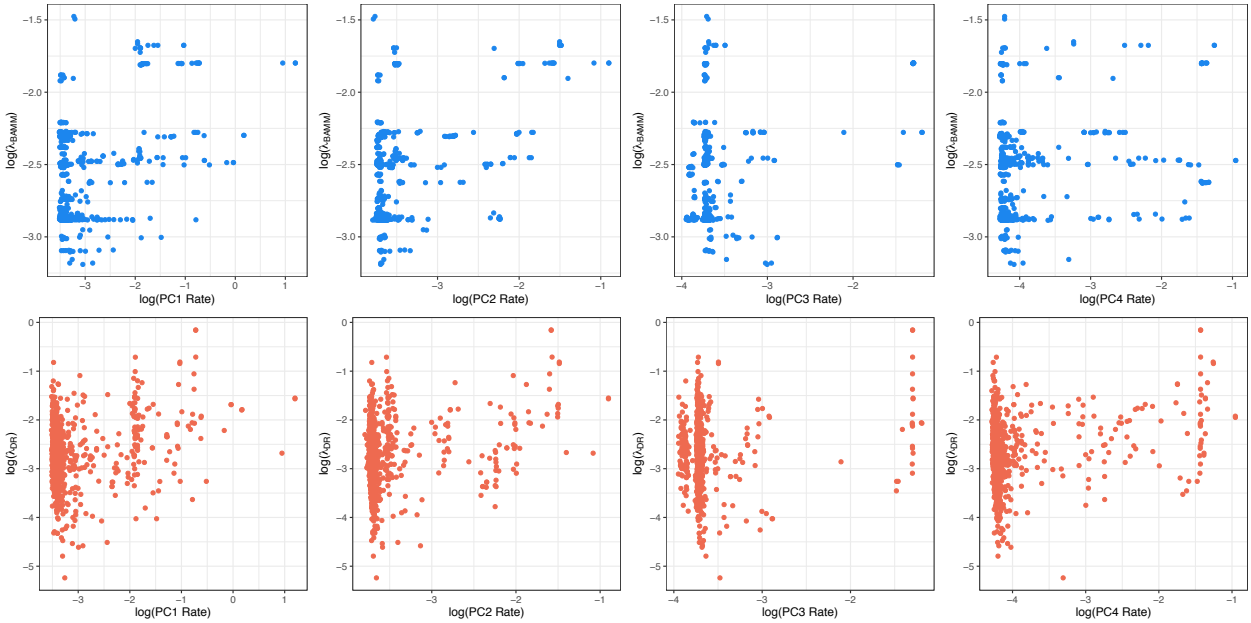

CHAPTER 3

Expansion And Packing Of Frog Morphospace Along The New World Latitudinal Diversity Gradient Revealed By Functional Traits

with Pascal O. Title and Daniel L. Rabosky

ABSTRACT

New World frogs show a steep latitudinal diversity gradient, but the underlying causes of this pattern are unknown. Whether the higher species richness in the tropics is accompanied by increased volume or denser packing of species in ecological niche space is also undetermined. Using morphological traits related to locomotion, habitat choice, and diet, we quantify how frog assemblage morphospace structure varies with species richness across the Americas. We find that morphospace volume increases and the distance between species in morphospace decreases with increasing species diversity, indicating that both niche expansion and packing occur. Overall, morphospace expansion accounts for the majority of species richness increases, but packing becomes the dominant pattern in comparisons between medium and high richness assemblages. This pattern sharply contrasts with the trend seen in birds, suggesting that the organization of morphospace and underlying patterns of phylogenetic and ecological structure may vary between clades along the latitudinal diversity gradient. Our study is an important step towards understanding the structure of frog morphospace along latitudinal and species richness gradients.

INTRODUCTION

One of the most striking and consistent patterns in the natural world, seen in nearly every major group of flora and fauna, is the stark difference in species richness between temperate and tropical regions (Hillebrand 2004). This pattern, known as the latitudinal diversity gradient (LDG), has been extensively studied, but the underlying mechanisms for its generation and maintenance remain undetermined despite intensive investigative effort and numerous hypotheses (Mittelbach et al. 2007; Fine 2015). A corollary to many of these hypotheses is that the gradient in species diversity will be accompanied by gradients in morphological and functional diversity. A classic framework for studying how niche utilization at the community or assemblage level might vary with species richness was presented by Macarthur (1965; Figure 3.1). Under this conceptual model, as species richness increases, the total volume of niche space used by a community could expand through addition of species that utilize niche space that is unavailable or unexplored at higher latitudes (MacArthur 1965). Niche packing adds species to a community by decreasing the distance between species in niche space without expanding niche volume through increasing specialization of species, increasing niche overlap, or filling of empty niche space (Klopfer and Macarthur 1961; Macarthur 1965). Of course niche expansion and packing are not mutually exclusive and both may occur as species richness increases (Pigot et al. 2016; Pellissier and Kissling 2018; Schumm et al. 2019).

There are theoretical reasons and empirical data to support that either or both patterns occur along the latitudinal gradient. Assemblage-level niche expansion could be facilitated by increased ecological opportunities in the tropics compared to temperate areas, a scenario that has been frequently hypothesized to be true (Schoener 1971). An example of this is the higher structural complexity in vertical vegetation could provide novel habitat options (Macarthur and

Macarthur 1961; Macarthur 1964; Proctor 1986). There is also the potential for expansion of trophic ecology and consumer diversity is indeed often tightly correlated with diversity at lower trophic levels in many systems (Schoener 1971; Kissling et al. 2007; Lewinsohn and Roslin 2008). On the other hand, there are many hypotheses that predict species in the tropic will be more ecologically specialized (Dobzhansky 1950; Pianka 1966), which would facilitate more species co-existing on the same volume of resources and generate a pattern of packing ecological space. Whether specialization increases in the tropics remains an unsettled question (Vázquez and Stevens 2004; Lewinsohn and Roslin 2008; Forister et al. 2015).

Few studies have explicitly attempted to simultaneously quantify niche expansion and packing along a gradient. Many of these studies have used birds as a study system, either along elevational gradients (Pigot et al. 2016; Schumm et al. 2019) or global gradients of net primary productivity (Pellissier and Kissling 2018) and found that both expansion and packing occur as species richness increases, with the latter being the dominant mechanism. A study comparing the structure of functional space between Europe and the more diverse eastern United States also found that species were packed within bounds of defined morphospace (Swenson et al. 2016). Given the limited taxonomic scope of these studies, the generality of these patterns across taxa and spatial scales remains unclear.

A major hurdle in establishing and linking patterns of functional diversity to those of species richness at large geographic scales is the lack of ecological data for species in many clades. Even when such data are available, categorization of species into functional categories or guilds can lead to results that are highly dependent on classification system and the detail of the underlying data (Vázquez and Stevens 2004). Morphology-based approaches offer an alternative to addressing these questions given that there is often a correlation between form and function

(Feilich and López-Fernández 2019). With these methods, functional traits are selected based on documented or putative ecomorphological relationships and used to construct a multidimensional trait space (morphospace) that can inform on how species utilize the ecological resources in relation to other species. This approach does have limitations in that it can be sensitive to the suite of selected morphological traits and apparent morphological redundancy of species may indicate that axes of ecological differentiation are not captured in the morphological data rather than ecological redundancy.

In this paper, we use morphological traits to investigate patterns of multidimensional morphospace structure in frog assemblages along the latitudinal diversity gradient in the Americas. Frogs present a useful study system for this question because they exhibit a strong latitudinal diversity gradient, such that tropical assemblages have an order of magnitude more species than a temperate assemblage. There is also a large literature on the ecomorphology of frogs that identifies traits relevant to locomotion (Zug 1972; Gomes et al. 2009; Lires et al. 2016), microhabitat usage (Gomes et al. 2009; Moen et al. 2013; Moen et al. 2016), and diet (Emerson 1985; Parmelee 1999; Moen and Wiens 2009), so that morphology can be treated as a coarse-scale proxy for ecological traits. We quantify how volume of morphological space (morphovolume) and distance between species in morphological space (morphodensity) covaries with species richness of frog assemblages to ask whether the high frog diversity of the tropics is mediated by niche expansion, niche packing or an interplay of the two.

MATERIALS AND METHODS

Geographic and trait data

All available digital distribution maps for frogs were obtained from IUCN Red List of Threatened Species (www.iucnredlist.org, accessed on 9 July 2018) and used to determine which species have native ranges falling within the Western Hemisphere. We retained maps of these 2,974 species and created a raster of species richness with 50km grid resolution in order to tally species richness for subsequent spatial analyses.

We retrieved a dataset of morphological traits of frogs from Larson et al. (Chapter 2). This dataset includes 11 linear external morphological traits: snout-vent length, head width, head length, internarial distance, interorbital distance, eye length, eye to naris distance, naris to snout distance, antebrachial length, femur length, and tibiofibula length. These measurements were selected by Larson et al. (Chapter 2) because they are relevant to microhabitat use (Gomes et al. 2009; Moen et al. 2013; Moen et al. 2016), locomotion (Zug 1972; Gomes et al. 2009; Lires et al. 2016) and diet (Emerson 1985; Parmelee 1999; Duellman 2005; Moen and Wiens 2009).

We parsed this dataset to retain only species whose native ranges fall within the Western Hemisphere by comparing it to the species list generated with IUCN range maps. To address inconsistent taxonomy between the IUCN and morphological datasets, we utilized the synonymMatch function within the R package *rangeBuilder* v. 1.5 (Rabosky et al. 2016). This resulted in morphological data for 434 species of Western Hemisphere frogs (~18% of Western Hemisphere species) with each species represented by a mean of 4 individuals (range: 1 – 9). For these species, we created another raster of species richness with 50km grid resolution with range maps from IUCN. We hereafter refer to the set of species located in a grid cell as an assemblage. For all subsequent spatial analyses, we only consider assemblages for which we have

morphological data of at least 40% of the total species. We refer to the number of species per cell with trait data as the sampled species richness to distinguish it from the total species richness as determined using IUCN distribution data.

Analyses

We performed a principal components analysis (PCA) on the correlation matrix of log-transformed species means to reduce dimensionality. We then normalized each PC axis to have a mean of 0 and standard deviation of 1 in order to give equal weighting to each axis during quantification of morphospace. Previous studies have demonstrated that axes with low explanatory power of morphological variance are still informative about ecological differentiation between species and that normalization is an important methodological step (Miles and Ricklefs 1984; Pigot et al. 2016).

We calculated the amount of morphospace occupied by each assemblage of frogs as the volume of a minimum convex polygon (MCPV), also referred to as a convex hull. Since hulls can only be reliably estimated when the number of data points (species per cell in this study) is greater than the number of dimensions, we retained only the first four PC axes for calculation of this metric and only considered the structure of morphospace of grid cells with an sampled richness of five species or greater. These four PC axes account for 96.5% of the morphological variation (Table S3.1). We used the convhulln function in the R package *geometry* v. 0.4.4 (Habel et al. 2019) to construct four-dimensional minimum convex polygons and calculate their volume. We quantified morphodensity by calculating mean nearest neighbor distance in Euclidean trait space with all eleven PC axes (MNND) using the R package *spatstat* v. 1.61.0 (Baddeley et al. 2015).

We also examined the evenness of species spacing within trait space using the functional evenness index (FEve) to understand whether species are clumped in morphospace or evenly distributed (Figure 3.1). This index is independent of species richness and calculates the regularity of branch lengths in a minimum spanning tree connecting species in multidimensional trait space and ranges from 0 (low evenness) to 1 (high evenness) (Villéger et al. 2008). We used the *dispRity* R package v. 1.3.1 to calculate FEve (Guillerme 2018).

Since MCPV and MNND can be sensitive to species richness, we compared observed values for all of our metrics to what we would expect given the species richness gradient. Null models were generated by randomly permuted PC data across species and recalculating our focal metrics (n = 999 replicates). We prefer this approach of permuting traits to randomizing species distributions because it maintains observed species richness, interspecific distribution patterns, and range continuity. For each of our three morphospace structure metrics, we calculated standardized effect size (SES) according to the following equation:

$$SES = \left(\frac{Metric_{obs} - Metric_{null}}{\sigma Metric_{null}}\right)$$

in which $Metric_{obs}$ is the observed value of the particular metric, $Metric_{null}$ is the mean value of the metric from the null model replicates, and $\sigma Metric_{null}$ is the standard deviation of the null distribution for that metric. Standardized effect size values were considered significant if the observed value of the metric was outside the 2.5 – 97.5% quantiles of the null distribution (Swenson 2014).

We regressed each of the three metrics, as well as the SES, against sampled richness, noting again that sampled and "true" richness are highly correlated (Fig S3.2). We accounted for spatial autocorrelation by applying simultaneous autoregressive (SAR) models (Kissling and Carl 2008) using the *spdep* R package v. 1.1.3 (Bivand and Wong 2018). We tested a range of

possible neighborhood sizes (50 km – 300 km in 50 km steps) and weighting styles before applying the model with the minimum residual spatial autocorrelation to our data (Table S3.2; Figure S3.1).

Since both morphospace expansion and packing can occur simultaneously, we quantified the relative contributions of each to increases in species richness by using the approach developed by Pigot et al. (2016). This method compares two assemblages of differing species richness and computes the number of species from the richer assemblage that could be contained in the morphovolume of the more depauperate assemblage. The iterative ("greedy search") algorithm sequentially removes species from the more diverse assemblage until its calculated morphovolume is equal to or less than that of the less diverse one. Species are removed based on their contributed volume increase in descending order and only unique species are considered; species shared between assemblages are not removed. The number of species removed from the richer assemblage represents the number of species that were added via morphovolume expansion and the remaining increase in richness is attributable to morphospace packing, ie increased morphodensity.

With this algorithm, we quantified the percentage of species richness increase attributable to morphovolume expansion by comparing assemblages from four richness categories: very low (5 species), low (10 species), medium (18 to 30 species), and high (40 to 68 specices). For the first three richness categories, we selected 20 unique assemblages, 10 from temperate areas and 10 from tropical areas. There are not any assemblages in the temperate zone with 40 species, so we have 10 tropical assemblages for this category (Figure 3.6). We performed all pairwise comparisons between assemblages in consecutive richness categories. We also compared very low richness assemblages against high richness ones to get an overall perspective.

RESULTS

Species richness and sampling

Our morphological dataset included measurements for 434 frog species (~18%) of the 2,974 species present in the Western Hemisphere, our geographical study area (IUCN). To limit the effects of incomplete sampling, we discarded any 50 km x 50 km grid cells for which we had sampled less than 40% of the recorded frog species. After additionally filtering out cells with a sampled richness less than five, our dataset consisted of 8,178 50 km^2 grid cells that we refer to as assemblages.

We found that sampled richness and total richness are tightly correlated ($r = 0.98$; Figure S3.2) and both show a strong latitudinal gradient (Figure 3.2). The mean sampling fraction for assemblages was 65%. There was a geographic bias to sampling depth with assemblages in higher northern latitudes being more completely sampled than assemblages at equivalent southern latitudes (Figure S3.3b), and with species rich communities tending towards lower sampling fractions (Figure S3.3a). We examined the relationship between each metric and the per-cell sampling fraction to investigate whether our results were driven by sampling. We did not detect any signal to suggest that our results are due to sampling artifacts (Figure S3.4).

Morphovolume

Morphovolume increased linearly with sampled species richness (Figure 3.3) and correcting for spatial autocorrelation with a simultaneous autoregressive model indicated that sampled species richness is a very strong predictor of morphovolume ($Z = 102.27$, $P < 0.001$). We also observed a strong inverse relationship between morphovolume and latitude, although the peak of the morphovolume curve was slightly south of the equator and therefore offset of

both total and sampled species richness maximums. For the most part, observed morphovolumes did not significantly differ from the null expectation, although 385 assemblages occupied a significantly greater volume of morphospace than expected by chance. These assemblages all have relatively low sampled richness, ranging from five to 33 species and are mostly located in low to mid-latitudes.

Using a linear SAR model, we found a statistically significant negative relationship between SES of MCPV and sampled species richness ($Z = -3.03$, $P < 0.01$), although the slope is shallow (Table S3.3). The relationship between SES of MCPV and latitude is complex and multimodal (Figure 3.3). Two peaks of values occur on either side of a relative dip at the equator and it is in these two peaks that most of the significant SES for MCPV are located. There appears to be a trend of increasing values from mid to high latitudes. Many of the significant SES values are observed in assemblages from the Yucatan Peninsula of Mexico. Other bands of unexpectedly large MCPV values appear to occur on the northern and southern edges of the Amazon rainforest.

Morphodensity

Mean nearest neighbor distance decreases with increasing sampled species richness ($Z = -48.54$, $P < 0.001$). There is a positive correlation between absolute latitude and MNND ($r = 0.7$) with minimum observed values of MNND occurring slightly south of the equator. On average, assemblages north of the equator are less densely packed in morphospace compared to assemblages south of the equator. From the equator through the southern mid-latitudes, MNND values generally remain small with a few outliers before rising. In contrast, MNND has a more pronounced and steady rise from the equator towards the high northern latitudes.

As with MCPV, most assemblages do not have MNND values that differ from the null expectation, although there are 161 assemblages that have higher MNND values than expected and 76 with values lower than expected. The highest values of SES for MNND values are observed at low and high latitudes. Values that are statistically greater than expected occur at low and high latitudes while statistically low values happen at low to mid-latitudes. Examining SES values for MNND against sampled species richness shows that all cases of smaller than expected MNND occur in relatively species poor assemblages. Cases of greater than expected MNND are seen in low to medium richness assemblages.

Morphological evenness

Functional evenness remains relatively consistent and high as assemblage richness varies, indicating that species are regularly spaced in most assemblages. The SAR model detected a significant negative relationship between FEve and species richness ($Z = 7.71$, $P < 0.001$), but the slope of the fitted model is nearly zero (Table S3.3). There is substantial variation between low richness assemblages (less than 20 species), with some higher values and a long tail of lower values. These lower values indicate that species within those assemblages are less regularly placed in morphospace. There appears to be a slight trend of decreasing FEve moving from high southern latitudes up to high northern latitudes. Above the equator, there is more heterogeneity in FEve values between assemblages at the same latitude, whereas values are more consistent below the equator.

Most assemblages have FEve values that do not significantly differ from the null expectations, indicating that most groups of frogs are not more or less clustered in morphospace than expected by chance. Some low richness assemblages ($n = 390$) are less evenly spaced and

some (n = 203) more evenly spaced than expected by chance. The assemblages in the former group are located mostly at high southern latitudes, whereas the latter are at high northern latitudes. Like with FEve, there is a negative relationshionsip between SES of FEve and species richness ($Z = 7.71$, $P < 0.001$), but the slope is nearly zero.

Relationships between metrics

Since morphovolume is tightly correlated with species richness, the shape of the pairwise relationships between MCPV and the other two metrics, MNND and FEve, are nearly identical to what is observed between the two metrics and sampled species richness (Figure S3.5). In other words, assemblages that occupy large areas of morphovolume, on average, are densely, but regularly packed in that space, whereas assemblages that fill smaller areas in morphospace show high variation in both density and evenness.

We considered the overlap of assemblages with significant MCVP and assemblages with significant SES for MNND and found that there were only five assemblages that fit these criteria. For all five, the SES for MNND and MCPV were positive indicating that these assemblages occupied more morphovolume and were less densely packed than expected by random sampling. These were species poor assemblages in low to mid latitude locations. We find a similar pattern of few assemblages with significant SES values for MCPV and FEve (n = 1), and MNND and FEve (n = 6). The lone assemblage in the first comparison is designated as significant due to the regularity of species arrangement in the large morphovolume. The latter set includes one assemblage with low density and uneven spacing, while the rest have low morphodensity and high evenness.

Relative contributions of expansion and packing

We found that expansion accounted for the large majority (mean: 88%; range: 70% - 100%) of species richness increase when comparing the highest richness communities (≥40 species) to very low richness communities (five species). Comparisons between assemblages of very low and low (10 species) sampled richness also showed a dominant role of morphovolume expansion (Figure 3.6) with expansion accounting for approximately 80% of the difference in species richness in these comparisons. In some pairwise comparisons, this value reached 100%, indicating that all species added to the community contributed to morphovolume expansion. Although expansion was still the most common pattern observed in comparisons between low to medium assemblages, its dominance was diminished, accounting for a mean 58% of species richness increases with high variance (range: 0% - 100%). The overall pattern was reversed when high richness assemblages were compared to medium richness ones and expansion only accounted for 40% of additional richness on average with a range of 0% to 100%. This means that packing becomes a more prevalent pattern in communities with high species richness. These patterns appear to be consistent irrespective of whether the two focal communities are in the same or different biomes, suggesting that they are not driven by differences in the taxonomic composition of temperate and tropical communities.

DISCUSSION

We tested how the structure of frog multidimensional morphospace varies in relation to species richness and latitude in the Western Hemisphere under the conceptual framework that increases in species richness should be accompanied by increases in occupied niche volume, increased density of species in a static niche volume, or a combination of both geometric patterns

(Macarthur 1965). Our results indicate that both morphospace expansion and packing accompany increases in frog species richness and that the relative importance of each varies along the richness gradient. However, expansion is the dominant pattern, and is by far the greatest difference between communities with low diversity and those with moderate to high diversity.

Recent studies on richness gradients in birds have found that morphospace packing is consistently the main pattern underlying species richness increases, although morphospace expansion is also detected (Pigot et al. 2016; Pellissier and Kissling 2018; Schumm et al. 2019). This pattern was consistently recovered despite the differences in spatial, taxonomic, and trait data employed by these studies. We find a strikingly different pattern in which increases in frog assemblage richness is strongly associated with increases in the volume of occupied morphospace. This provides evidence against a general pattern in morphospace structure across taxa underlying shared species richness gradients. Interestingly, we observe that this reverses in comparisons of high richness assemblages to medium richness ones and species are largely added *within* occupied morphospace, with minimal expansion. This difference in how additional species are accommodated may indicate an initial increase in morphologically distinct species until saturation of morphotypes is achieved and further richness occurs through addition of morphologically redundant species. We note though that this approach to quantifying the relative contributions of expansion and packing does not consider absolute morphospace position of assemblages, so it is possible that assemblages may occupy different areas in global morphospace without overlap.

It is also important to note that an apparent accumulation of morphologically redundant species does not necessarily signify that these species are ecologically equivalent. The mean position of a species in morphospace provides an approximation of the species' ecological role,

absolutely and in relation other species, but may not have suitable power to distinguish fine-scale resource partitioning. Additionally, our dataset doesn't permit us to distinguish the role of specialization or increased overlap in the increased density of species. This is because without additional information on intraspecific variability, position in morphospace does not inform about the breadth of ecological space used by the species, which is essential to determining a species' degree of specialization and the amount of overlap in ecological space between species. For example, an extreme position in morphospace could indicate the potential to utilize a novel ecological resource, but does not preclude the species from overlapping in ecological space with more centrally located species (Bellwood et al. 2006); such overlap is a function of intraspecific variability, which need not have any relationship to the mean position of a species in morphospace (Bolnick et al. 2003). In the same way, two species that are close in morphological space, indicating similar morphologies, are not guaranteed to have high ecological overlap. Position in morphospace is also highly dependent upon the selected functional traits. Due to these constraints, the frequency and magnitude of morphological packing might overestimate the prevalence of ecological niche packing.

While we find a strong positive correlation between species richness and assemblage morphovolume, the observed patterns are largely consistent with our null model. However, it is still informative that volume increased with rising species richness since a lack of morphovolume expansion along a species richness gradient would indicate that species in the low richness communities already occupy the full range of morphologies that are accessible to frogs based on physical and evolutionary constraints of the frog body plan. In this extreme scenario, the hard bounds of morphospace would have been reached already, precluding further expansion by morphological innovation and the only way to increase species richness would be

to add species within the boundaries of this predefined space. Our method of quantifying morphovolume as the volume of a minimum convex polygon would detect this potential pattern as a constant morphovolume value across all assemblages, regardless of species richness. Instead we find that low richness assemblages occupy a subset of this global morphospace and niche expansion does occur along the LDG. Interestingly, the peak values of morphovolume do not correspond to peak values of either sampled or total richness.

We also found that the density of species in morphospace decreases with increasing species richness at a rate that was mostly consistent with our null model. Interpreted in isolation, this result suggests that morphological similarity is not a major constraint on assemblage richness of frogs along this latitudinal gradient at this spatial scale. However, the other metric that quantifies the positioning of species within morphospace in relation to others, functional evenness, was decoupled from species richness and was nearly constant across all latitudes and richnesses. The high and consistent value of functional evenness across all assemblages means that species were regularly spaced within the morphovolume utilized by each assemblage and suggests that limiting similarity could be a strong force in the structuring of frog communities. This is not inconsistent with the MNND result. Instead, it suggests that the magnitude of the allowable similarity is variable, so that species in some assemblage are able to be closer together in trait space, but there is a limit to this proximity. It is also plausible that these patterns of distance between species in morphospace do not directly connect to underlying interspecific interactions and ecological processes given the relatively broad spatial scale at which assemblages are defined, 50 km x 50 km map grid cells.

A previous study on patterns of functional diversity in all birds along global gradients of species richness and net primary productivity used standardized effect sizes of functional volume

to infer the presence or absence of both expansion and packing (Pellissier and Kissling 2018). In that framework, a significant negative SES value was interpreted as evidence of increased packing without directly measuring whether species in such assemblages were indeed closer in trait space. We cannot test whether this assumption is true in our dataset or not since we did not detect assemblages with morphovlumes that were significantly smaller than expected. We can however say that mean nearest neighbor distances, a direct measure of how closely species are packed in morphospace, indicated that many assemblages had significantly higher morphodensity than expected. For our dataset at least, species can be densely packed within morphospace without occupying a significantly small morphovolume. In other words, if we had taken the approach of using SES of MCPV to infer patterns of expansion and packing within our dataset, we would not have detected any assemblages with significant packing. In light of this, we recommend calculating a metric that directly measures the distance between species in functional space if characterizing patterns of species density in trait space is one of the research goals.

ACKNOWLEDGEMENTS

We thank Greg Schneider for access to specimens (University of Michigan Museum of Zoology) and Monica West, Erich Eberhard, Abraham Weiner, and Yoshio Wagner for helping collect data. We are grateful to Ivan Prates for helpful discussions. JGL was supported by a NSF Graduate Research Fellowship and a University of Michigan Rackham Predoctoral Fellowship.

DATA AVAILABILITY

Raw morphological measurements used in this study are available on Deep Blue Data,

https://doi.org/10.7302/4rf6-fk68

REFERENCES

Baddeley, A., E. Rubak, and R. Turner. 2015. Spatial Point Patterns: Methodology and Applications with {R}. Chapman and Hall/CRC Press, London.

Bellwood, D. R., P. C. Wainwright, C. J. Fulton, and A. S. Hoey. 2006. Functional versatility supports coral reef biodiversity. Proceedings of the Royal Society B: Biological Sciences 273:101–107.

Bivand, R., and D. W. S. Wong. 2018. Comparing implementations of global and local indicators of spatial association. TEST 27:716–748.

Bolnick, D. I., R. Svanba, J. A. Fordyce, L. H. Yang, J. M. Davis, C. D. Hulsey, and M. L. Forister. 2003. The Ecology of Individuals : Incidence and Implications of Individual Specialization. American Naturalist 161:1–28.

Dobzhansky, T. 1950. Evolution in the tropics. American Scientist 38:209–221.

Duellman, W. E. 2005. Cusco Amazonico. Comstock Pub. Associates, Ithaca, NY.

Emerson, S. B. 1985. Skull Shape in Frogs : Correlations with Diet. Herpetologica 41:177–188.

Feilich, K. L., and H. López-Fernández. 2019. When Does Form Reflect Function ? Acknowledging and Supporting Ecomorphological Assumptions. Integrative and Comparative Biology 59:358–370.

Fine, P. V. A. 2015. Ecological and Evolutionary Drivers of Geographic Variation in Species Diversity. Annual Review of Ecology and Systematics 46:369–392.

Forister, M. L., V. Novotny, A. K. Panorska, L. Baje, Y. Basset, and P. T. Butterill. 2015. The global distribution of diet breadth in insect herbivores. Proceedings of the National Academy of Sciences USA 112:442–447.

Gomes, F. R., E. L. Rezende, M. B. Grizante, and C. A. Navas. 2009. The evolution of jumping performance in anurans : morphological correlates and ecological implications. European Society for Evolutionary Biology 22:1088–1097.

Guillerme, T. 2018. dispRity : A modular R package for measuring disparity. Methods in

Ecology and Evolution 2018:1755–1763.

Habel, K., R. Grasman, R. B. Gramacy, P. Mozharovskyi, and D. C. Sterratt. 2019. geometry: Mesh Generation and Surface Tessellation.

Hillebrand, H. 2004. On the Generality of the Latitudinal Diversity Gradient. American Naturalist 163:192–211.

Kissling, D. W., C. Rahbek, and K. Böhning-Gaese. 2007. Food plant diversity as broad-scale determinant of avian frugivore richness. Proceedings of the Royal Society B: Biological Sciences 274:799–808.

Kissling, W. D., and G. Carl. 2008. Spatial autocorrelation and the selection of simultaneous autoregressive models. Global Ecolog and Biogeography 17:59–71.

Klopfer, P. H., and R. H. Macarthur. 1961. On the Causes of Tropical Species Diversity: Niche Overlap. American Naturalist 95:223–226.

Lewinsohn, T. M., and T. Roslin. 2008. Four ways towards tropical herbivore megadiversity. Ecology letters 11:398–416.

Lires, A. I., I. M. Soto, and R. O. Gómez. 2016. Walk before you jump : new insights on early frog locomotion from the oldest known salientian. Paleobiology 42:612–623.

Macarthur, R. H. 1964. Environmental Factors Affecting Bird Species Diversity. American Naturalist 98:387–397.

Macarthur, R. H. 1965. Patterns of Species Diversity. Biological Reviews 40:510–533.

Macarthur, R. H., and J. W. Macarthur. 1961. On Bird Species Diversity. Ecology 42:594–598.

Miles, D. B., and R. E. Ricklefs. 1984. The correlation between ecology and morphology in deciduous forest passerine birds. Ecology 65:1629–1640.

Mittelbach, G. G., D. W. Schemske, H. V Cornell, A. P. Allen, J. M. Brown, M. B. Bush, S. P. Harrison, et al. 2007. Evolution and the latitudinal diversity gradient: speciation, extinction and biogeography. Ecology letters 10:315–31.

Moen, D. S., D. J. Irschick, and J. Wiens. 2013. Evolutionary conservatism and convergence both lead to striking similarity in ecology, morphology and performance across continents in frogs. Proceedings of the Royal Society B: Biological Sciences 280:20132156.

Moen, D. S., H. Morlon, and J. J. Wiens. 2016. Testing convergence versus history: convergence dominates phenotypic evolution for over 150 million years in frogs. Systematic Biology 65:146–160.

Moen, D. S., and J. J. Wiens. 2009. Phylogenetic evidence for competitively driven divergence: Body-size evolution in caribbean treefrogs (Hylidae: Osteopilus). Evolution 63:195–214.

Parmelee, J. R. 1999. Trophic Ecology of a Tropical Anuran Assemblage. Scientific Papers Natural History Museum the University of Kansas 11:1–59.

Pellissier, V., and W. D. Kissling. 2018. Niche packing and expansion account for species richness – productivity relationships in global bird assemblages. Global Ecolog and Biogeography 27:604–615.

Pianka, E. R. 1966. Latitudinal Gradients in Species Diversity : A Review of Concepts. American Naturalist 100:33–46.

Pigot, A. L., C. H. Trisos, J. A. Tobias, and A. L. Pigot. 2016. Functional traits reveal the expansion and packing of ecological niche space underlying an elevational diversity gradient in passerine birds.

Proctor, J. 1986. Tropical rain forest : structure and function. Progress in Physical Geography 10:383–400.

Rabosky, A. R. D., C. L. Cox, D. L. Rabosky, P. O. Title, I. A. Holmes, A. Feldman, and J. A. Mcguire. 2016. Coral snakes predict the evolution of mimicry across New World snakes. Nature Communications 7:1–9.

Schoener, T. W. 1971. Large-Billed Insectivorous Birds : A Precipitous Diversity Gradient. Condor 73:154–161.

Schumm, M., A. E. White, K. Supriya, and T. D. Price. 2019. Ecological limits as the driver of bird species richness patterns along the east Himalayan elevational gradient. American Naturalist.

Swenson, N. G. 2014. Functional and Phylogenetic Ecology in R. Springer, New York, New York.

Swenson, N. G., M. D. Weiser, L. Mao, S. Normand, M. Á. Rodríguez, L. Lin, M. Cao, et al. 2016. Constancy in Functional Space across a Species Richness Anomaly. American Naturalist 187.

Vázquez, D. P., and R. D. Stevens. 2004. The latitudinal gradient in niche breadth: concepts and evidence. The American naturalist 164:E1–E19.

Villéger, S., N. W. H. Mason, and D. Mouillot. 2008. New multidimensional functional diversity indices for a multifaceted framework in functional ecology. Ecology 89:2290–2301.

Zug, G. R. 1972. Anuran Locomotion : Structure and Function . I . Preliminary Observations on

Relation between Jumping and Osteometrics of Appendicular and Postaxial Skeleton. Copeia 1972:613–624.

Figure 3.1: Conceptual framework for how morphospace structure can vary with increased species richness. Blue dots represent species.

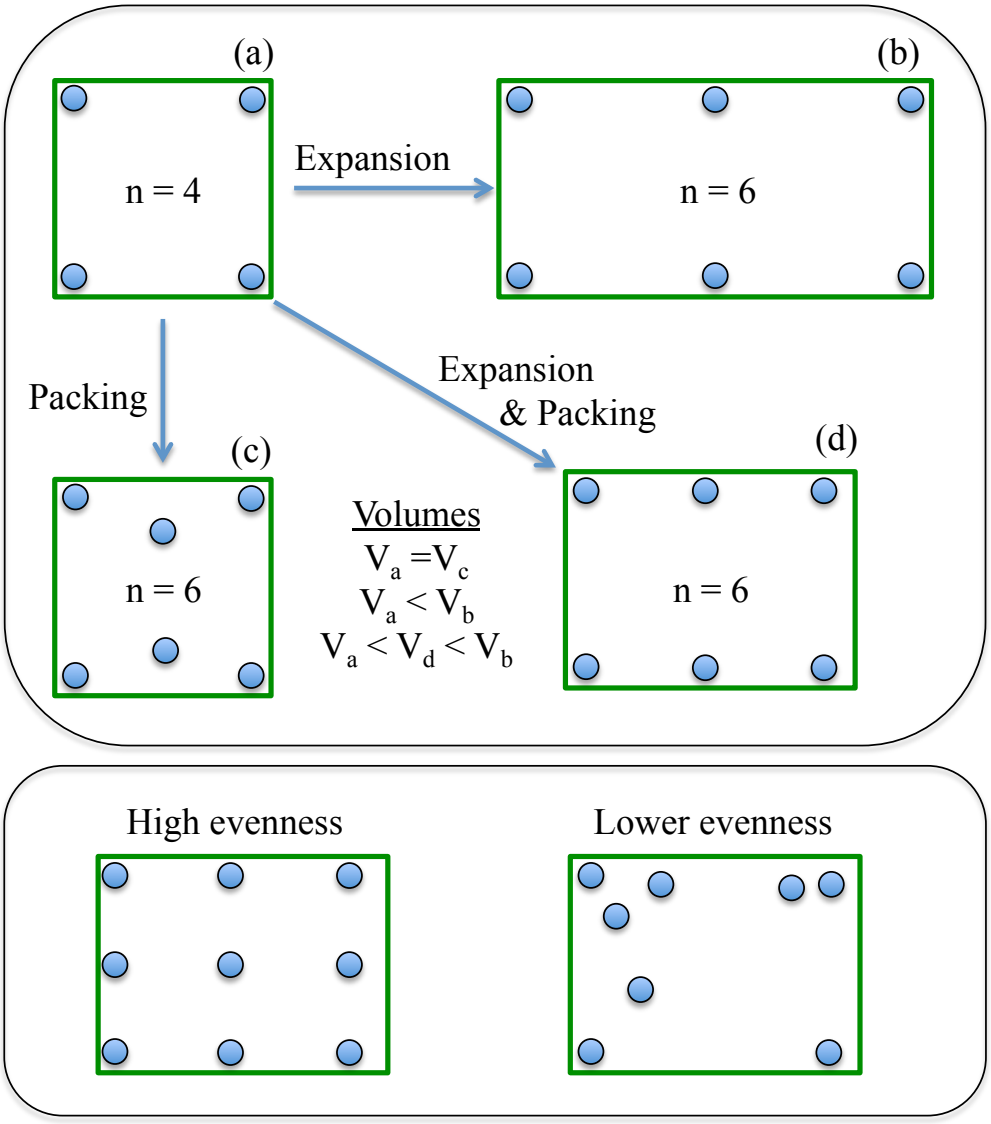

Figure 3.2: Spatial patterns of frog species richness in the Western Hemisphere. (*a*) Spatial distribution of all frog species with range information available from IUCN (n = 2,974 species). (*b*) Spatial distribution of the species with morphological data used in this study (n = 434 species) showing a strong correlation to distributional patterns of total richness in *a*. (*c*) Relationship between total frog species richness and latitude of 50 km x 50 km map grid cells. (*d*) Relationship between sampled frog species richness of assemblages with respect to latitude. Locally-weighted regressions shown by green lines in (*c*) and (*d*).

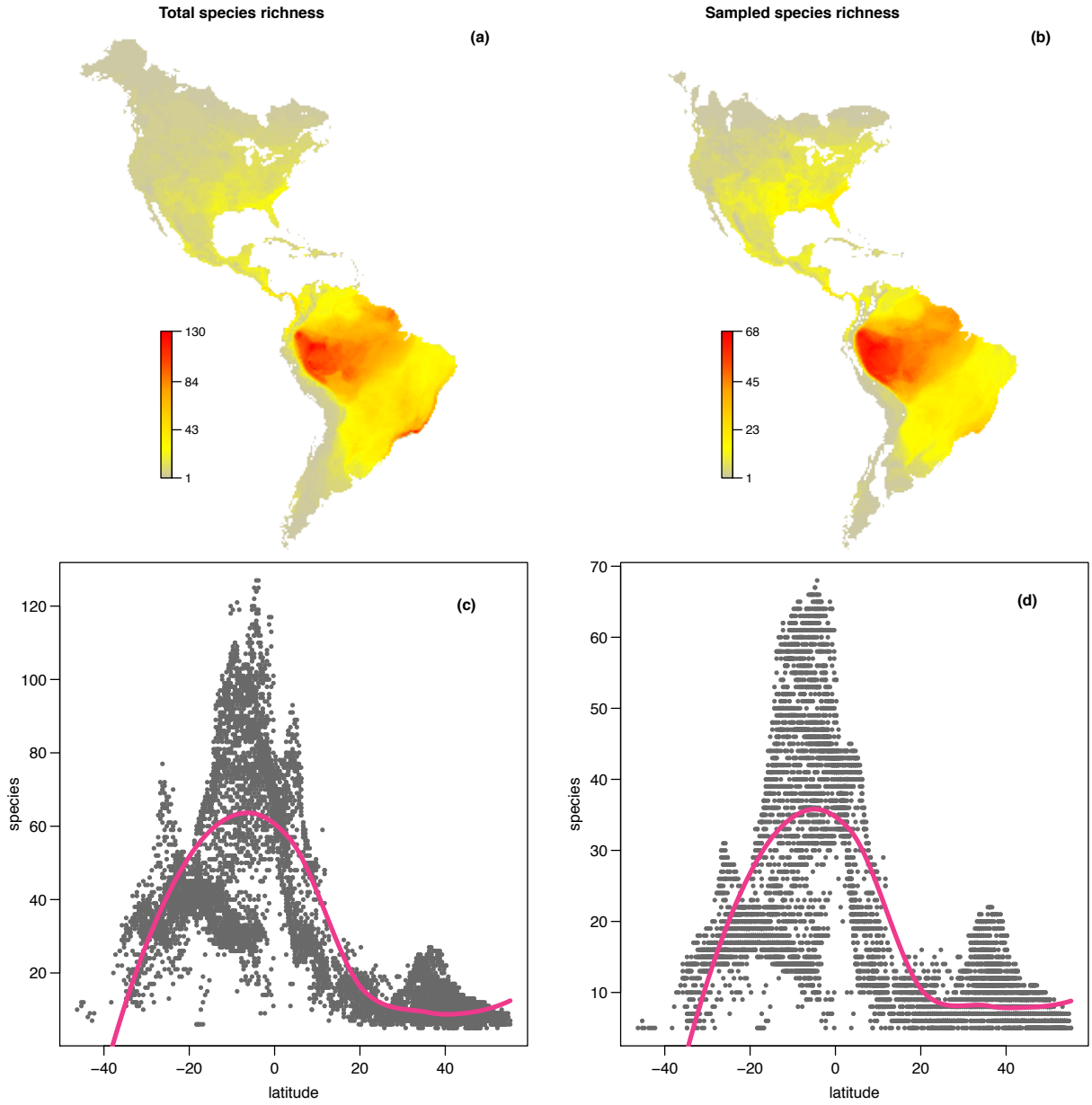

Figure 3.3: Morphospace expansion occurs along the latitudinal diversity gradient. Scatterplots showing the relationship between morphovolume (MCPV) and (*a*) sampled species richness and (*b*) latitude. Scatterplots showing the relationship between standard effect size of morphovolume (SES of MCPV) and (*d*) sampled species richness and (*e*) latitude. Maps showing the spatial distribution of (*c*) MCPV and (*f*) SES of MCPV. Blue indicates an assemblage that has a significant SES of MCPV.

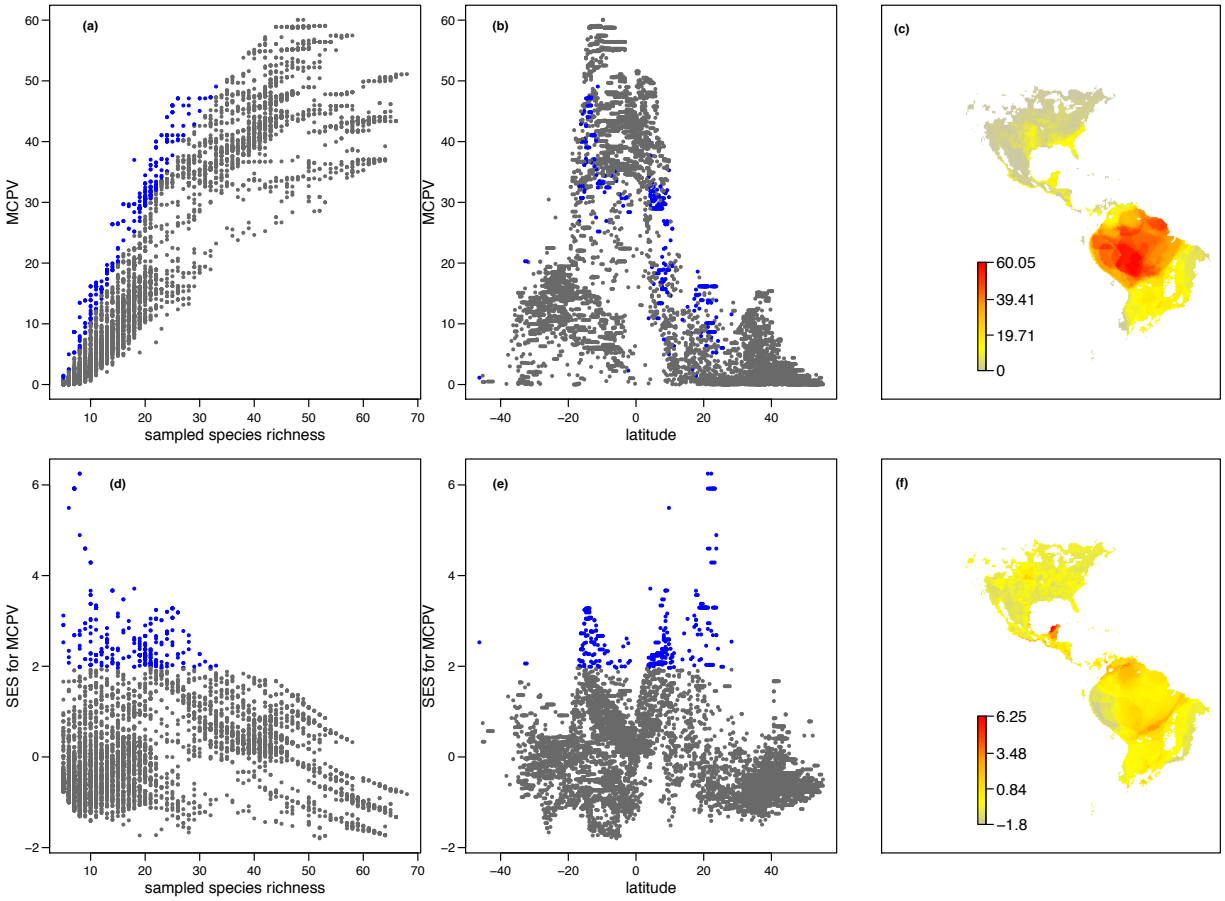

Figure 3.4: Morphospace packing occurs along the latitudinal diversity gradient. Scatterplots showing the relationship between morphodensity, measured as mean nearest neighbor density (MNND), and (*a*) sampled species richness and (*b*) latitude. Scatterplots showing the relationship between standard effect size of morphodensity (SES of MNND) and (*d*) sampled species richness and (*e*) latitude. Maps showing the spatial distribution of (*c*) MNND and (*f*) SES of MNND. Blue indicates an assemblage that has a significant SES of MNND.

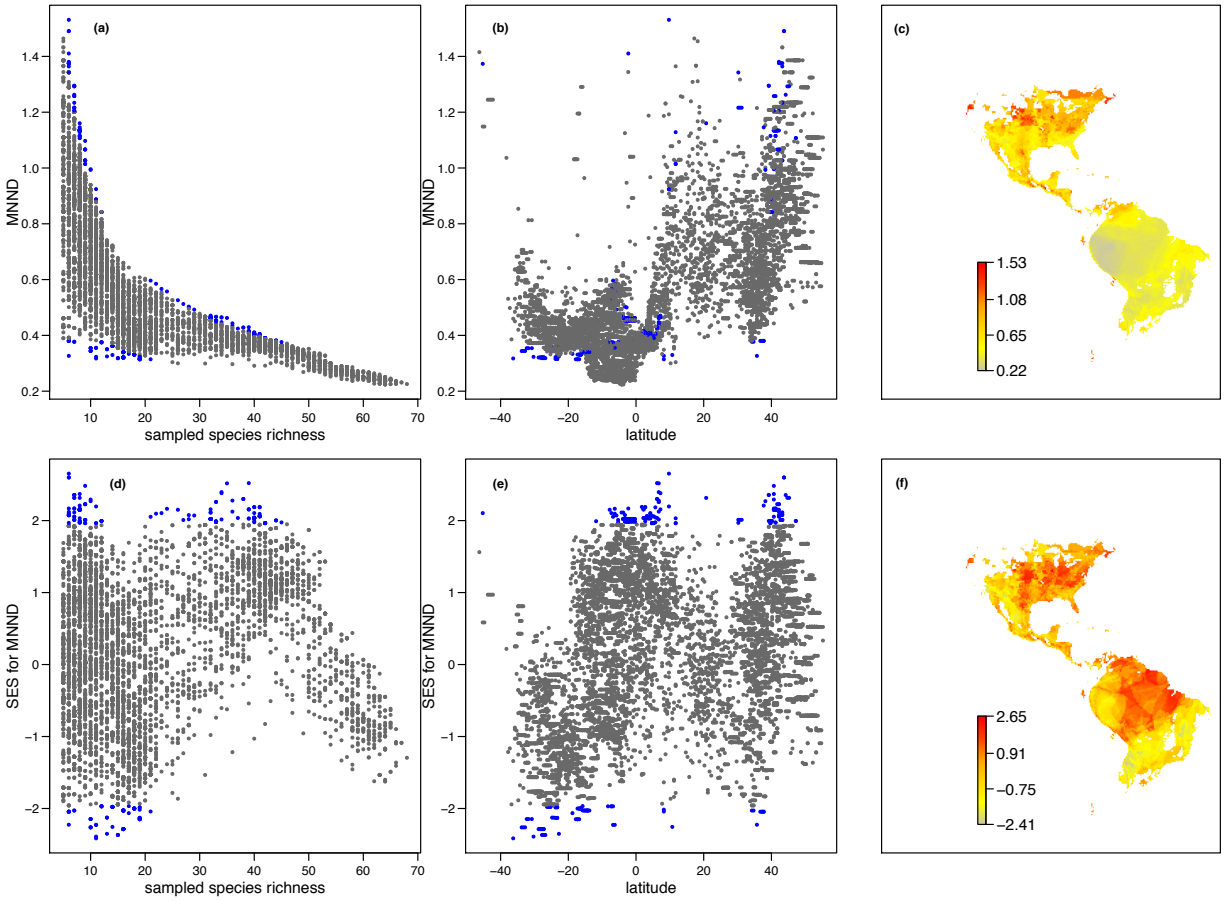

Figure 3.5: Morphospace evenness remains consistent along the latitudinal diversity gradient. Scatterplots showing the relationship between functional evenness (FEve) and (*a*) sampled species richness and (*b*) latitude. Scatterplots showing the relationship between standard effect size of functional evenness (SES of FEve) and (*d*) sampled species richness and (*e*) latitude. Maps showing the spatial distribution of (*c*) FEve and (*f*) SES of Feve. Blue indicates an assemblage that has a significant SES of Feve.

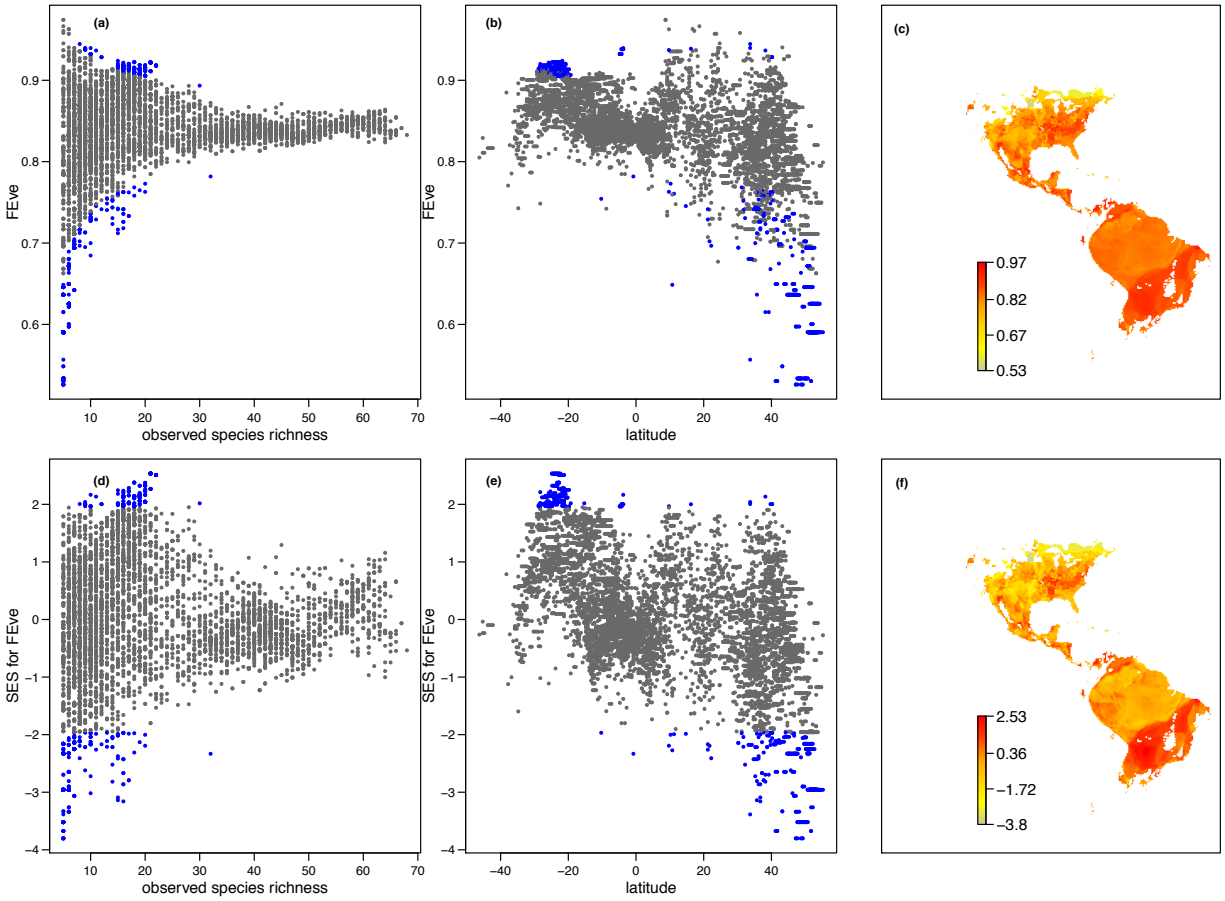

Figure 3.6: Relative contributions of expansion and packing of morphospace with increasing frog species richness. Map colors represent spatial patterns of sampled species richness. Plotted are 10 unique assemblages with high species richness and 20 unique assemblages for each of the other three richness categories. Violin plots show results of pairwise comparisons of assemblages and quantification of the proportion of species richness difference attributable to morphospace expansion. Results are displayed based on the species richness categories involved in the comparison (top) and the biome from which the assemblages were drawn (bottom). For inter-biome comparisons, the location of the assemblage with less species is given first.

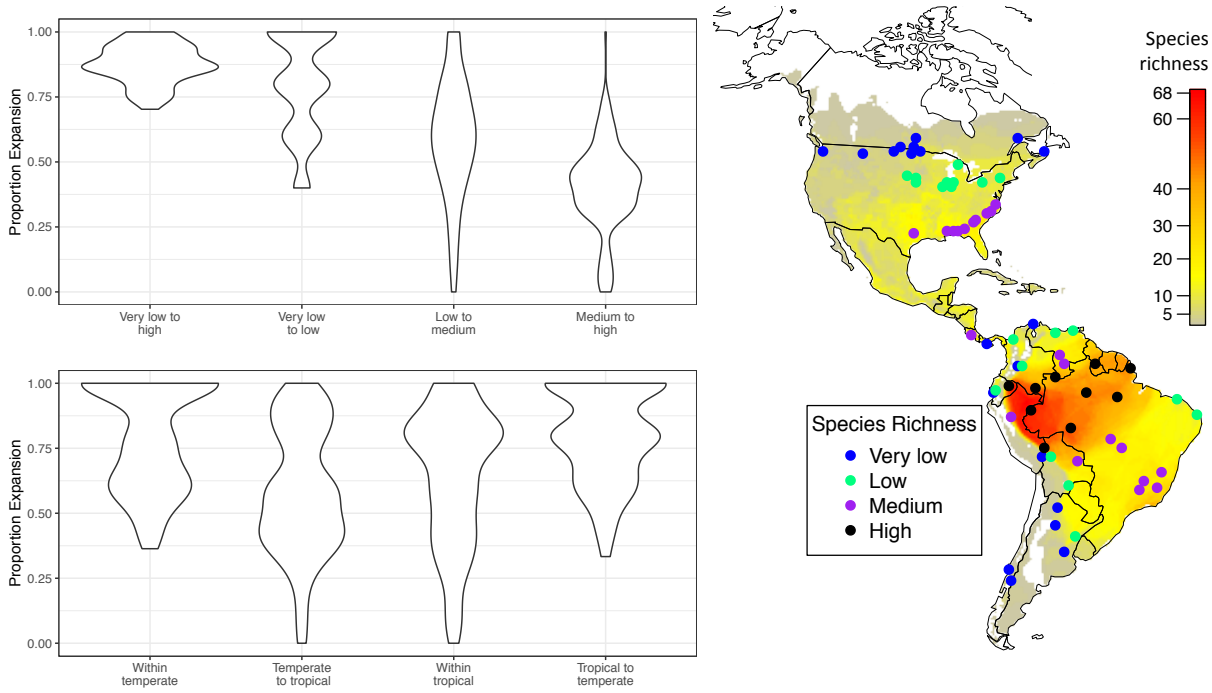

Table S3.1: Loadings of the eleven log-transformed morphological traits for the principal component (PC) axes.

	PC1	**PC2**	**PC3**	**PC4**	**PC5**	**PC6**	**PC7**	**PC8**	**PC9**	**PC10**	**PC11**
Snout to vent length	0.31	0.22	-0.13	0.12	-0.28	0.01	0.00	-0.19	0.84	-0.04	-0.04
Head width	0.31	0.17	-0.02	0.26	0.06	0.18	0.15	-0.54	-0.29	0.56	-0.27
Head length	0.32	0.12	-0.10	-0.03	0.21	0.10	-0.02	-0.45	-0.22	-0.74	0.14
Internarial distance	0.26	-0.70	0.26	0.42	-0.15	-0.37	-0.13	-0.11	0.00	-0.08	-0.02
Interorbital distance	0.30	-0.01	0.48	0.07	-0.13	0.39	0.61	0.32	-0.02	-0.11	0.10
Eye length	0.31	-0.01	-0.14	0.12	0.83	-0.21	0.13	0.28	0.20	0.11	0.02
Eye to naris distance	0.30	0.03	0.49	-0.30	0.14	0.30	-0.67	0.05	0.06	0.13	0.01
Naris to snout distance	0.27	-0.53	-0.58	-0.30	-0.10	0.43	0.01	0.11	-0.02	0.09	0.01
Antebrachial length	0.30	0.33	-0.27	0.47	-0.25	0.01	-0.32	0.49	-0.29	-0.07	-0.03
Femur length	0.31	0.13	-0.04	-0.30	-0.20	-0.41	0.08	-0.06	-0.14	0.26	0.70
Tibiofibula length	0.31	0.08	0.04	-0.48	-0.15	-0.43	0.13	0.13	-0.12	-0.11	-0.63
Proportion of Variance	**0.878**	**0.048**	**0.025**	**0.014**	**0.011**	**0.008**	**0.006**	**0.004**	**0.002**	**0.001**	**0.001**
Cumulative Proportion	**0.878**	**0.927**	**0.952**	**0.965**	**0.976**	**0.985**	**0.991**	**0.995**	**0.997**	**0.999**	**1**

Table S3.2: Results from simultaneous autoregressive models with combinations of neighbor distances and coding styles of the weighted matrix. These models link a) morphovolume, b) standardized effect size of morphovolume, c) minimum nearest neighbor distance and d) standardized effect size of minimum nearest neighbor distance, with sampled richness. We tested three weighting styles: C, globally standardized; S, variance-stabilizing coding; and W, row standardized. We use MinRSA, the minimum residual autocorrelation of the SAR models, to select the combination of neighbor distance and weighting style. The combination with the smallest MinRSA is bolded.

(a)

Neighbor distance (km)	Weighting style	AIC	MinRSA
50	C	30908.00	0.69
100	C	31013.98	0.69
150	C	32786.52	1.14
200	C	34381.71	1.61
250	C	36011.43	2.20
300	C	37190.51	2.71
50	S	30480.67	0.58
100	S	30445.29	0.46
150	S	32073.04	0.82
200	S	33599.65	1.33
250	S	35180.09	1.95
300	S	36350.86	2.51
50	W	30960.99	0.71
100	**W**	**30678.67**	**0.43**
150	W	32175.40	0.76
200	W	33605.42	1.33
250	W	35115.34	1.96
300	W	36294.91	2.46

(b)

Neighbor distance (km)	Weighting style	AIC	MinRSA
50	C	7682.62	1.08
100	C	7208.55	0.85
150	C	8406.32	1.35
200	C	9448.55	1.78
250	C	10473.69	2.26
300	C	11237.97	2.64
50	S	6680.88	0.88
100	**S**	**6009.35**	**0.46**
150	S	7093.30	0.75
200	S	8131.68	1.09
250	S	9155.01	1.38

Neighbor distance (km)	Weighting style	AIC	MinRSA
300	S	9907.47	1.71
50	W	6260.96	0.97
100	W	5456.60	0.35
150	W	6387.17	0.61
200	W	7383.94	0.98
250	W	8432.49	1.36
300	W	9268.48	1.67

(c)

Neighbor distance (km)	Weighting style	AIC	MinRSA
50	C	-17080.37	0.87
100	C	-17666.74	0.63
150	C	-16644.80	0.95
200	C	-15661.16	1.27
250	C	-14658.74	1.63
300	C	-13993.57	1.92
50	S	-17642.71	0.86
100	**S**	**-18475.39**	**0.36**
150	S	-17557.86	0.57
200	S	-16602.13	0.91
250	S	-15609.43	1.27
300	S	-14945.19	1.62
50	W	-17832.99	1.10
100	W	-18839.79	0.37
150	W	-18022.75	0.53
200	W	-17127.73	0.85
250	W	-16188.29	1.32
300	W	-15555.62	1.69

(d)

Neighbor distance (km)	Weighting style	AIC	MinRSA
50	C	9395.73	1.12
100	C	8674.66	0.57
150	C	9612.43	0.82
200	C	10458.37	1.18
250	C	11410.91	1.57
300	C	12069.07	1.89
50	S	8858.62	1.01
100	**S**	**7938.67**	**0.36**
150	S	8824.32	0.58

Neighbor distance (km)	Weighting style	AIC	MinRSA
200	S	9659.82	0.97
250	S	10620.53	1.38
300	S	11285.56	1.62
50	W	8829.51	1.18
100	W	7762.42	0.38
150	W	8560.04	0.59
200	W	9371.60	0.94
250	W	10319.38	1.36
300	W	10969.30	1.70

Table S3.3: Results of best-fit SAR models for each metric of morphospace structure.

	Slope	Z value	p-value of Z	Nagelkerke pseudo-R-squared
MCPV ~ sampled richness	0.8636727	102.267	< **0.001**	0.99223
SES of MCPV ~ sampled richness	-0.0062985	-3.0309	< **0.01**	0.87031
MNND ~ sampled richness	-0.0224399	-48.539	< **0.001**	0.90379
SES of MNND ~ sampled richness	-0.0139879	-6.0587	< **0.001**	0.85104
FEve ~ sampled richness	0.00118534	7.7136	< **0.001**	0.82325
SES of FEve ~ sampled richness	0.0090414	3.412	< **0.001**	0.82879

Figure S3.1: Comparison of Moran's I for linear model (black) and the best fit SAR model (red) indicates that most of the spatial autocorrelation in the data is removed by the SAR model.

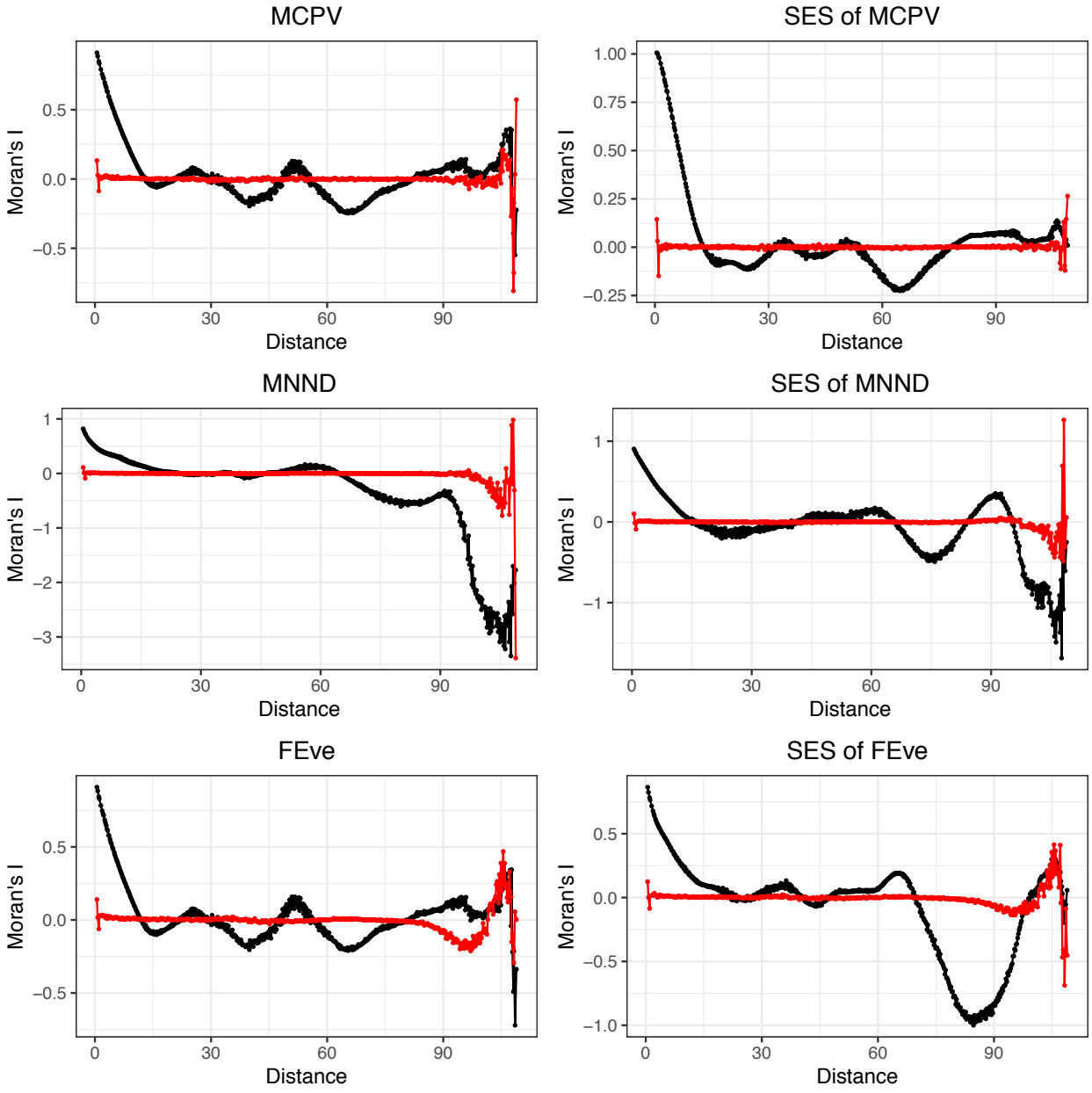

Figure S3.2: Relationship between total frog species richness and sampled frog species richness for 50 x 50 km map grid cells.

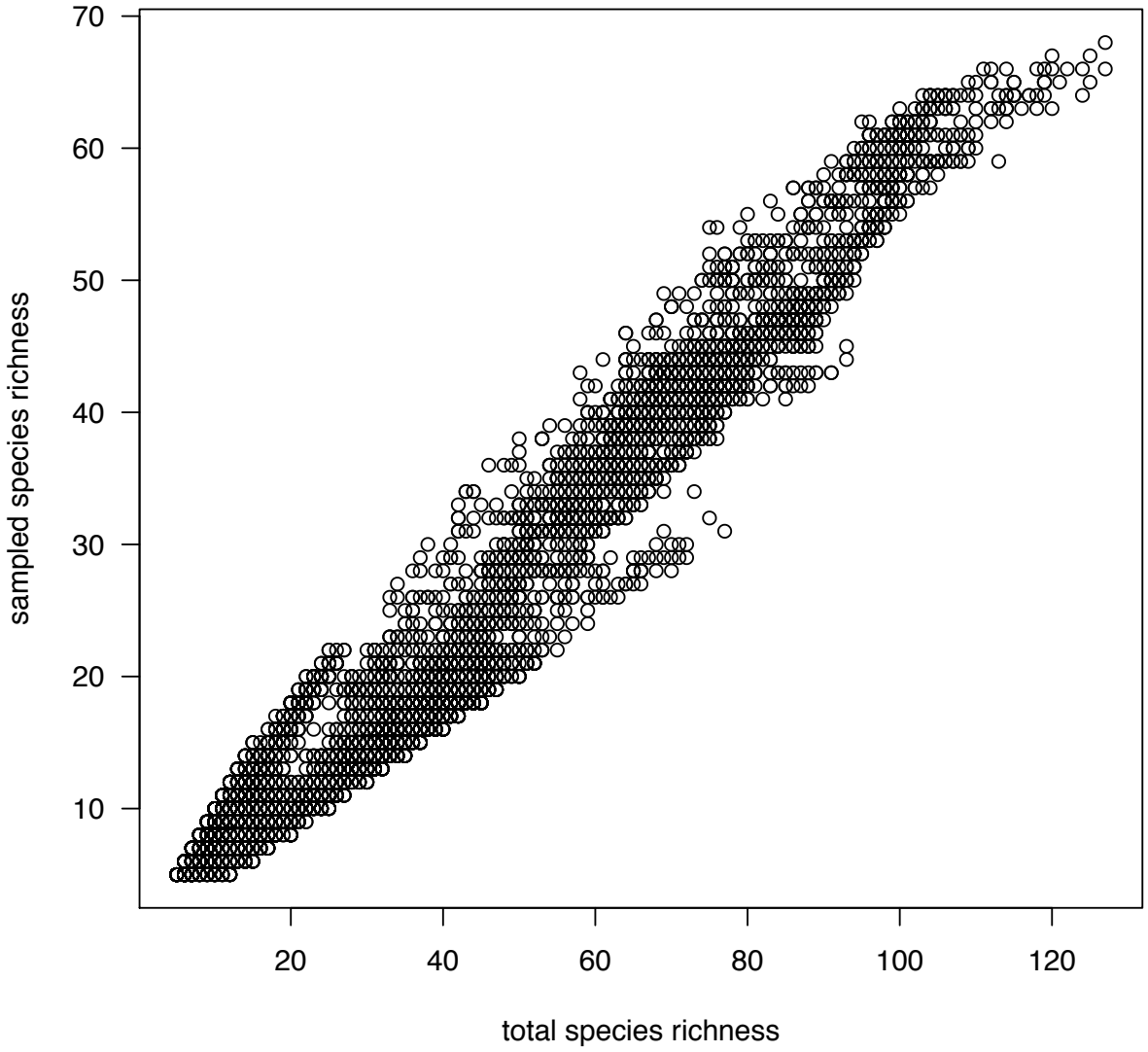

Figure S3.3: Sampling fraction of assemblages in relation to total species richness and latitude, as well as spatial distribution of sampling.

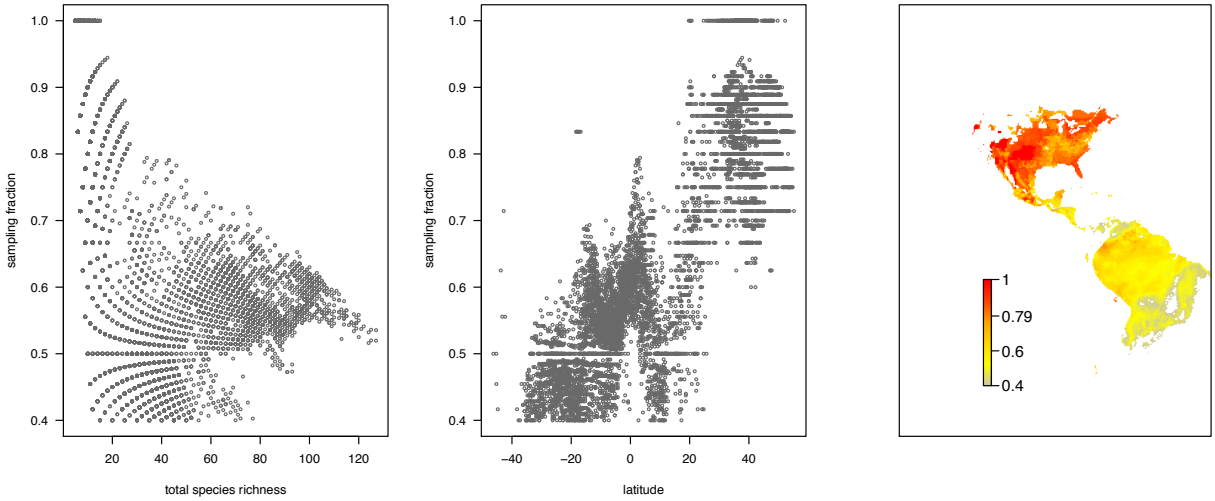

Figure S3.4: Sampling fraction of assemblages compared to each metric of morphospace structure. Blue indicates an assemblage with a significant SES value for the relevant metric.

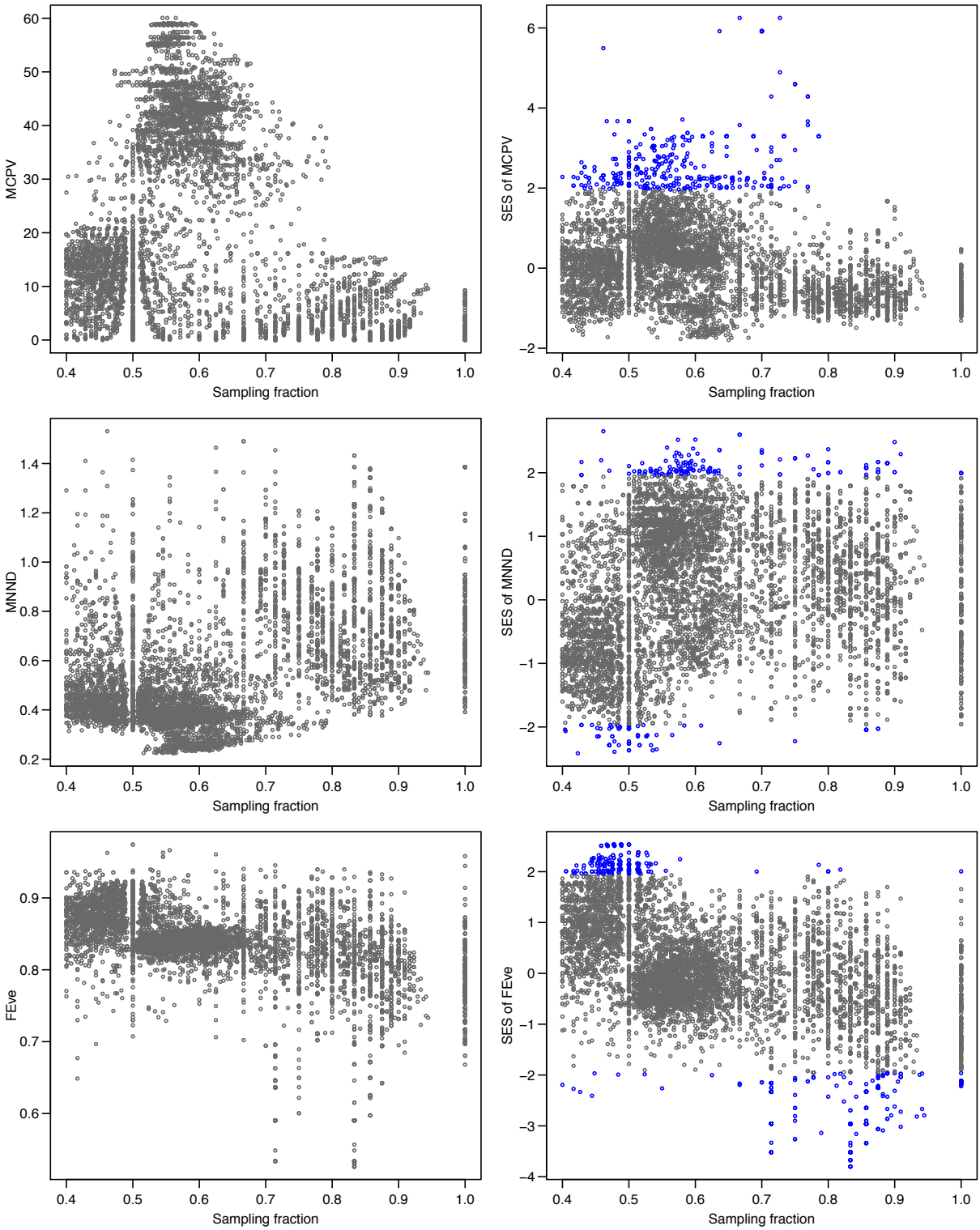

Figure S3.5: Comparison of morphospace metrics by assemblage. Color indicates absolute latitude, ranging from red (high latitude) to blue (low latitude).

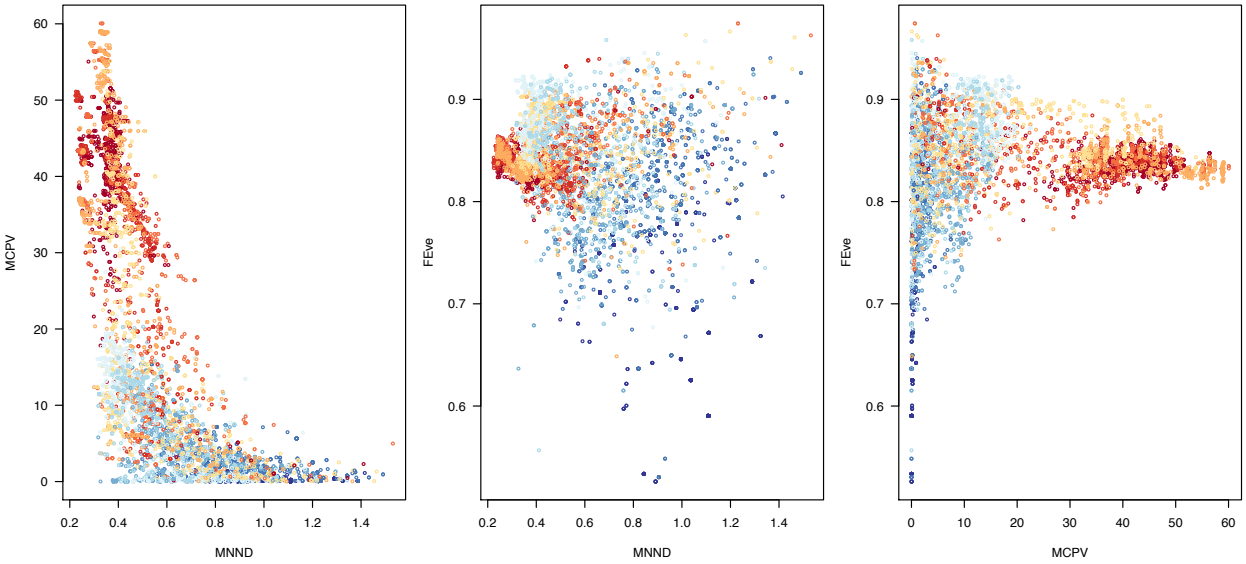

CHAPTER 4

Evaluation Of Taxonomic And Phylogenetic Descriptors Of Diet Diversity And Dissimilarity In A Community Of Tropical Frogs

With Nicholas Ferrugia, Leslie Hamar, Courtney Whitcher, and Daniel L. Rabosky

ABSTRACT

Diet is one of the most important components of a species' biology, yet challenges associated with collecting detailed dietary information have previously made it complicated to quantify this crucial niche axis. DNA metabarcoding of dietary samples has alleviated some of these barriers as it can rapidly generate high-resolution dietary information, but it raises new questions about the appropriate level of prey identification (LPI) to use in analyses and whether to incorporate the phylogenetic relationships between dietary resources into quantifications of diet. With DNA metabarcoding, we created high-resolution diet profiles for 22 sympatric frog species from a lowland tropical community in southeastern Peru and used these data to explore how understanding of dietary niche breadth and diet similarity between frog species varies depending on whether prey items are identified taxonomically to species or order level. We also test how these taxonomic metrics correlate with metrics that incorporate phylogenetic relationships between prey items. While all approaches to quantifying diet breadth are significantly correlated, they are not entirely congruent and choice of metric can influence conclusions about diet breadth. The phylogenetic approaches provided more nuanced

characterizations of relative diet breadths and capture differences between species in resource use that taxonomy-based measures are unable to do, revealing that frogs can be phylogenetic specialists, but taxonomic generalists. Taxonomic estimates of diet dissimilarity are correlated, but differences between species are always greater when computed with species LPI. Estimates of taxonomic diet dissimilarity with order LPI and phylogenetic diet similarity are uncorrelated, indicating that each approach is capturing different dimensions of dietary diversity. Our study also finds that prey species accumulation curves continue to rise sharply, even with 70 diet observations, indicating that hundreds - perhaps thousands - of diet records would be necessary to adequately describe diet breadth at species LPI, at least for diverse lowland rainforest communities. Since this sampling depth is beyond the scope of most studies, taxonomic metrics with order LPI data or phylogenetic metrics offer more accessible and reliable assessments of frog dietary specialization and interspecfic dietary similarity.

INTRODUCTION

Diet is one of the most central aspects of a species' ecology and is therefore relevant to myriad questions in ecology and evolutionary biology. There are innumerable studies in the literature focused on questions such as how species within communities partition food resources (Winemiller and Pianka 1990), how dietary specialization evolves (Darst et al. 2005) and varies along biotic and abiotic gradients (Belmaker et al. 2012), and the evolution of dietary strategies (Román-Palacios et al. 2019) to name just a few. Underlying all of these studies are datasets that vary widely in how diet items are identified and grouped. Level of prey identification (LPI) and categorization scheme is determined by the research question, but is also constrained by the data themselves. Until recently, most dietary studies have identified prey items to order or family

level (Caldwell and Vitt 1999; Parmelee 1999) or assigned consumers to broad categories (e.g. granivore, herbivore) (Belmaker et al. 2012; Price et al. 2012) due to the multitude of challenges associated with collecting fine-scale dietary data. It has been shown that this level of prey resolution and consumer categorization has potential to obscure patterns of resource partitioning and mischaracterize dietary niche breadth in an unpredictable manner (Greene and Jaksić 1983; Winemiller and Pianka 1990; Kartzinel et al. 2015). For example, using species LPI to study the interactions between sympatric birds of prey dramatically altered conclusions about which species were most likely to be the strongest competitors for food (Greene and Jaksić 1983). Despite most authors acknowledging the potential for these issues in their studies and the loss of ecologically relevant information by using coarse diet data, they are often limited to using broad categories or higher level taxonomy because of methodological issues related to the generation and analysis of more specific diet information.

The recent advent of high-throughput sequencing technology and metabarcoding methodology has revolutionized the way in which researchers can generate dietary information (Pompanon et al. 2012). This approach allows for species level prey identification from bulk samples such as feces or gut contents in a time and cost-effective manner. This has been highly advantageous for dietary studies of species that feed on soft-bodied organisms that are rapidly digested (McInnes et al. 2017), species that feed on groups that are hard to identify based on morphology (Burgar et al. 2014), and species that macerate diet items beyond the point of morphological identification from gut contents (Siegenthaler et al. 2019). Metabarcoding studies have uncovered previously unappreciated patterns of resource specialization and intra-community resource partitioning that had been obscured by use of higher taxonomy identification of food items (Kartzinel et al. 2015).

Since metabarcoding allows for the rapid generation of species level diet data, it might seem like all dietary studies that use this method should conduct analyses at the species LPI. However, it remains an unresolved question of what the most appropriate LPI is for studying diet. There is a case to be made for the use of higher taxonomic classification or broader categories, since this could provide a more accurate picture of "functional" niche breadth under the assumption that prey species in the same taxonomic order will have more similar handling and digestive requirements and nutritional profiles than ones from different orders. For example, consider a case of a consumer that eats two ant species and another consumer that eats one ant and one beetle species. These two consumers would be equally specialized if species LPI is used, but the former would be more specialized if order LPI is used. This scenario provides strong support for the use of broader categories to capture ecological differentiation. However consider another example, in which two consumers both eat only ants, but one consumes any ant that it encounters and the other feeds solely on one ant species. Use of order LPI, which would show equal specialization, is misleading in the scenario and it is easy to argue that species LPI would be more appropriate. These two examples highlight the challenges of selecting a LPI for describing and analyzing dietary niche breadth.

The issue of how prey classification can influence conclusions is particularly acute when we consider diet overlap or diet similarity. Estimates of dietary overlap that use order LPI nearly always overestimate overlap compared to when it is calculated at species LPI (Greene and Jaksić 1983). In fact, diet overlap with broad categories or higher taxonomy can indicate that two consumers have complete overlap in diets, when in actuality they share no prey species and are therefore not competing for resources. Like with dietary niche breadth however, use of species LPI for calculation of diet similarity is not free of biases. Allopatric consumers might not have

access to the same prey species, but nevertheless have very similar diets in terms of the functional traits of their consumed prey that would be revealed using order LPI. A standard presence-absence dissimilarity or overlap index does not take functional or taxonomic similarity into account and species LPI of prey items can therefore result in an artificially high dissimilarity of diets. Ultimately, using categorizations of prey types at any taxonomic level may result in a loss of ecological information about diet.

Another caveat to selection of an appropriate LPI is the practical consideration of sampling depth in the dietary data. For most analyses that utilize taxonomic categories to compute measures of diet, it is preferable that accumulation of prey taxonomic categories reaches an asymptote for each consumer species. However, in biomes with extremely diverse resources, such as lowland Amazonian forests, very large sample sizes might be required to capture the full range of prey species used by all but the most extremely specialized consumers. Richness at higher taxonomic levels will plateau more rapidly than species richness and might therefore provide a more complete picture of dietary resource diversity than species LPI in these types of environments.

The use of metabarcoding to enumerate and identify diet items offers an alternative to describing diet in terms of taxonomic units. With the genetic information generated for every prey taxon, it is easily feasible to reconstruct the evolutionary relationships between prey taxa. The incorporation of the phylogenetic relationships between prey species can provide a more nuanced means of studying diet that may retain more ecological information than taxonomic or functional categories and facilitates calculation of diet similarity between allopatric species. The idea of considering the phylogenetic relationships of prey or dietary items in quantifications of diet breadth was presented by Symons & Beccaloni (Symons and Beccaloni 1999) and discussed

in the context of understanding specialization of herbivorous insects. Although several subsequent papers on this study system have incorporated the phylogenetic relationships of host plant species to quantify the diet specialization of herbivorous insects (e.g. Pellissier et al. 2012; Jorge et al. 2014; Forister et al. 2015; Jorge et al. 2017), the use of phylogenetic indices has not been widely leveraged in other dietary studies despite the rise of metabarcoding diet studies in recent years (but see Burgar et al. 2014).

There has been limited evaluation of how phylogenetic metrics of diet correspond and perform relative to taxonomic metrics of diet. A recent paper found that species level taxonomic dietary diversity and phylogenetic dietary diversity were negatively or not significantly correlated in a community of large mammalian herbivores (Kartzinel and Pringle 2020). Since the focus of that study was on quantifying dietary specialization with diet items resolved to species level, it did not evaluate the correspondence between phylogenetic dietary descriptors and taxonomic descriptors of diet using order LPI nor did it not evaluate the impact of taxonomic versus phylogenetic dietary descriptors on estimated diet similarity. The nature of these relationships therefore remains unclear, as does the extension of their findings to other study systems.

In this study, we investigate how conclusions about resource utilization by frogs are dependent on the use of taxonomic and phylogenetic metrics of diet breadth and similarity. We also evaluate how level of prey identification used in taxonomic approaches can influence conclusions. With molecular dietary data, we evaluate diet breadth and similarity with three approaches: phylogenetic metrics, taxonomic metrics at species LPI, and taxonomic metrics at order LPI. Focusing on 22 sympatric frog species from a lowland forest in southeastern Peru, we use DNA metabarcoding to cluster prey items into molecular operational taxonomic units

(MOTUs) and assign taxonomy by comparison to an annotated genetic database. We assess whether species LPI is tractable for this study system or whether the diverse resource base renders this level of prey identification uninformative given realistic levels of diet sampling. Based on previous study of overlap in frog diets in another lowland Amazonian frog community (Parmelee 1999), we predict that species LPI will show low overlap across species, especially in contrast to order-level LPI. We also test whether measures of frog dietary breadth and diet similarity are correlated across metrics and provide insight into how DNA metabarcoding can be leveraged to study frog trophic ecology.

METHODS

Study sites and sample collection

We collected stomach contents through gastric lavage or dissection of animals immediately after euthanasia at the Los Amigos Research Station in southeastern Peru (Figure S4.1). Samples were stored in 96% ethanol at room temperature and subsequently at -80°C in the laboratory prior to processing. Sampling was conducted over four field seasons, each lasting for one month in March 2016, November 2016, November 2017, and December 2018. We caught frogs during daytime and nighttime visual encounter surveys and through the use of funnel and pitfall traps. Stomach contents were extracted as soon after capture as possible to minimize digestion of prey items. All procedures that involved handling live animals were reviewed and approved by the University of Michigan Committee on Use and Care of Animals (UCUCA Protocol #PRO00006234). We conducted research and collected biological samples in Peru under permits issued by the Peruvian government SERFOR (Servicio Nacional Forestal y de Fauna Silvestre;

permit numbers: 029-2016-SERFOR-DGGSPFFS, 405-2016-SERFOR-DGGSPFFS, 116-2017-SERFOR-DGGSPFFS).

Metabarcoding

We examined samples under a microscope with a camera and photographed each prey item with a digital scalebar. Items that were too large to be photographed under the microscope were photographed using a smart phone camera and physical scalebar. Prey items were placed in a 1.5 mL cryovial; large prey items were subsampled. Then we dried samples in a Savant SpeedVac concentrator. After all ethanol was evaporated, we added two 2.5 mm stainless steel beads and 180 µL – 720 µL of ATL buffer from a Qiagen DNeasy extraction kit; we added the buffer in 180 µL increments until the sample was just barely covered. To homogenize samples, we then used a FastPrep-24 (MP Biomedical) set at 5.5 m/sec for 60 seconds, after which we added 20 µL of proteinase K for every 180 µL of ATL buffer. We then vortexed samples and spun them down in a microcentrifuge for one minute at 12,000 rpm to ensure that all fragments of prey items were covered in reagent. Samples were subsequently incubated at 56°C for at least 36 hours, following which they were briefly vortexed and spun down in a microcentrifuge at 4,000 rpm for three minutes. We removed the supernatant into a sterile 1.5 mL microcentrifuge tube and subsequently followed the standard Qiagen DNeasy extraction protocol to extract DNA, using Ultrapure water for the final elution. We used a Qubit fluorometer to quantify the amount of DNA in the extractions and standardized aliquots to 0.69 ng/µL via dilution or concentration. We found that this relatively low concentration was required to overcome the presence of PCR inhibitors.

We amplified a 300-400 bp fragment of the SSU 18S rRNA gene using universal eukaryotic primers: SSU-FO4 (5'-GCTTGTCTCAAAGATTAAGCC) and SSU-R22 (5'-GCCTGCTGCCTTCCTTGGA) (Blaxter et al 1998). We also amplified a fragment of CO1, but since we do not consider the resultant data for this study we do not provide extensive description of methods specific to its generation. The targeted genomic regions were amplified in separate PCRs. The 18S PCR recipe consisted of: 3.75 µL of eluted DNA for a total of 2.5 ng of input DNA, 1 µL of each primer at 5 mM, 0.5 µL of DMSO, 6.25 µL of GoTaq Mastermix for a total volume of 12.5 µL. Cycler conditions were: 95ºC for 4 min; 30 cycles of 95ºC for 30 s; 48ºC for 30 s; 72ºC for 3 min, and a final extension of 72ºC for 10 min.

We pooled PCR products by sample and removed unincorporated reagents using AMPure XP magnetic beads (Beckman Coulter) at a ratio of 0.8X. We then performed a short cycle PCR to attach dual index barcodes and P5 and P7 Illumina sequencing adapters to these cleaned PCR products. This short cycle PCR recipe was: 3 µL of PCR product, 3 µL each of the N5 and N5 indices at 5 mM, 0.25 µL Phusion High Fidelity DNA polymerase (ThermoFisher), 5 µL of 5X Phusion HF Buffer, 0.5 µL dNTPs at 10 mM and 10.25 µL of water for a total reaction volume of 25 µL. Cycler conditions for the second PCR were: 95°C for 3 minutes; 8 cycles of 95°C for 30 seconds, 55°C for 30 seconds, 72°C for 30 seconds; and a final extension of 72°C for 5 minutes.

We purified and size selected libraries with AMPure XP beads (0.6X), quantified them using a Qubit fluorometer, and pooled libraries with sufficient DNA concentration in equimolar amounts. Libraries constructed with samples from our study site, Los Amigos Research Station, were combined samples from other sampling locations to form four pooled libraries that contained 380, 373, 370, and 372 samples, respectively. Pooled libraries were sequenced at the

University of Michigan Advanced Genomics Core on an Illumina MiSeq platform using v2 chemistry (500 cycle; 2 x 250 bps).

Bioinformatics

Sequences were delivered demultiplexed. We merged read pairs using VSEARCH (v2.14.1; Rognes et al. 2016) with the default parameters of the –fastq_mergepairs command (--fastq_maxdiffs 10). In the same step, we separated 18S and CO1 amplicons by merged read length. We do not use CO1 sequences beyond this point, so all further mention of sequence data refers solely to the 18S amplicons. Primers were removed and sequences quality filtered with a Maxee value of 1.0. Filtered and truncated reads were pooled by sampling region to improve downstream clustering analyses; the samples from our focal community of Los Amigos Research Station were pooled with samples from other sampling sites in Peru and Brazil to the exclusion of samples from the USA. We then dereplicated pooled sequences using full length matching (--derep_fulllength) and unique sequences represented by less than 10 reads were discarded (--minuniquesize 10). We clustered dereplicated sequences into molecular operational taxonomic unites (MOTUs) at 97% similarity and checked for chimeras using the uchime-denovo algorithm (Edgar, Haas, Clemente, Quince, & Knight 2011), implemented in VSEARCH as --uchime3_denovo. Taxonomy was assigned to each MOTU using the SILVA 18S database (v123). For the purposes of this study, assigning a specific name to an MOTU is not essential, but higher level taxonomy is required. For MOTUs that were not assigned ordinal level taxonomy, sequences were manually BLASTed on NCBI to obtain this information. Sequence reads were then mapped onto the MOTUs with –-usearch_global.

Using Qiime 2.0 2019.10 (Bolyen et al. 2019), we filtered out non-prey items by taxonomy using the q2-taxa plugin. First, we retained only OTUs identified as metazoan and discarded all others. Frogs have not been documented to consume any non-metazoan species (Wells 2007) nor did we detect any evidence for this during visual inspection of gut samples. We did observe plant material in some samples, but this was consistent with incidental ingestion in the process of consuming targeted prey items. We further removed any MOTUs belonging to Nematoda and Platyhelminthes because these are assumed to be parasites rather than prey items. Samples that had less than 1000 reads at this point were considered to be unsuccessful and not processed further.

A challenge in extracting DNA from a whole animal, such as an intact prey item, rather than targeting a tissue subsample, such as liver or muscle, is that there will be DNA of other organisms included in the extraction. This includes genetic material from the microbiome, parasites, and secondary prey items. We were able to address some of these concerns with the taxonomic filtering described above, but this was not guaranteed to be effective for removing secondary prey items. This is because frogs consume taxa that have high potential diet overlap with frogs. For example, spiders were frequently observed in our samples prior to metabarcoding and spiders, like frogs, eat mainly arthropods. By comparing MOTU profiles to the photographed prey items, we determined that we could remove secondary prey items by removing MOTUs from samples if they were represented by less than 5% of the remaining sequence reads. Since some frogs are anurophagous, we hand curated MOTUs identified as vertebrates at this stage. We consulted photographs of prey items for frogs with a vertebrate MOTU in their profile to determine whether these sequence reads represented detection of a prey item or were consumer DNA. We converted MOTU tables to binary presence and absence tables. We do not utilize

relative read abundance data in our analyses because these data can be misleading with metabarcoding of stomach contents because prey items can be at differing levels of digestion (Deagle et al 2018).

We identified samples from our focal study site, Los Amigos Biological Station, and species for which we had a least ten individuals from that site. These records were then merged by species to create MOTU tables at the level of the frog species. Presence records were summed, so that values indicate the number of frog individuals that had consumed a prey species. We also collapsed MOTUs to order level taxonomy and summed observations.

We aligned the sequences for the MOTUs using MAFFT (Katoh and Standley 2013) (via q2-alignment) and estimated an unrooted phylogeny using fasttree2 (Price et al. 2010) (via q2-phylogeny) within the Qiime 2 platform (Bolyen et al. 2019). Then we rooted this tree in R using the root function in the *ape* R package ver 5.3 R package (Paradis and Schliep 2019) with Chordata as the outgroup to Annelida, Mollusca, and Arthropoda. For each frog species, we generated species and order richness accumulation curves for pooled diet samples using the rarefy function in the vegan R package *vegan* ver 2.5.6 (Oksanen et al. 2019).

Diet Breadth

To quantify taxonomic dietary diversity (TDD), we use Simpson's Diversity Index, which is calculated as: $1 - \sum(\frac{n}{N})^2$, where *n* is the number of observations of a prey taxon and *N* is the total number of diet observations for the frog species. It ranges between 0 (no diversity) and 1 (infinite diversity). Since this formulation of dietary niche breadth uses the proportional utilization of each prey type, prey taxa that are not major components of diet are not given equal

weight as more regularly consumed items. We used this formula for TDD at species and order LPI.

To quantify diet breadth from a phylogenetic perspective, we used two metrics: abundance-weighted unrooted Faith's phylogenetic diversity (PDD) and mean phylogenetic distance (MPD). For PDD calculations, we used R code from Swenson (2014). We use unrooted PD because this modified version results in a value of 0 if a consumer species eats only one prey taxon. The original formulation of Faith's PD includes the root in all calculations, which results in a non-zero value for a monophagous consumer. Since we are concerned with the phylogenetic breadth of diet rather than depth of evolutionary history, we opt for using an unrooted metric. We also calculated the mean phylogenetic distance (MPD) between prey items within each frog species' diet as this can provide more insight into the specialization of diet as opposed to PDD, which is theoretically a descriptor of diet volume. To do this, we use the mpd function in the R package *picante* (Kembel et al. 2010).

To account for different numbers of diet observations between species, the diet records for each species were subsampled without replacement to 15 diet observations (N = 15) before calculation of the four metrics. We did this for 1000 iterations and calculated the mean and 95% confidence intervals. To assess how different measures of diet breadth impact characterization of relative diet specialization between species, we tested for pairwise correlation using Spearman's rank order correlation and Pearson tests.

Diet dissimilarity

To quantify diet dissimilarity, we utilized the Bray-Curtis dissimilarity index, which varies between 0 (complete overlap) for complete overlap to 1 (no overlap). It also incorporates

information on the abundance of individual prey items within the pooled sample of diet across all individuals for a given species, so that a prey item consumed by multiple conspecific frog individuals will be given more weight than a prey item consumed by a single frog individual. We calculated Bray-Curtis dissimilarity matrices with the species LPI (BC, species LPI) and order LPI (BC, order LPI) data. As a measure of phylogenetic beta diversity, we calculated the mean phylogenetic distance (MPBD) between species using the comdist function in picante, weighted by number of observations. This metric calculates the expected phylogenetic distance between two prey species drawn randomly from different frog species. A smaller value indicates that two frog species eat phylogenetically similar and larger values indicate greater dissimilarity in diet. For these three metrics, we also subsampled the diet profile of each frog species without replacement and took the mean of 1,000 iterations. To test the correlation between diet dissimilarity based on these three metrics, we applied Mantel tests to each set of distance matrices using the R package vegan (Oksanen et al. 2019).

RESULTS

Our dataset included 22 species that each had diet data for at least 10 individuals (mean: 15.5; range: 10 - 29). The number of diet observations per species ranged from 15 to 68, with a mean of 34. Across all of these individuals, we identified 254 prey MOTUs from 33 orders. Species accumulation curves did not reach an asymptote for any of the frog species, even the most heavily sampled ones, and continued to rise sharply (Figure 4.1 and S4.2). At the order level, richness accumulation appeared to be slowing for many species, but did not fully reach a plateau (Figure 4.1 and S4.2).

Diet breadth

Niche breadth of a frog species calculated with order LPI with the Simpson Diversity Index (TDD, order LPI) was always smaller than when it was calculated using species LPI (TDD, species LPI). Niche breadth estimated using unrooted and abdundance-weighted Faith's phylogenetic distance (PDD) showed the most variation in values between species. TDD, species LPI estimated that most species were roughly similar in niche breadth with only *Engystomops freibergi* clearly differentiated with a relatively small diet breadth (Figure 4.2). A similar pattern emerged with TDD, order LPI, except that two additional species, *Hampytophryne boliviana* and *Ameerega trivittata*, are identified as having relatively limited diet breadths like *E. freibergi*. In contrast, PDD and MPD show much greater variation in diet breadth between species. As with both TDD measures, *E. freibergi* is identified as having the smallest diet breadth. *Hampytophryne boliviana* and *Ameerega trivittata* have similarly small PDD and MPD values. With PDD, there is a group of three species, *Ctenophryne geayi*, *Phyllomedusa vaillantii*, and *Hypsiboas lanciformis*, that have slightly higher PDD values than the three specialized species and above these are 15 species that arranged in a gradient of PDD values. At the high end of the spectrum is *Pristimantis reichlei,* which has a distinctly high PDD, whereas it is not noteworthy with either TDD measure. MPD also indicates that *P. reichlei* has a generalized diet, but that *Ceratophrys cornuta* has the highest observed value of MPD within this dataset.

When we consider the correlation between values of niche breadth across the three metrics, we find that they are highly to moderately correlated (Figure 4.3) based on either Pearson or Spearman's rank order correlation. This indicates that understanding of relative dietary specialization within this set of frogs is relatively consistent across metrics. The lowest correlations are between TDD, species LPI and the two phylogenetic metrics, PDD and MPD,

but even these values indicate moderately strong correlations (Figure 4.3). We find that despite some differences in relative specialization orderings, MPD and PDD are highly correlated. These findings are robust to the removal of *Engystomops freibergi*, an outlier, with the exception of the relationship between MPD and TDD, species LPI that is not significant after this species is removed (Table S4.1).

Diet dissimilarity

We quantified diet dissimilarity between the 22 focal sympatric species and found noticeably different patterns with the three different methods (Figure 4.4). Unsurprisingly, we found that diet dissimilarity was always higher when it was calculated with taxonomic data at species LPI than with order LPI. In fact, BC with species LPI indicated that there was very limited overlap between most frog species. Two groupings of species with relatively greater overlap emerge, one consisting of *Osteocephalus castaneicola*, *Phyllomedusa camba*, *Phyllomedusa vaillantii*, and *Hypsiboas lanciformis*, all of which are large treefrogs (Figure S4.3). The other grouping includes *Ctenophryne geayi, Hamptophryne boliviana, Adenomera andreae, Ameerega trivittata, Ameerega hahneli*, and *Amazophrynella javierbustamantei*, which all have a high proportion of Hymenoptera in their diets (Figure S4.3).

Diet dissimilarity quantified as BC with order LPI had more variability in overlap. The most obvious pattern with this metric is the unique diet of *Engystomops freibergi*, which is likely driven by the high proportion of termites in their diet. While other species in this community were recorded to eat termites, it was not a proportionally important prey order to them. As with BC, species LPI, the species with high proportions of ants and large treefrogs showed higher than average overlap.

The two taxonomic measures were moderately correlated, as was BC at species LPI with the phylogenetic metric, MPBD (Table 4.2). The correlation between BC using order LPI and MPBD was not significantly different than zero, indicating that these two metrics are quantifying different axes of dietary divergence.

DISCUSSION

We explored the impact of prey identification level and incorporation of phylogenetic information about prey items on understanding of the relative specialization and dietary overlap of 22 species of frogs from a tropical community in southeastern Peru. We found a strong positive relationship between taxonomy-based and phylogeny-based dietary diversity metrics. Our results provide a counterpoint to a recent study that examined the relationship between phylogenetic and taxonomic descriptors of diet breadth for a community of mammalian herbivores and found no correlation or a weakly negative one (Kartzinel and Pringle 2020). Our finding of a strong correlation in relative specialization of species between all metrics suggests that analyses of dietary niche breadth in frogs could be robust to metric selection. However, despite strong correlations between specialization metrics, we found that dietary taxonomic diversity can accumulate without phylogenetic or higher level taxonomic diversity also accumulating (Figure 4.3).

Even though different niche metrics did not substantially differ in the rankings of frog species' relative niche breadths, they differed in the degree to which they clustered and differentiated between species' diet breadths (Figure 4.2). As hypothesized, metrics that incorporate the phylogenetic relationships of prey items produced more nuanced perspectives on the diet breadth and relative specialization of frog species. With TDD at species LPI, 21 of our

22 frog species have diet breadths that are nearly identical. This decreases slightly with TDD at order LPI to 19 species with indistinguishable values, but our data support the view that frogs do not differ greatly in their relative diet specialization. Both phylogenetic metrics, PDD and MPD, present a more complicated picture, with multiple clusters of diet breadth, likely because they are computed using more continuous data compared to the TDD metrics that rely on taxonomic categories. This suggests that phylogenetic metrics might detect meaningful differences between species dietary breadths better than taxonomy-based metrics when sampling per species is insufficient to achieve plateauing of (dietary) richness accumulation curves, as in this study. In fact, the observed consistency in TDD across species might be an artifact of insufficient sampling depth rather than an accurate ecological pattern and we predict that greater differentiation in TDD at both species and order LPI would begin to emerge with greater sampling.

The species accumulation curves for species in this study reveal that frog species in this community consume a large number of prey species and that even with more than 40 dietary observations we were unable to detect a decrease in the rate of prey species accumulation. The constant slope of these species accumulation curves prevented us from predicting with any confidence the total number of prey species consumed by these frogs, but it appears that upwards of 100 dietary observations are necessary to estimate this value. This suggests that using species LPI will rarely be feasible in locations such as lowland Amazonian forests that have exceptionally large resource bases.

The occasional disconnect of taxonomic dietary diversity and phylogenetic dietary diversity indicates that metric choice has the potential to influence which species would be considered relative dietary generalists or specialists. Degree of diet specialization is highly

relevant for extinction risk assessments for frogs, a group that is threatened by many factors (Hof et al. 2011; Grant et al. 2016) and given the emerging concerns about arthropod population declines (Forister et al. 2019; Sánchez-Bayo and Wyckhuys 2019), it is important that we improve our understanding of the breadth of dietary resources used by frogs. Only one species, *Engystomops freibergi*, appeared to have a specialized diet based on species LPI data, although as we previously noted, increased sampling might reveal that other species also have specialized diets at species LPI. We detected relatively restricted diets for more species at higher LPI and in terms of phylogenetic diversity. This is similar to a pattern seen in herbivorous insects that are specialized at the level of genus for host plants (Barone 1998; Novotny et al. 2002). For frogs, this trend of diet specialization is driven by species that eat a high proportion of ants or termites. Highlighting the value of integrating the phylogenetic relationships of prey items is the discovery that *Osteocephalus castaneicola*, *Phyllomedua vaillantii*, and *Hypsiboas lanciformis* have relatively specialized diets from the perspective of MPD and PDD, but neither TDD metric. These three treefrog species have high proportions of orthopterans in their diets. Our results suggest that the diets of these species might warrant further investigation to determine the extent of their specialization and flexibility to use other prey clades.

We only considered sympatric species in this study and it is therefore possible that all species had access to the same resource base and the potential to overlap in diet at species LPI. At this scale of LPI, we find generally low overlap in frog diets, which could indicate weak interspecific competition for food resources or reflect that our sampling did not recover the full richness of prey species utilized by these focal frog species. Despite this incomplete dietary profile and our hypothesis that there would be limited to no overlap in sampled diets at species LPI, most pairwise comparisons of frog diets revealed some degree of overlap. Interestingly, the

species showing the highest overlap in diet at species LPI are also the ones identified as having relatively specialized diets (Figure S4.3). The species that heavily consume hymenopterans (specifically ants) overlap in diet. Given the ant diversity of lowland Amazonian rainforest (Guénard and Economo 2015), it is remarkable that there is any overlap. The other group showing relatively high overlap in prey species is the large-bodied treefrogs: *Osteocephalus castaneicola*, *Phyllomedusa camba, Phyllomedua vaillantii*, and *Hypsiboas lanciformis*. Future work should explore whether this overlap in prey species is the result of prey selectivity or reflects prey availability in the environment.

In studies of allopatric species, it would be ineffectual to use species LPI because the geographic ranges of prey species would impact diet dissimilarity and it would be hard to disentangle these effects from meaningful resource partitioning. Dissimilarity indices calculated with higher LPI or phylogenetic distances can be applied in these situations. Intriguingly, the complete lack of correlation between BC at order LPI and MPBD indicates that these two metrics are measuring fundamentally different axes of diet dissimilarity. An illustrative example of this is diet comparisons between *Ceratophrys cornuta* with other species. From an order LPI perspective, *C. cornuta* shares moderate overlap in diet with several species, particularly *Pristimantis toftae*. However, these similarities are greatly reduced when diet dissimilarity is quantified using MPBD and *C. cornuta* has a distinct diet from *P. toftae*. We expect that this shift is driven by MPBD accounting for the fact that *C. cornuta* is the only species observed to eat vertebrates, which are deeply evolutionarily divergent to all other prey groups in the dataset.

In conclusion, we find that a very high number of diet observations is required to adequately describe the richness of prey species consumed by any given frog species, at least from the high-diversity lowland rainforest community studied here. Without extremely large

intraspecific sample sizes, use of diet data with prey items identified to species level will not be informative for most studies of frog diet specialization and similarity. Instead, we consider the use of metrics that rely on order LPI data or the phylogenetic relationships between prey items to quantify aspects of frog diets to be a more tractable and ecologically informative approach. Given the accessibility of both taxonomic and phylogenetic data about prey items from metabarcoding datasets, we recommend the quantification of both metric types because this can reveal interesting patterns of resource use and partitioning that are invisible or easily missed if only one axis of dietary diversity is considered.

DATA AVAILABILITY

FASTA sequences and photographs of stomach contents samples will be available through the University of Michigan Library Digital Collections.

REFERENCES

Barone, J. A. 1998. Host specificity of folivorous insects in a moist tropical forest. Journal of Animal Ecology 67:400–409.

Belmaker, J., C. H. Sekercioglu, and W. Jetz. 2012. Global patterns of specialization and coexistence in bird assemblages. Journal of Biogeography 39:193–203.

Bolyen, E., J. Rideout, M. Dillon, N. Bokulich, C. Abnet, G. Al-Ghalith, H. Alexander, et al. 2019. Reproducible, interactive, scalable and extensible microbiome data science using QIIME 2. Nature biotechnology 37:852–857.

Burgar, J. M., D. C. Murray, M. D. Craig, J. Haile, J. Houston, V. Stokes, and M. Bunce. 2014. Who's for dinner? High-throughput sequencing reveals bat dietary differentiation in a biodiversity hotspot where prey taxonomy is largely undescribed. Molecular Ecology 23:3605–3617.

Caldwell, J. P., and L. J. Vitt. 1999. Dietary asymmetry in leaf litter frogs and lizards in a transitional northern Amazonian rain forest. Oikos 84:383–397.

Darst, C. R., P. A. Menéndez‐Guerrero, L. A. Coloma, and D. C. Cannatella. 2005. Evolution of Dietary Specialization and Chemical Defense in Poison Frogs (Dendrobatidae): A Comparative Analysis. The American Naturalist 165:56–69.

Forister, M. L., V. Novotny, A. K. Panorska, L. Baje, Y. Basset, and P. T. Butterill. 2015. The global distribution of diet breadth in insect herbivores. Proceedings of the National Academy of Sciences USA 112:442–447.

Forister, M. L., E. M. Pelton, and S. H. Black. 2019. Declines in insect abundance and diversity : We know enough to act now. Conservation Science and Practice 1:e80.

Grant, E. H. C., D. A. W. Miller, B. R. Schmidt, M. J. Adams, S. M. Amburgey, T. Chambert, S. S. Cruickshank, et al. 2016. Quantitative evidence for the effects of multiple drivers on continental-scale amphibian declines. Scientific Reports 6:1–9.

Greene, H. W., and F. M. Jaksić. 1983. Food-Niche Relationships among Sympatric Predators : Effects of Level of Prey Identification. Oikos 40:151–154.

Guénard, B., and E. P. Economo. 2015. Additions to the checklist of the ants (Hymenoptera: Formicidae) of Peru. Zootaxa 4040:225–235.

Hof, C., M. Araújo, W. Jetz, and C. Rahbek. 2011. Additive threats from pathogens, climate and land-use change for global amphibian diversity. Nature 480:516–519.

Jorge, L. R., V. Novotny, S. T. Segar, G. D. Weiblen, S. E. Miller, Y. Basset, and T. M. Lewinsohn. 2017. Phylogenetic trophic specialization : a robust comparison of herbivorous guilds. Oecologia 185:551–559.

Jorge, L. R., P. I. Prado, M. Almeida-Nato, and T. M. Lewinsohn. 2014. An integrated framework to improve the concept of resource specialisation. Ecology letters 17:1341–1350.

Kartzinel, T. R., P. A. Chen, T. C. Coverdale, D. L. Erickson, W. J. Kress, M. L. Kuzmina, D. I. Rubenstein, et al. 2015. DNA metabarcoding illuminates dietary niche partitioning by African large herbivores. Proceedings of the National Academy of Science 112:8019–8024.

Kartzinel, T. R., and R. M. Pringle. 2020. Multiple dimensions of dietary diversity in large mammalian herbivores. Journal of Animal Ecology 2020:1–15.

Katoh, K., and D. M. Standley. 2013. MAFFT Multiple Sequence Alignment Software Version 7 : Improvements in Performance and Usability. Molecular biology and evolution 30:772–780.

Kembel, S. W., P. D. Cowan, M. R. Helmus, W. K. Cornwell, H. Morlon, D. D. Ackerly, S. P. Blomberg, et al. 2010. Picante: R tools for integrating phylogenies and ecology.

Bioinformatics 26:1463--1464.

McInnes, J. C., R. Alderman, M.-A. Lea, B. Raymond, B. E. Deagle, R. A. Phillips, A. Stanworth, et al. 2017. High occurrence of jellyfish predation by black-browed and Campbell albatross identified by DNA metabarcoding. Molecular Ecology 26:4831–4845.

Novotny, V., Y. Basset, S. E. Miller, G. D. Weiblen, B. Bremer, L. Cizek, and P. Drozd. 2002. Low host specificity of herbivorous insects in a tropical forest. Nature 416:841–844.

Oksanen, J., F. G. Blanchet, R. Kindt, P. Legendre, P. R. Minchin, R. B. O'Hara, G. L. Simpson, et al. 2019. vegan: Community Ecology Package. R package version 2.5-6 https://CRAN.R-project.org/package=vegan.

Paradis, E., and K. Schliep. 2019. ape 5 . 0 : an environment for modern phylogenetics and evolutionary analyses in R. Bioinformatics 35:526–528.

Parmelee, J. R. 1999. Trophic Ecology of a Tropical Anuran Assemblage. Scientific Papers Natural History Museum the University of Kansas 11:1–59.

Pellissier, L., K. Fiedler, C. Ndribe, A. Dubuis, J. Pradervand, A. Guisan, and S. Rasmann. 2012. Shifts in species richness, herbivore specialization, and plant resistance along elevation gradients. Ecology and evolution 2:1818–1825.

Pompanon, F., B. E. Deagle, W. O. C. Symondson, D. S. Brown, S. N. Jarman, and P. Taberlet. 2012. Who is eating what: Diet assessment using next generation sequencing. Molecular Ecology 21:1931–1950.

Price, M. N., P. S. Dehal, and A. P. Arkin. 2010. FastTree 2 – Approximately Maximum-Likelihood Trees for Large Alignments. PloS one 5:e9490.

Price, S. A., S. S. B. Hopkins, K. K. Smith, and V. L. Roth. 2012. Tempo of trophic evolution and its impact on mammalian diversification. Proceedings of the National Academy of Science 109:7008–7012.

Román-Palacios, C., J. P. Scholl, and J. J. Wiens. 2019. Evolution of diet across the animal tree. Evolution Letters 3:339–347.

Sánchez-Bayo, F., and K. A. G. Wyckhuys. 2019. Worldwide decline of the entomofauna : A review of its drivers. Biological Conservation 232:8–27.

Siegenthaler, A., J. Campos, O. S. Wangensteen, C. Benvenuto, and S. Mariani. 2019. DNA metabarcoding unveils multiscale trophic variation in a widespread coastal opportunist. Molecular biology and evolution 28:232–249.

Symons, F. B., and G. W. Beccaloni. 1999. Phylogenetic Indices for Measuring the Diet Breadths of Phytophagous Insects. Oecologia 119:427–434.

Winemiller, K. O., and E. R. Pianka. 1990. Organization in Natural Assemblages of Desert Lizards and Tropical Fishes. Ecological Monographs 60:27–55.

Table 4.1: Metrics of diet breadth or specialization and dissimilarity utilized in this study.

Metric	Acronym in this study	Application	Interpretation
Simpson's Diversity Index calculated with prey items identified to species level	TDD, species LPI	Diet breadth	0: highly specialized 1: highly generalized
Simpson's Diversity Index calculated with prey items identified to order level	TDD, order LPI	Diet breadth	0: highly specialized 1: highly generalized
Unrooted, abundance-weighted Faith's phylogenetic diversity	PDD	Diet breadth	Lower PDD: more specialized Higher PDD: less specialized
Mean pairwise phylogenetic distance between prey items within a frog species' diet	MPD	Diet specialization	Lower MPD: more specialized Higher MPD: less specialized
Bray-Curtis dissimilarity calculated with prey items identified to species level	BC, species LPI	Diet dissimilarity	0: no overlap or similiarity 1: complete overlap/identical
Bray-Curtis dissimilarity calculated with prey items identified to order level	BC, order LPI	Diet dissimilarity	0: no overlap or similiarity 1: complete overlap/identical
Mean phylogenetic distance separating prey items between frog species' diets; phylogenetic beta diversity between frog species	MPBD	Diet dissimilarity	Lower MPBD: more similar Higher MPBD: less similar

Table 4.2: Mantel test results comparing diet dissimilarity matrices. Pearson correlation coefficients (r) and Spearman's rank order correlation coefficients (r_s) provided. BC, order LPI: Bray-Curtis dissimilarity calculated using order LPI. BC, species LPI: Bray-Curtis dissimilarity calculated using species LPI. We applied a Bonferroni correction for multiple comparisons; with 6 comparisons and alpha = 0.05, a p-value ≥ 0.008 was required for significance.

	BC, order LPI ~ BC, species LPI	BC, order LPI ~ MPBD	BC, species LPI ~ MPBD
r	0.52*	0.02	0.40*
r_s	0.45*	0.004	0.31

Figure 4.1: Species and order richness accumulation curves for the six frog species in our dataset with the most diet observations.

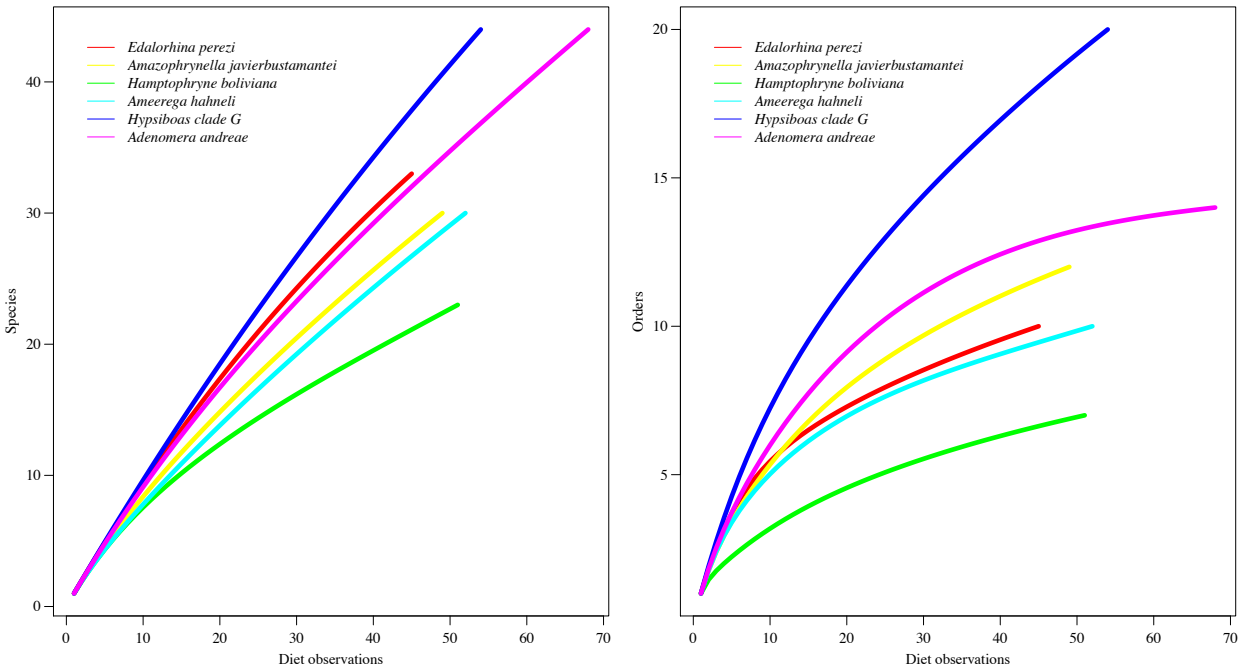

Figure 4.2: Diet niche breadths with 95% confidence intervals estimated for 22 frog species using four different metrics. Species are rank ordered. TDD, species LPI: Simpson's Diversity Index using species level of prey taxonomic identification; TDD, order LPI: Simpson's Diversity Index using order level of prey taxonomic identification; PDD: abundance-weighted unrooted phylogenetic diversity of prey; MPD: mean phylogenetic distance between prey items with abundance weighting.

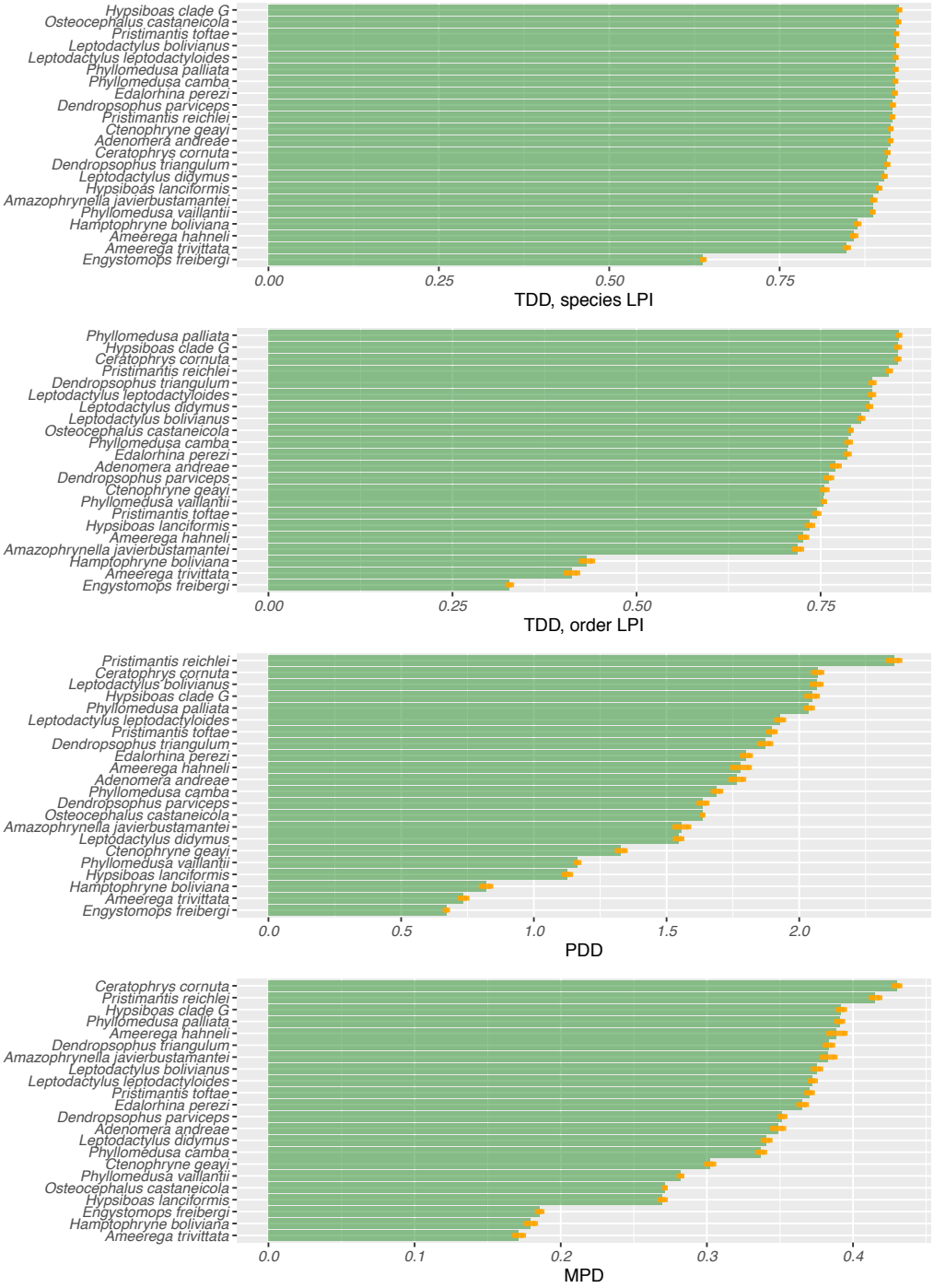

Figure 4.3: Pairwise comparison of diet breadth by species. TDD, species LPI: Simpson's Diversity Index using species level of prey taxonomic identification; TDD, order LPI: Simpson's Diversity Index using order level of prey taxonomic identification; PDD: abundance-weighted unrooted phylogenetic diversity of prey; MPD: mean phylogenetic distance between prey items with abundance weighting. Spearman rank order (r_s) and Pearson correlation (r) coefficients for dietary niche breadth with significant values indicated by an asterisk. We applied a Bonferroni correction for multiple comparisons; with 12 comparisons and alpha = 0.05, a p-value ≥ 0.004 was required for significance. Species that are mentioned in the Results and Discussion are noted with colored symbols: green asterisk is *Engystomops freibergi*; red circle is *Pristimantis reichlei*; blue square and triangle are *Ameerega trivittata* and *Hamptophryne boliviana*, respectively. *Engystomops freibergi* feeds predominantly on termites and *A. trivittata* and *H. boliviana* have high proportions of ants in their diets. Since *E. freibergi* appears to be an outlier and might be driving the positive correlations between metrics, we calculated the correlations between metrics without *E. freiberg*i. Results were unchanged (Table S4.1), with the exception of the relationship between MPD and TDD, species LPI, which was no longer significant.

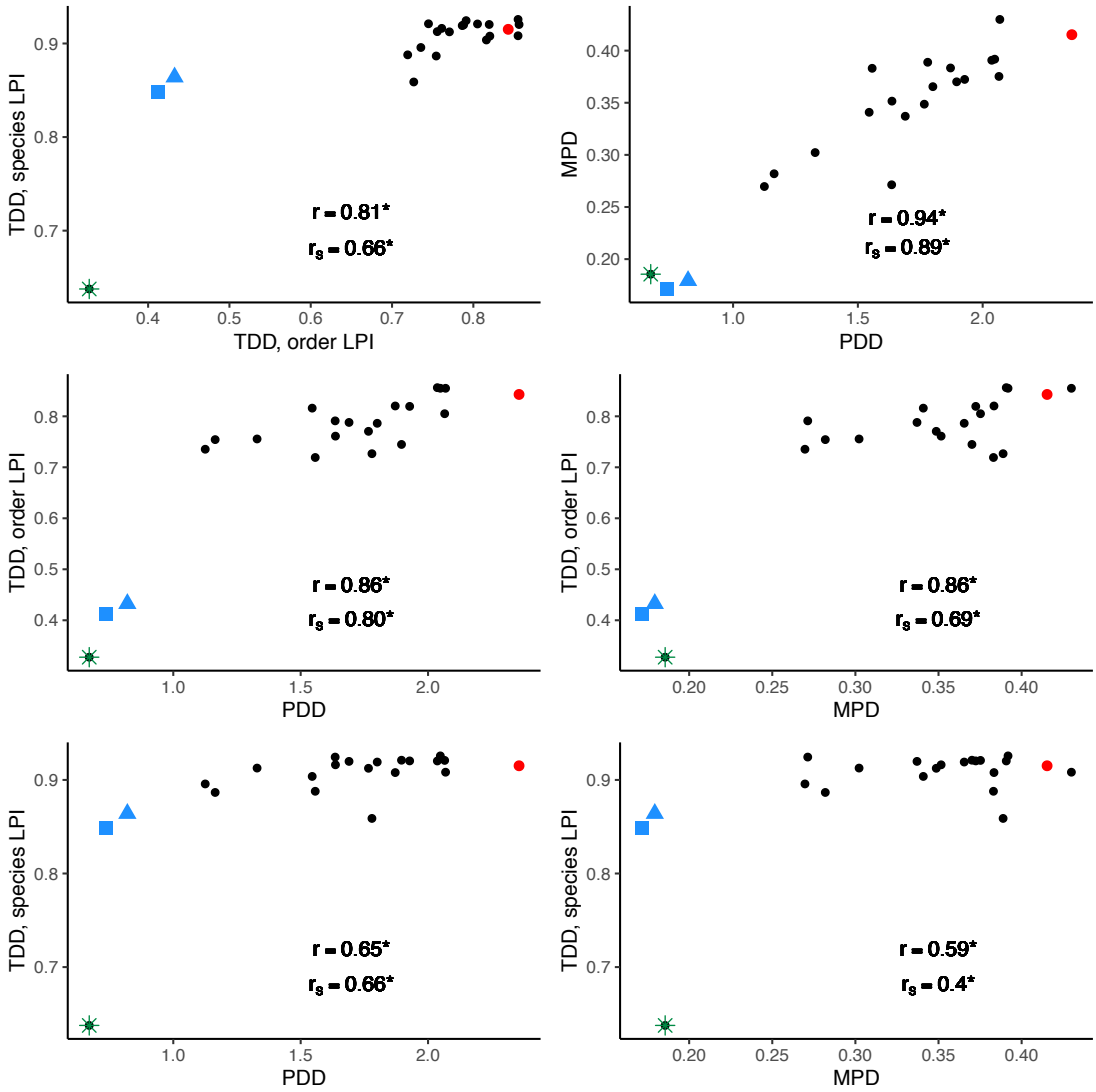

Figure 4.4: Diet dissimilarity matrices. Red indicates greater distance between species. Circle size also indicates magnitude of distance. The Bray-Curtis can vary from 0 to 1 and absolute values calculated at species and order LPI can be compared directly. MPBD does not have an inherent limit, so absolute values are not comparable to Bray-Curtis dissimilarity values. Family membership indicated by bars on right side of each panel: A, Bufonidae; B, Ceratophryidae; C, Dendrobatidae; D, Hylidae; E, Leptodactylidae; F, Microhylidae; G, Strabomantidae**.**

Table S4.1: Pairwise comparison of diet breadth by species without *Engystomops freibergi*. TDD, species LPI: Simpson's Diversity Index using species level of prey taxonomic identification; TDD, order LPI: Simpson's Diversity Index using order level of prey taxonomic identification; PDD: abundance-weighted unrooted phylogenetic diversity of prey; MPD: mean phylogenetic distance between prey items with abundance weighting. Spearman rank order (r_s) and Pearson correlation (r) coefficients for dietary niche breadth with significant values indicated by an asterisk. We applied a Bonferroni correction for multiple comparisons; with 12 comparisons and alpha = 0.05, a p-value ≥ 0.004 was required for significance.

	PDD~MPD	PDD~TDD, species LPI	PDD~TDD, order LPI	MPD~TDD, species LPI	MPD~TDD, order LPI	TDD, order LPI~ TDD, species LPI
Pearson	0.92*	0.70*	0.83*	0.58	0.84*	0.80*
Spearman	0.88*	0.61*	0.76*	0.31	0.65*	0.61*

Figure S4.1: Map of Peru showing sample collection location. Color indicates elevation. Los Amigos Biological Research Station is in the lowland rainforest.

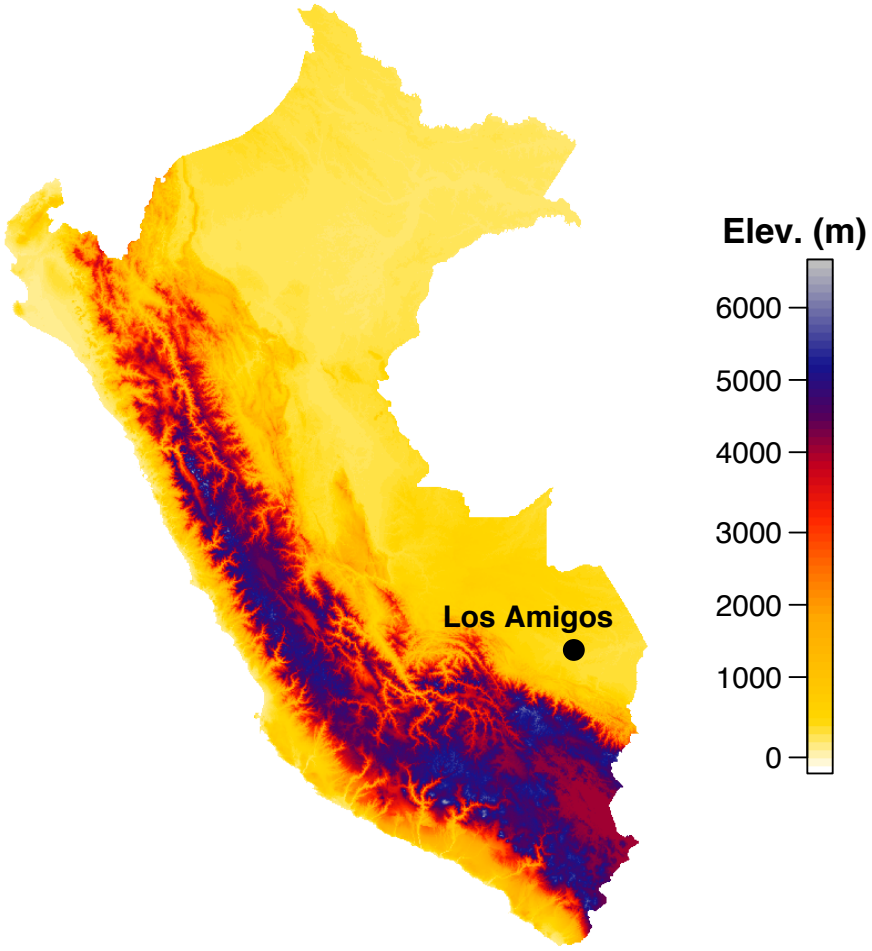

Figure S4.2: Species and order richness accumulation curves for sampled diets in our dataset.

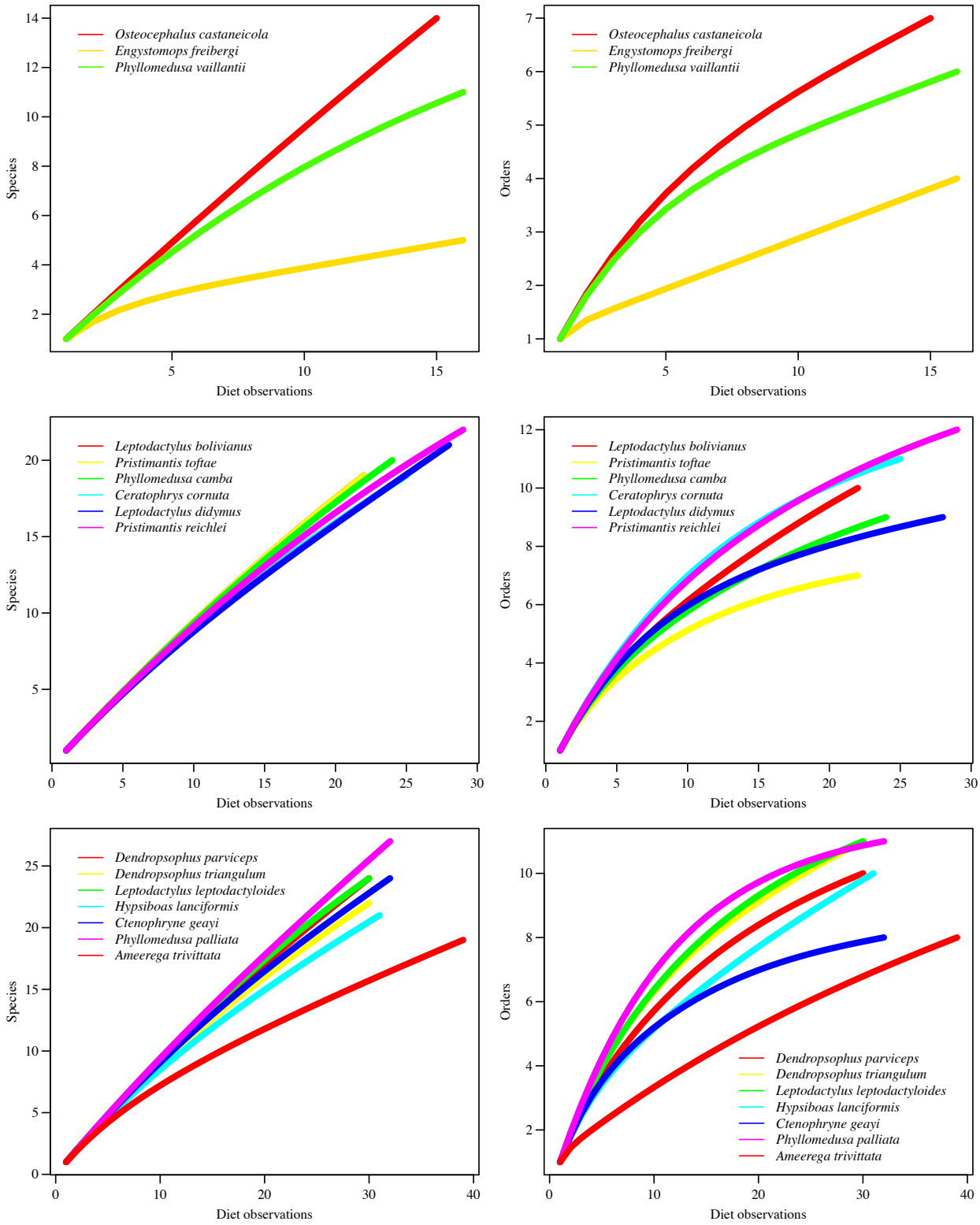

Figure S4.3: Diet dissimilarity calculated with Bray-Curtis dissimilarity index using species LPI. This is the same information as in Figure 4.4, shown here using a different coloring scheme to accentuate patterns in the data. Family membership indicated by bars on right side of each panel: A, Bufonidae; B, Ceratophryidae; C, Dendrobatidae; D, Hylidae; E, Leptodactylidae; F, Microhylidae; G, Strabomantidae.

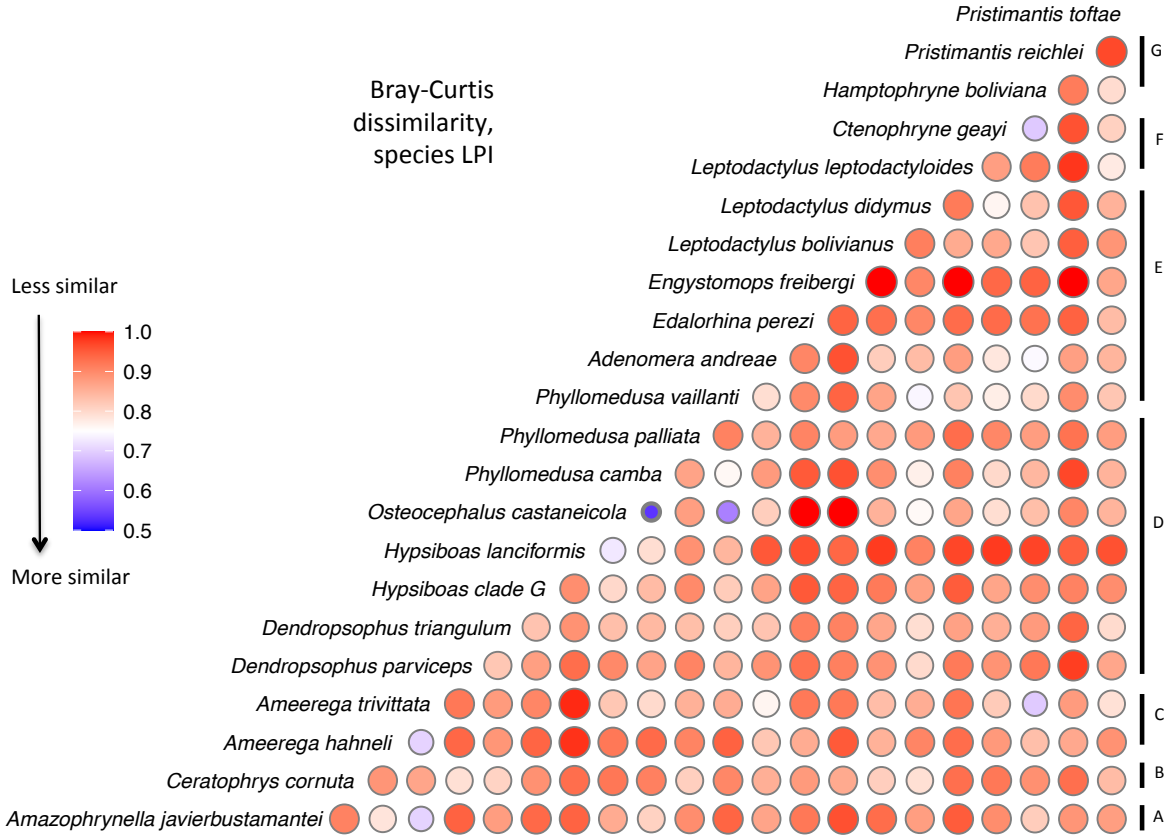

CHAPTER 5

The Impacts Of Evolutionary History On Frog Diets

With Alison Davis Rabosky, Ísis Arantes, Guarino Colli, and Daniel L. Rabosky

ABSTRACT

Diet and the trophic niche are fundamental facets of species' biology, but the evolutionary dynamics of trophic ecology remains poorly understood for many groups of animals. Previous studies suggest that the trophic niche is conserved in some clades over vast spans of evolutionary time (Deep History Hypothesis), whereas evidence from recent evolutionary radiations suggests that trophic niches can evolve quickly and represent a primary axis of divergence. Here we apply a novel metabarcoding approach to quantify the trophic niche of 111 species of frogs in ten families and test whether present-day trophic ecology in frogs shows conservatism congruent with the Deep History Hypothesis or whether it is a more labile trait, shaped by more recent events. We find that evolutionary history has a limited power to explain interspecific differences in diet composition. Frog phylogenetic and taxonomic diet dissimilarity is weakly, but significantly correlated with phylogenetic distance between frog species. Frog diets are remarkably similar despite the large amount of evolutionary time spanned by the clade and we do not find strong evidence of notable shifts in diet composition or trophic innovations. Rather than fitting into a framework of diet reflecting deep history or recent radiations, frog trophic ecology

appears to fit an alternative paradigm of extreme trophic generalism that has not been observed in other vertebrate groups.

INTRODUCTION

Trophic ecology can dramatically and rapidly evolve, as seen in adaptive radiations such as the honeycreepers of Hawaii (Lovette et al. 2002) or the cichlids of the African rift lakes (Seehausen 2006). In these clades, diet is highly labile in both the type and number of prey items. Other groups, such as squamates, appear to display phylogenetic inertia in trophic strategy with major dietary divergences having occurred in deep time (Vitt and Pianka 2005; Colston et al. 2010). Even within snakes, a clade with remarkable trophic diversity (Greene 1997), evolutionary history seems to play a key role in determining how extant species utilize trophic resources, despite lability on other ecological axes (Cadle and Greene 1993; Grundler and Rabosky 2014). Studies on phytophagous insects have also found evidence for taxonomic conservatism in host plant use (Futuyma and Moreno 1988; Crespi and Sandoval 2000; Janz et al. 2001).

In comparison to other vertebrate groups, the question of diet conservatism in frogs has received little direct study. This may stem from the widespread perception that frogs are opportunistic invertivore generalists that will eat any animal they encounter and that will fit in their mouth (Wells 2007). Such an assumption implies that there is little to no variability in diet composition or dietary specialization. However, these conclusions are based on morphological identification of stomach contents. There have been some detailed studies describing frog diets based on frog gut contents (e.g. Toft 1981; Parmelee 1999), but prey have generally been identified to taxonomic rank of order or family because there are significant challenges to morphology-based identification of invertebrates. This level of prey identification can mask

significant specialization and dietary niche differentiation (Burgar et al. 2014; Kartzinel et al. 2015). Despite the limitations on existing data and presumption that frogs select prey largely based on size, there are indications that prey selection is occurring beyond the level of size selection and that it has an evolutionary component (Caldwell and Vitt 1999). Two anecdotal examples of this are found in groups of frogs that appear to have dietary specialization on ants (myrmecophagy) and frogs (anurophagy). Ants are not an energetically profitable prey item due to their small size, high level of indigestible chitin, and chemical defenses, such as formic acid (Redford and Dorea 1984), and specialized ant-feeding behaviors have evolved repeatedly in other groups of vertebrates. Several frog families, such as Bufonidae (true toads) and Dendrobatidae (poison dart frogs) are reported to feed exclusively on or have high proportions of ants in their diets (Wells 2007). Likewise, anurophagy also appears in several lineages with a strong taxonomic bias (Measey et al. 2015). These two trophic strategies are widespread in the frog families in which they occur, but are not common in other clades. It is unclear whether these observations indicate inheritance of a trophic strategy from a common ancestor (phylogenetic conservatism) or lability in diet that facilitated the repeated evolution of a trophic strategy within a clade.

In this paper, we test whether present-day frog diets fit the Deep Time Hypothesis (Vitt and Pianka 2005), such that interspecific differences reflect ancient dietary divergences that have been conserved through time, or whether frogs exhibit high lability in trophic ecology. We leverage molecular metabarcoding methods to generate finely resolved dietary data for 111 frog species from 10 taxonomic families. With these data, we test three hypotheses: i) dietary specialization differs between families of frogs; ii) diet similarity and phylogenetic distance

between frogs are positively correlated; and iii) variation in present-day diets can be explained by dietary shifts in the deep history of frog evolution.

METHODS

Sample collection

We collected stomach contents from eight sites (Table S5.1). Two sites were in Michigan, USA, one in North Carolina, USA, one in the cerrado of Brazil, and four from the lowland Amazonian forests of Peru. Samples were collected through gastric lavage or dissection of frogs immediately after euthanasia. We caught frogs during night and day visual encounter surveys, as well as in pitfall and funnel traps, and removed stomach contents as quickly after capture as possible to reduce digestion of prey items. We stored samples in 96% ethanol at room temperature in the field and subsequently in a -20C or -80C freezer. All procedures that involved handling live animals were reviewed and approved by the University of Michigan Committee on Use and Care of Animals (UCUCA Protocol #PRO00006234). Permits to conduct research and collect biological samples were obtained for all field sites.

Metabarcoding

We processed stomach contents from1,540 frog individuals. For each one, we examined it visually and photographed every prey item with a scale bar. Small prey items were photographed with a microscope and integrated camera system. Larger prey items were photographed with cellphone cameras, and very large prey items were subsampled for DNA extraction. All small prey items and subsamples of large prey items were placed in a 1.5 mL cryovial per sample and dried in a Savant DNA Speed Vac Concentrator. We added two stainless steel beads (1.5 mm) to

each tube and ATL digestion buffer from the Qiagen DNeasy Extraction Kit in 180 µL amounts until the sample was just covered. To homogenize samples, we used a FastPrep machine set at 5.5 m/sec for 60 seconds. We subsequently added Proteinase K in 20 µL aliquots in equal number to the added ATL buffer aliquots, vortexed samples, and briefly centrifuged them to ensure that all fragments of prey items were covered by the digestion mixture. We incubated samples at 56°C for at least 36 hours, after which we briefly vortexed samples and then centrifuged them at 4,000 rpm for three minutes. We transferred the supernatant to a clean 1.5 mL centrifuge tube and then followed the standard Qiagen DNesasy extraction protocol for animal tissues, using UltraPure water for the final elution step. After quantifying extracted DNA with a Qubit flurometer, we standardized each sample to 0.69 ng/µL by dilution or concentration. We found that this relatively low concentration was required to mitigate the impact of PCR inhibitors. Seven extractions did not have sufficient yield and those samples were not processed further.

We used a two-step PCR protocol to prepare amplicon libraries. Based on literature and observation of diet samples, we expected that frogs in our study had consumed mostly arthropods, but that there were also other distantly related taxa, such as Mollusca and Annelida, in their diet samples. In light of this, we targeted a 300-400 bp fragment of the SSU 18S rRNA because the primer binding sites are highly conserved and there are universal primers that reliably amplify this region across all eukaryotes. Specifically, we used the primers SSU-FO4 (5'-GCTTGTCTCAAAGATTAAGCC) and SSU-R22 (5'-GCCTGCTGCCTTCCTTGGA) (Blaxter et al 1998) because they have been used successfully to metabarcode diverse environmental samples with similar taxonomic profiles to our samples (Andújar et al. 2018). We also amplified a 412 bp region of CO1, but since we do not use the resultant sequence data for this paper, we do not discuss amplification conditions for it in detail. We used modified primers that included an

overhang adapter sequence following the Illumina protocol for nested PCRs (16S Library Preparation Protocol at http://support.illumina.com). The two target gene regions were amplified in separate PCR reactions. For the 18S fragment, the PCR recipe consisted of: 3.75 µL of eluted DNA for a total of 2.5 ng of input DNA, 1 µL of each primer at 5 mM, 0.5 µL of DMSO, 6.25 µL of GoTaq Mastermix for a total volume of 12.5 µL. Cycler conditions were: 95ºC for 4 min; 30 cycles of 95ºC for 30 s; 48ºC for 30 s; 72ºC for 3 min, and a final extension of 72ºC for 10 min.

PCR products for CO1 and 18S were pooled by sample and cleaned using a 0.8X AMPure XP magnetic beads (Beckman Coulter) to remove unincorporated reagents. We then performed a short-cycle PCR to attach dual-index barcodes and P5 and P7 Illumina sequencing adapters. This short cycle PCR recipe was: 3 µL of PCR product, 3 µL each of the N5 and N5 indices at 5 mM, 0.25 µL Phusion High Fidelity DNA polymerase (ThermoFisher), 5 µL of 5X Phusion HF Buffer, 0.5 µL dNTPs at 10 mM and 10.25 µL of water for a total reaction volume of 25 µL. Barcodes could be combined to uniquely tag 384 samples (Baym et al. 2015). Cycler conditions for the second PCR were: 95°C for 3 minutes; 8 cycles of 95°C for 30 seconds, 55°C for 30 seconds, 72°C for 30 seconds; and a final extension of 72°C for 5 minutes. We used a 0.6X ratio of AMPure XP magnetic beads (Beckman Coulter) to clean these PCR products and remove all fragments shorter than our targeted amplicons. Then we quantified each sample using a Qubit fluorometer. There were 38 libraries with very low concentrations and these were discarded as failed library constructions. With the remaining 1,495 samples, we created four pooled libraries with samples combined in equimolar concentrations. We pooled samples so that each library consisted of uniquely tagged samples. The four pools contained 380, 373, 370, and 372 samples, respectively. Libraries were sequenced on Illumina MiSeq v2 platforms (500 cycles; 2 x 250 bp

paired-end reads) at the University of Michigan Advanced Genomics Core with a full lane per pooled library.

Bioinformatics

We received demultiplexed sequences from the Advanced Genomics Core and processed them using VSEARCH v2.14.1 (Rognes et al. 2016). We merged paired reads with the default parameters of the –fastq_mergepairs command (--fastq_maxdiffs 10). During this step, we separated CO1 and 18S amplicons based on merged read length. We did not process CO1 sequences further and all subsequent references to sequences in this paper refer solely to the 18S data. We trimmed reads to remove primer sequences and quality filtered (Maxee = 1.0). These quality-filtered and trimmed reads were then separated into two pools based on geographic origin to improve the downstream clustering step. One pool contained all samples from the USA and the other consisted of the samples from Peru and Brazil. Sequences in these pools were then dereplicated using full length matching (--derep_fulllength) and we discarded unique sequences represented by less than 10 reads (--minuniquesize 10). We clustered dereplicated sequences into molecular operational taxonomic unites (MOTUs) at 97% similarity and checked for chimeras using the uchime-denovo algorithm (Edgar et al. 2011), implemented in VSEARCH as --uchime3_denovo. We assigned taxonomy to MOTUs using the SILVA 18S database (v123) and mapped reads onto these annotated MOTUs with the --usearch_global command.

Since we used universal eukaryotic primers, some of our MOTUs corresponded to non-prey items, such as the frog consumers, incidentally ingested plant material, parasites, and secondary prey items. To address some of these issues, we filtered sequences by taxonomy using the q2-taxa plugin within Qiime 2.0 2019.10 (Bolyen et al. 2019). Our first step was to discard all

MOTUs that were not identified as metazoans, a decision based on observation of diet samples prior to DNA extraction and published literature (Wells 2007). We also removed all sequences identified as Nematoda or Platyhelminthes, which are parasites. The 110 samples with less than 1,000 reads at this point in the pipeline were considered to be unsuccessful libraries and not processed further.

Distinguishing between prey items and secondary prey items is a significant concern for this study given that there is potential for a large overlap in the diets of frogs and some of their prey items. For example, spiders, a frequent prey item of frogs, also consume arthropods and it is therefore not possible to remove secondary prey items through taxonomic filtering. We chose to use relative read abundance (RRA) to filter out secondary prey items under the assumption that secondary prey items would have lower RRAs relative to primary prey items. To select a threshold RRA, we compared the MOTU profiles with RRA of a subset of frog individuals against the photographs of diet samples. Based off of these comparisons, we set a minimum threshold of 5% RRA by sample for an MOTU to be retained as a primary prey item. Since our primary goal is to elucidate the diet of frogs at the species rather than individual level, we adopted this high threshold to prioritize removal of false positives, potentially at the expense of introducing false negatives, although we expect this number to be low or zero. Also, for most species, we have diet samples from multiple individuals and if a prey species is an important component of the species' diet it will be detected in more than one sample, so a false negative in one sample will not deeply impact our results.

A final consideration for analysis of this sample type is the phenomena of anurophagy, which we knew to be present in our samples. We hand curated all MOTUs identified as vertebrates, using photographs of prey items to determine whether sequences corresponded to a

vertebrate prey item or consumer DNA. We then converted the MOTU tables to binary presence or absence data because RRA for metabarcode data of stomach contents is not a reliable estimator of biomass, since prey items can be at varying levels of digestion (Deagle et al. 2018). Tables were then merged by frog species with records summed across individuals, such that values reflect the number of frog individuals observed to have eaten a particular prey taxon.

Within the Qiime 2 platform (Bolyen et al. 2019), we constructed a phylogeny of the prey MOTUs. We created a multiple sequence alignment using MAFFT (Katoh and Standley 2013) (via q2-alignment) and estimated an unrooted phylogeny using fasttree2 (Price et al. 2010) (via q2-phylogeny). We rooted this tree using the *root* function in the ape ver 5.3 R package (Paradis and Schliep 2019) with Chordata as the outgroup to Annelida, Mollusca, and Arthropoda.

Frog diet breadth and evolutionary history

One of our main hypotheses is that dietary niche breadth will vary between frog species and that dietary specialization will be evolutionarily conserved once it evolves. We estimated dietary niche breadth as the phylogenetic diversity of diet items (PDD). Specifically, we calculated this as the abundance-weighted unrooted Faith's phylogenetic distance (Faith 1992) using R code from (Swenson 2014). We modified this code to assign a value of zero to any species that consumed only one prey taxon. Since we have unequal sampling between frog species and PDD is sensitive to sampling, we subsampled diet observations to five per species before calculating this metric and took the mean of 1,000 iterations in order to have comparable values for each species. We did this for the 111 frog species that had a minimum of five diet observations. As a complementary approach, we also computed a metric of taxonomic dietary diversity (TDD), using Simpson's Diversity Index with prey items identified to order level.

Although TDD and PDD in frogs is often positively correlated, variance between the two approaches can reveal informative patterns of resource use (Chapter 4).

We calculated phylogenetic signal in PDD and TDD to test whether this is a labile or evolutionarily conserved trait in frogs. For a phylogenetic framework of frog species, we utilized a published time-calibrated phylogeny of amphibians (Jetz and Pyron 2018). Because reliance on phylogenies that include species placed using polytomy resolvers rather molecular data can result in biased estimates of trait evolution (Rabosky 2015), we only consider the 92 frog species in our dataset that are in the molecular backbone of the phylogeny.

We also used one-way phylogenetic ANOVAs to test whether PDD and TDD vary between frog families. Phylogenetic ANOVAs were implemented using the phylANOVA function in the R package *phytools* ver. 0.6.99 (Revell 2012). Assignment of species to family was based on the taxonomic framework of AmphibiaWeb (2020) and the 92 species were separated into ten families.

Frog diet similarity and evolutionary history

We test the relationship between frog evolutionary history and diet similarity using two complementary approaches: correlations between distance matrices for frog phylogenetic relationships and diet dissimilarity and a canonical phylogenetic ordination (CPO). The first approach uses Mantel tests to evaluate whether interspecific diet dissimilarity is correlated with the phylogenetic distance between species. The limitation of this method is that it assesses associations across the full frog tree and does not have the ability to detect important dietary shifts within the tree. While also finding associations between matrices, CPO also determines the importance of shifts in diet at nodes in the phylogeny (Ter Braak and Verdonschot 1995;

Giannini 2003). A form of constrained ordination, CPO, associates variation within the matrix of dietary resource use to the variation in a matrix of frog phylogenetic relationships.

For testing how diet dissimilarity is correlated with phylogenetic distance between frog species, we consider the same set of 92 frog species that were used to compute phylogenetic signal in PDD and TDD. We use the *cophenetic* function in ape (Paradis and Schliep 2019) to calculate the phylogenetic distance between frog species based on the phylogeny of Jetz and Pyron (2018). We use the same function to compute the phylogenetic distance between prey MOTUs based on the phylogeny we constructed. As a measure of phylogenetic diet dissimilarity, we calculate the mean pairwise phylogenetic distance (MPBD) of diets between frog species using the *comdist* function in picante (Kembel et al. 2010), which is a measure of phylogenetic beta diversity. It is the expected pairwise phylogenetic distance between diet observations from different frog species. We also calculated the Bray-Curtis dissimilarity index using order LPI as a measure of differences in taxonomic dietary composition, since this metric and MPBD have been shown to be uncorrelated in frogs and measuring distinct dimensions of dietary diversity (Chapter 4). To test the relationship between these diet dissimilarity matrices and phylogenetic dissimilarity between frogs, we implemented a Mantel test in the R package *vegan* (Oksanen et al. 2019).

To test whether interspecific dietary variation can be explained by dietary shifts in deep time, we utilized a CPO following the approach of Vitt and Pianka (2005). Our dietary matrix included the dietary profiles for 111 frog species, with prey grouped at the order level. The independent variable was a binary matrix indicating the family membership of each frog species (Giannini 2003; Colston et al. 2010). We tested each independent variable individually using symmetric scaling to determine the amount of variation it explained and calculated F and P

values using Monte Carlo permutation tests (n = 9,999). We then added variables to the model in decreasing order of explained variance, stopping after subsequent variables were not significant.

Finally, we test whether the proportional utilization of Hymenoptera displays phylogenetic signal. Figure 5.1 indicates that there is variation in importance of ants and wasps in the diets of frogs and species that heavily utilize this prey category appear to be phylogenetically clustered. We apply a logit transformation to the utilization proportion of Hymenoptera across the 92 species represented in the molecular phylogeny and calculate Pagel's λ.

RESULTS

DNA sequencing

After quality filtering and removing libraries that were not from amphibian consumers, we had 1,325 successful libraries. These provided data on the diets of 152 species of frogs, three species of salamanders, and one species of caecilian. We identified 741 MOTUs in these samples from 44 orders, 12 classes, and four phyla. After restricting the dataset to only frog species with at least five diet observations, we had a dataset of 111 frog species that had dietary observations for 725 MOTUs from 43 orders, 12 classes, and four phyla (Figure 5.1). The mean number of diet observations per species was 24.5 (range: 5 – 145).

Dietary niche breadth

We calculated PDD and TDD for 111 species of frog, which each had at least five dietary observations and found that there is clear variation in the PDD between frog species, with slightly less variation in TDD (Figure 5.2). However, when we estimated phylogenetic signal in PDD across the 92 frog species for which a molecular-based phylogenetic framework exists (Jetz and

Pyron 2018; Figure S5.1), we did not find support for our hypothesis that phylogenetic dietary niche breadth would reflect the evolutionary history of frogs. Instead we find that PDD does not show phylogenetic signal, with Pagel's lambda = 0.39 (P = 0.75). When we considered distribution of TDD (Figure 5.2 and Figure S5.1), we found less interspecific variation, but statistical support for phylogenetic signal ($\lambda = 0.70$; $P < 0.001$).

We also tested whether PDD or TDD differ between frog families with phylogenetic one-way ANOVAs and found that neither are statistically different between families (PDD: F= 2.38, P=0.977; TDD: F = 4.80, P= 0.826).

Dietary similarity

To test whether similarity in diet between frog species is influenced by evolutionary history, we applied a Mantel test to the matrices of pairwise phylogenetic distances between frogs and phylogenetic diet dissimilarity, which was calculated as the mean pairwise phylogenetic distance. The results, Mantel statistic r = 0.24 (P = 0.005), indicate that there is a significant positive correlation between the two metrics, although the low Mantel statistic indicates that it is relatively weak correlation (Figure S5.2). We discovered a similarly significant, but weak correlation between frog phylogenetic distances and diet dissimilarity calculated as Bray-Curtis dissimilarity with prey identified to order level (r = 0.24; P = 0.001; Figure S5.2).

Using CPO, we found that variance in diet was significantly reduced by six frog families: Pipidae, Ceratophryidae, Bufonidae, Ranidae, Dendrobatidae, and Hylidae, (Figure 5.3; Table 1). These clades explained 29.66% of the total residual variance observed in the dataset. The most basal divergence in our dataset, the split between Pipidae and all the other clades, accounts for 16.29% residual variation. The single pipid species, *Pipa pipa*, sits in a distinct spot within the

CPO plot, driven by the high proportion of fish in its diet (Figures 5.1 and 5.4); in our dataset, 50% of the diet observations for this species are Siluriformes, catfish. The single representative species of Ceratophryidae, *Ceratophrys cornuta*, is also positioned far from other species in the CPO plot because of anurophagy (Figure 5.4). Aside from these two outlier species, all the frog species and prey categories are located near the center of the ordination space, indicating that most species are highly similar in diet. There is a gradient along CCA2 that roughly corresponds to the proportion of hymenopteran prey in the diet. The vectors for Bufonidae and Dendrobatidae, species of which consume high proportions of ants, are oppositely aligned to those of Ranidae, Hylidae, and Ceratophryidae, all of which do not as heavily feature hymenopterans in their diets (Figures 5.1 and 5.4). We found that the proportional utilization of Hymenoptera showed strong phylogenetic signal ($\lambda = 0.82$; $P < 0.001$).

DISCUSSION

We examined the relationship between evolutionary history and present-day diets across 111 species of frogs and found a striking lack of association. Our results indicate that there is an effect of evolutionary history on observed frog diets, but that it is not a major determinant. We identified nodes in the phylogeny at which statistically significant splits in diet occurred, but these events only account for a little less than 30% of the observed variation in diet. This stands in sharp contrast to deep history dietary divergences within squamates and snakes that explain nearly 80% and 70% of present-day variation, respectively (Vitt and Pianka 2005; Colston et al. 2010). The correlation between phylogenetic distance between frog species and diet dissimilarity across the phylogeny also supported a limited effect of phylogeny on diet because, while statistically significant, it is not strong.

At the same time that we cannot ascribe variance in diet to divergences in deep history, we also cannot attribute this lack of association to rapid and dramatic divergence in trophic strategy in recent history as we see in certain adaptive radiations, such as cichlids (Seehausen 2006) and honeycreepers (Lovette et al. 2002). Instead, it appears that frogs have remained startlingly consistent in diet composition over the course of their evolutionary history with few divergences from a broad diet of invertebrates (Figures 5.1 and 5.4). The majority of diet observations are concentrated within several invertebrate orders. Even though these are orders, it is startling that frogs have not taxonomically diversified more in diet, given that frogs are an ancient lineage with its origins in the Mesozoic. Given these results, we propose a novel paradigm, the Phylogenetically Widespread Hyper-Generalism Hypothesis, to describe frog trophic ecology. This framework is characterized by generalized diets, high interspecific overlap, and limited specialization despite the amount of evolutionary time spanned by the clade.

The few frog species that exhibit exceptions to the general pattern of generalist invertivory are also in the clades identified by canonical phylogenetic ordination as the ones that most significantly reduce residual variation. Pipidae, the clade that accounted for the most variation, is represented by *Pipa pipa,* which is the only truly aquatic frog represented in this study and has a highly distinct diet. It captures and ingests prey in a way that sets it apart from other frogs, since it lacks a tongue and captures prey through inertial suction (Carreño and Nishikawa 2001).

Consumption of vertebrates has previously been documented in dozens of frog species and families (Wells 2007; Measey et al. 2015). The diet of *Ceratophrys cornuta* (Ceratophryidae) has been documented to have a high proportion of vertebrates (Duellman and Lizana 1994) and this is reflected in our dataset, with anurans forming 16% of the diet observations that we have

for the species. We also detected what we believe to be the first record of *Oreobates* eating a vertebrate. Specifically, we found that an adult *O. quixensis* had eaten a juvenile, perhaps hatchling, *Cerscosaura* sp., a small leaf litter lizard (Gymnothalmidae).

Although molluscivory has generally been considered to be rare in frogs (Wells 2007), we observed this behavior in 17 species across five families. While previous reports have been confined to terrestrial frog species, we documented molluscivory in six hylid tree frog species.

One axis of dietary divergence that emerges is whether species consume hymenopterans as an important component of their diet or not. Figure 5.1 conveys that most frog species consume hymenopterans to some degree and that hymnopterans compose 50% of more of the diets for many species. In fact, *Elachistocleis muirquitan* was observed eating only ants. "Ant specialization" appears to be concentrated in Bufonidae, Dendrobatidae, and Microhylidae and we find a strong phylogenetic signal in the proportional utilization of this prey category. Heavy consumption of ants occasionally appears within families that otherwise do not primarily eat ants. A prime example of this is the two species within Hylidae, *Sphaenorhynchus carneus* and *S. lacteus*, for which over 50% of the diet observations are hymenopteran species. We would not term this a major trophic innovation or shift however, because these species merely shift the relative proportions of ants in diets rather than adding a taxonomically or phylogenetically novel prey category.

In conclusion, we find that evolutionary history has limited power to explain diet of present-day frogs and frogs are strikingly homogeneous in diet despite the long evolutionary history of the clade. They do not fit within the paradigms of phylogenetic conservatism or lability applied to the trophic ecology of other groups of animals, and instead require a new framework defined by the strong trend towards a hypergeneralist diet.

DATA AVAILABILITY

FASTA sequences and photographs of stomach contents samples will be available through the University of Michigan Library Digital Collections.

REFERENCES

AmphibiaWeb. 2020. <https://amphibiaweb.org> University of California, Berkeley, CA, USA. Accessed 22 Jan 2020.

Andújar, C., P. Arribas, C. Gray, C. Bruce, G. Woodward, D. W. Yu, and A. P. Vogler. 2018. Metabarcoding of freshwater invertebrates to detect the effects of a pesticide spill. Molecular Ecology 27:146–166.

Baym, M., S. Kryazhimskiy, T. D. Lieberman, H. Chung, M. M. Desai, and R. Kishony. 2015. Inexpensive multiplexed library preparation for megabase-sized genomes. PloS one 10:1–15.

Bolyen, E., J. Rideout, M. Dillon, N. Bokulich, C. Abnet, G. Al-Ghalith, H. Alexander, et al. 2019. Reproducible, interactive, scalable and extensible microbiome data science using QIIME 2. Nature biotechnology 37:852–857.

Burgar, J. M., D. C. Murray, M. D. Craig, J. Haile, J. Houston, V. Stokes, and M. Bunce. 2014. Who's for dinner? High-throughput sequencing reveals bat dietary differentiation in a biodiversity hotspot where prey taxonomy is largely undescribed. Molecular Ecology 23:3605–3617.

Cadle, J. E., and H. W. Greene. 1993. Phylogenetic patterns, biogeography, and the ecological structure of neotropical snake assemblages. Species diversity in ecological communities: historical and geographical prespectives 281–293.

Caldwell, J. P., and L. J. Vitt. 1999. Dietary asymmetry in leaf litter frogs and lizards in a transitional northern Amazonian rain forest. Oikos 84:383–397.

Carreño, C. A., and K. C. Nishikawa. 2001. Aquatic feeding in pipid frogs : the use of suction for prey capture. Journal of Experimental Biology 213:2001–2008.

Colston, T. J., G. C. Costa, and L. J. Vitt. 2010. Snake diets and the deep history hypothesis. Biological Journal of the Linnean Society 101:476–486.

Crespi, B. J., and C. P. Sandoval. 2000. Phylogenetic evidence for the evolution of ecological specialization in Timema walking-sticks. Journal of Evolutionary Biology 13:249–262.

Deagle, B. E., L. J. Clarke, A. C. Thomas, J. C. Mcinnes, E. J. Vesterinen, E. L. Clare, T. R. Kartzinel, et al. 2018. Counting with DNA in metabarcoding studies : How should we convert sequence reads to dietary data ?

Duellman, W. E., and M. Lizana. 1994. Biology of a Sit-and-Wait Predator , the Leptodactylid Frog Ceratophrys cornuta. Herpetologica 50:51–64.

Edgar, R. C., B. J. Haas, J. C. Clemente, C. Quince, and R. Knight. 2011. UCHIME improves sensitivity and speed of chimera detection. Bioinformatics 27:2194–2200.

Faith, D. P. 1992. Conservation evaluation and phylogenetic diversity. Biological Conservation 61:1–10.

Futuyma, D. J., and G. Moreno. 1988. The evolution of ecological specialization. Annual Review of Ecology and Systematics 19:207–233.

Giannini, N. P. 2003. Canonical Phylogenetic Ordination. Systematic biology 52:684–695.

Greene, H. W. 1997. No TitleSnakes: the evolution of mystery in nature. University of California Press, Berkeley, CA.

Grundler, M. C., and D. L. Rabosky. 2014. Trophic divergence despite morphological convergence in a continental radiation of snakes. Proceedings of the Royal Society B: Biological Sciences 281:20140413.

Janz, N., K. Nyblom, and S. Nylin. 2001. Evolutionary dynamics of host-plant specialization : a case study of the tribe Nymphalini. Evolution 55:783–796.

Jetz, W., and R. A. Pyron. 2018. The interplay of past diversification and evolutionary evolutionary isolation with present imperilment across the amphibian tree of life. Nature Ecology & Evolution 2:850–858.

Kartzinel, T. R., P. A. Chen, T. C. Coverdale, D. L. Erickson, W. J. Kress, M. L. Kuzmina, D. I. Rubenstein, et al. 2015. DNA metabarcoding illuminates dietary niche partitioning by African large herbivores. Proceedings of the National Academy of Science 112:8019–8024.

Katoh, K., and D. M. Standley. 2013. MAFFT Multiple Sequence Alignment Software Version 7 : Improvements in Performance and Usability. Molecular biology and evolution 30:772–780.

Kembel, S. W., P. D. Cowan, M. R. Helmus, W. K. Cornwell, H. Morlon, D. D. Ackerly, S. P. Blomberg, et al. 2010. Picante: R tools for integrating phylogenies and ecology. Bioinformatics 26:1463-1464.

Lovette, I. J., E. Bermingham, and R. E. Ricklefs. 2002. Clade-specific morphological diversification and adaptive radiation in Hawaiian songbirds. Proceedings of the Royal Society B: Biological Sciences 269:37–42.

Measey, G. J., G. Vimercati, F. Andr, M. M. Mokhatla, S. J. Davies, and S. Edwards. 2015. Frog eat frog : exploring variables influencing anurophagy. PeerJ 3:e1204:1–16.

Oksanen, J., F. G. Blanchet, R. Kindt, P. Legendre, P. R. Minchin, R. B. O'Hara, G. L. Simpson, et al. 2019. vegan: Community Ecology Package. R package version 2.5-6 https://CRAN.R-project.org/package=vegan.

Paradis, E., and K. Schliep. 2019. ape 5 . 0 : an environment for modern phylogenetics and evolutionary analyses in R. Bioinformatics 35:526–528.

Parmelee, J. R. 1999. Trophic Ecology of a Tropical Anuran Assemblage. Scientific Papers Natural History Museum the University of Kansas 11:1–59.

Price, M. N., P. S. Dehal, and A. P. Arkin. 2010. FastTree 2 – Approximately Maximum-Likelihood Trees for Large Alignments. PloS one 5:e9490.

Rabosky, D. L. 2015. No substitute for real data : A cautionary note on the use of phylogenies from birth – death polytomy resolvers for downstream comparative analyses. Evolution 69:3207–3216.

Redford, H., and J. G. Dorea. 1984. The nutritional value of invertebrates with emphasis on ants and termites as food for mammals. Journal of Zoology 203:385–395.

Revell, L. J. 2012. phytools : an R package for phylogenetic comparative biology (and other things). Methods in Ecology and Evolution 2012:217–223.

Rognes, T., T. Flouri, B. Nichols, C. Quince, and F. Mahé. 2016. VSEARCH : a versatile open source tool for metagenomics. PeerJ 4:e2584.

Seehausen, O. 2006. African cichlid fish : a model system in adaptive radiation research. Proceedings of the Royal Society B: Biological Sciences 273:1987–1998.

Swenson, N. G. 2014. Functional and Phylogenetic Ecology in R. Springer, New York, New York.

Ter Braak, C. J. F., and P. F. M. Verdonschot. 1995. Canonical correspondence analysis and related multivariate methods in aquatic ecology. Aquatic Sciences 57:255–289.

Toft, C. A. 1981. Feeding Ecology of Panamanian Litter Anurans : Patterns in Diet and Foraging Mode. Journal of Herpetology 15:139–144.

Vitt, L. J., and E. R. Pianka. 2005. Deep history impacts present-day ecology and biodiversity. Proceedings of the National Academy of Science 102:7877–7881.

Wells, K. D. 2007. The ecology and behavior of amphibians. University of Chicago Press, Chicago, IL.

Table 5.1: Results of a canonical phylogenetic ordination, ranked in descending order by the amount of residual variance explained by each clade.

Clade	Variation	Variation %	*F* value	*P* value
Pipidae	0.503	16.288	24.399	0.0001
Ceratophryidae	0.135	4.372	6.538	0.00859
Hylidae	0.09	2.914	4.382	0.0001
Bufonidae	0.052	1.684	2.514	0.0343
Ranidae	0.086	2.785	4.165	0.0221
Dendrobatidae	0.05	1.619	2.431	0.031
Leptodactylidae	0.036	1.166	1.741	0.068
Microhylidae	0.031	1.004	1.526	0.138
Craugastoridae	0.022	0.712	1.072	0.259
Strabomantidae	0.022	0.712	1.072	0.259

Figure 5.1: Proportional utilization of prey orders by frog species with phylogenetic relationships between from pruned from Jetz and Pyron (2018).

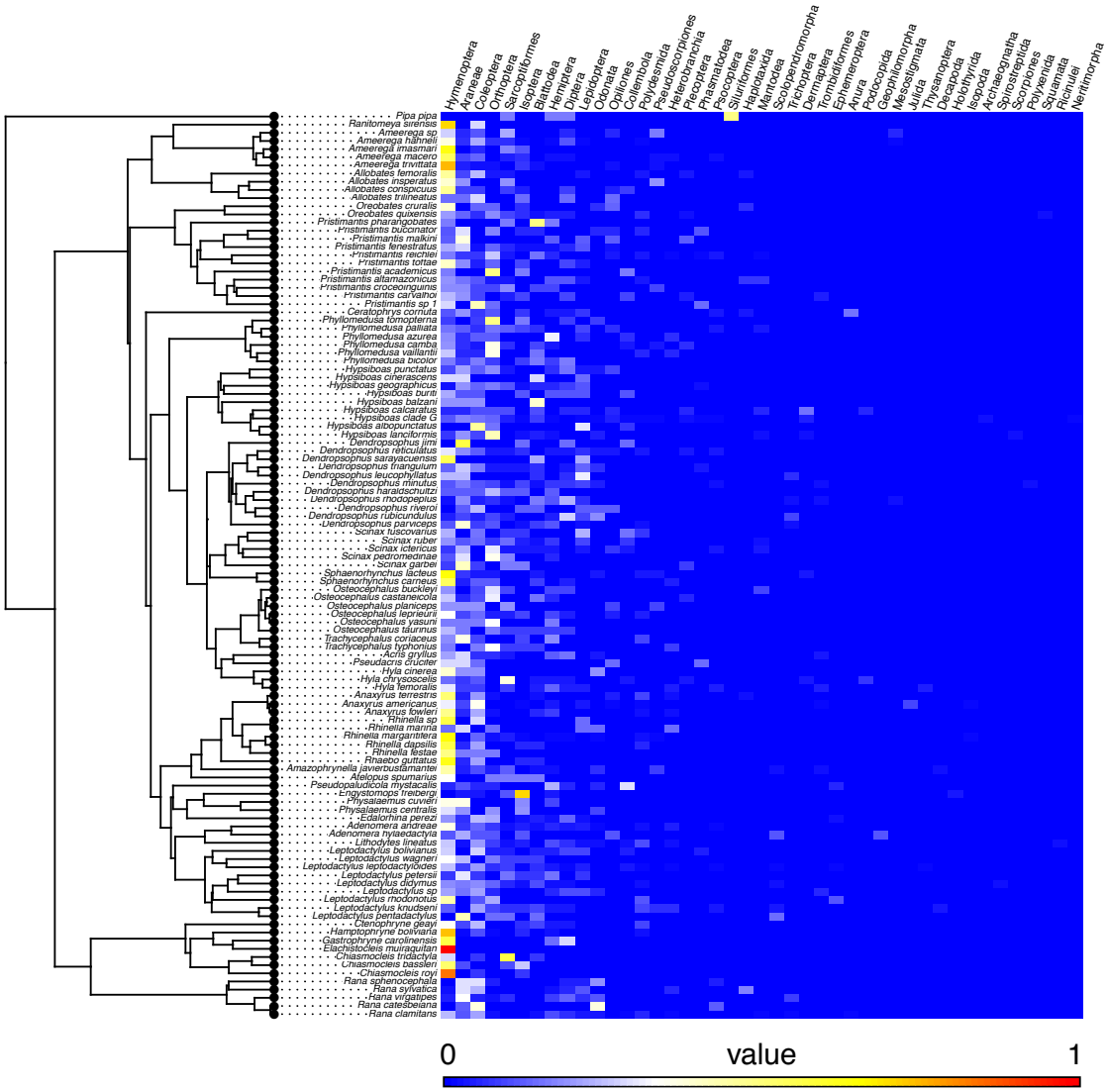

Figure 5.2: Taxonomic and phylogenetic dietary diversity distribution across frogs. Results of a one-way phylogenetic ANOVA testing whether (a) phylogenetic dietary diversity (PDD) or (b) taxonomic dietary diversity (TDD) differs between frog taxonomic families. No significant differences were detected. Time-calibrated molecular phylogeny pruned from Jetz and Pyron (2018).

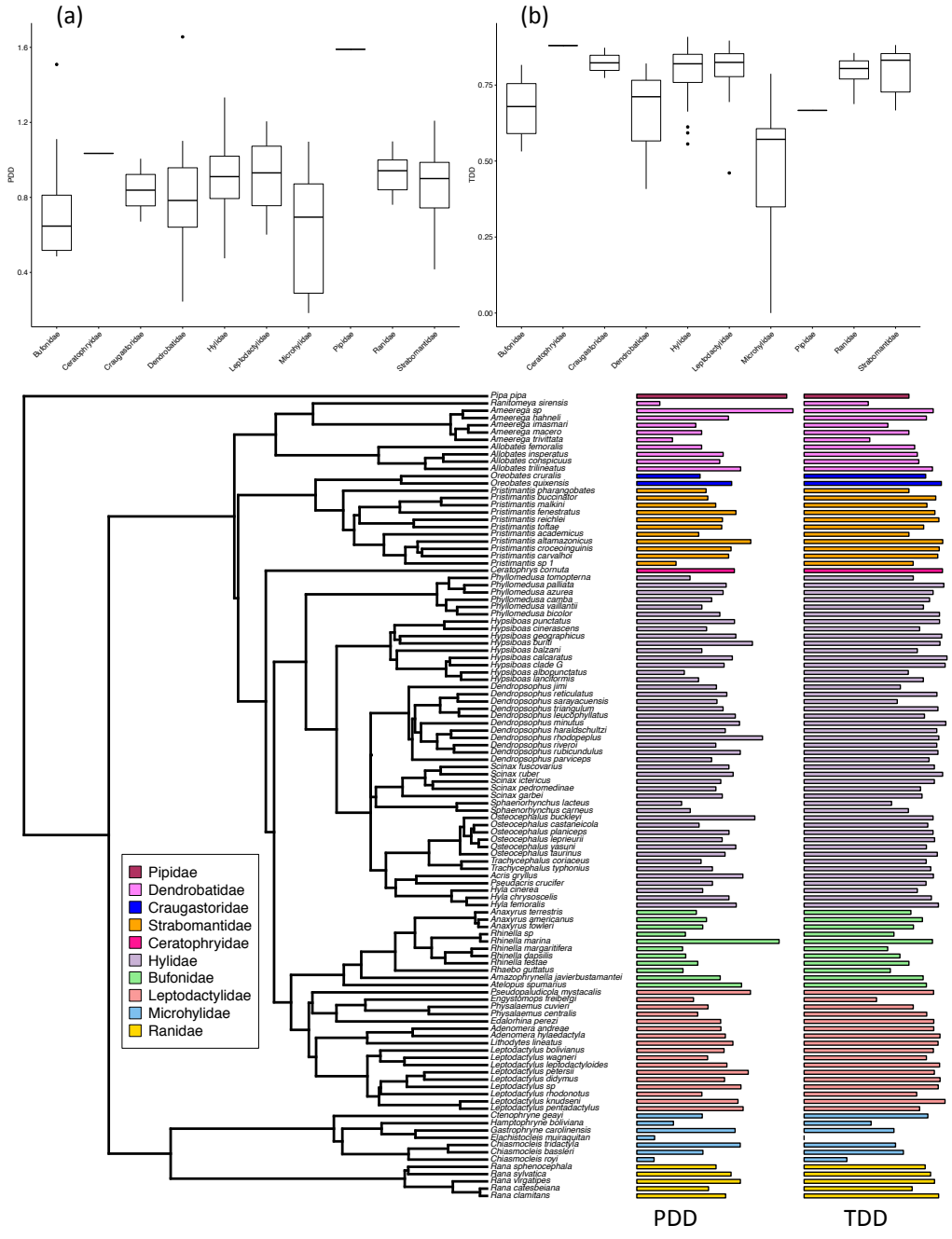

Figure 5.3: Phylogenetic relationships between the species used in this study. Solid blue circles indicate clades that were significant in the stepwise canonical phylogenetic ordination (CPO). Phylogeny pruned from Jetz and Pyron (2018). Photographs courtesy of Consuelo Alarcon Rodriguez.

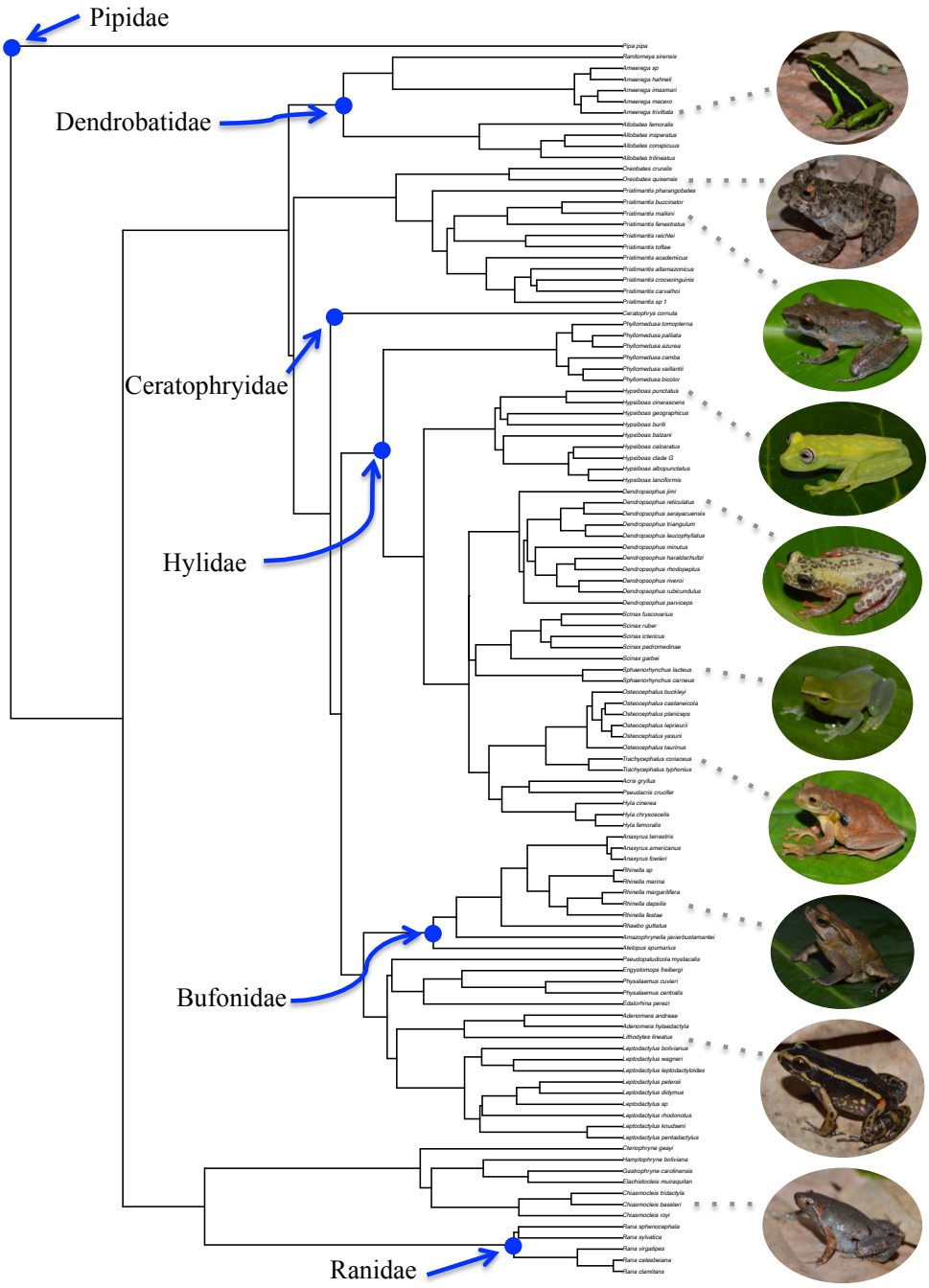

Figure 5.4: Results of a canonical phylogenetic ordination. Clades that significantly reduce variation are plotted with the length of the vector indicating strength of significance.

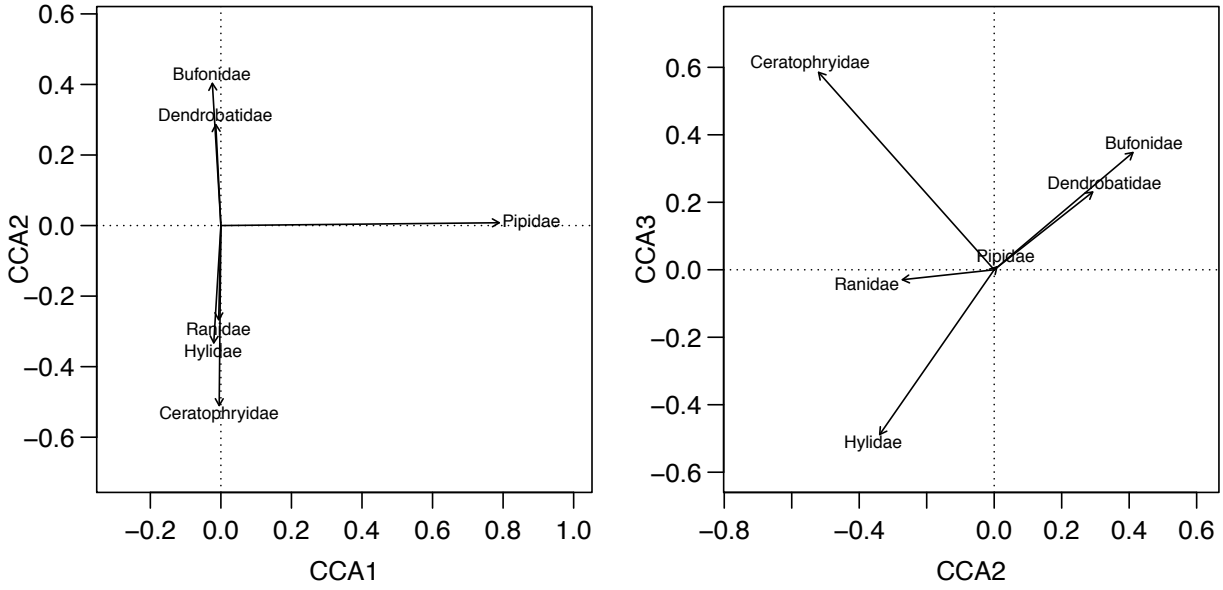

Table S5.1: Sampling location information.

Location	Coordinates
West Park, Ann Arbor, Michigan, USA	42.282867 -83.755727
E. S. George Reserve, Pinckney, Michigan, USA	42.46101 -84.02527
Sandhills Gameland, Hoffman, North Carolina, USA	34.97489 -79.59613
Santa Cruz Research Station, Loreto, Peru	-3.52859599 -73.1790750
Madre Selva Research Station, Loreto, Peru	-3.61722222 -72.23555556
Villa Carmen Research Station, Cusco, Peru	-12.8955 -71.4038
Los Amigos Research Station, Madre de Dios, Peru	-12.5969167 -70.100111
Brasília, Federal District, Brazil	-15.638363 -47.683767

Figure S5.1: TDD and PDD for the 92 species found in the molecular backbone phylogeny of Jetz and Pyron (2018).

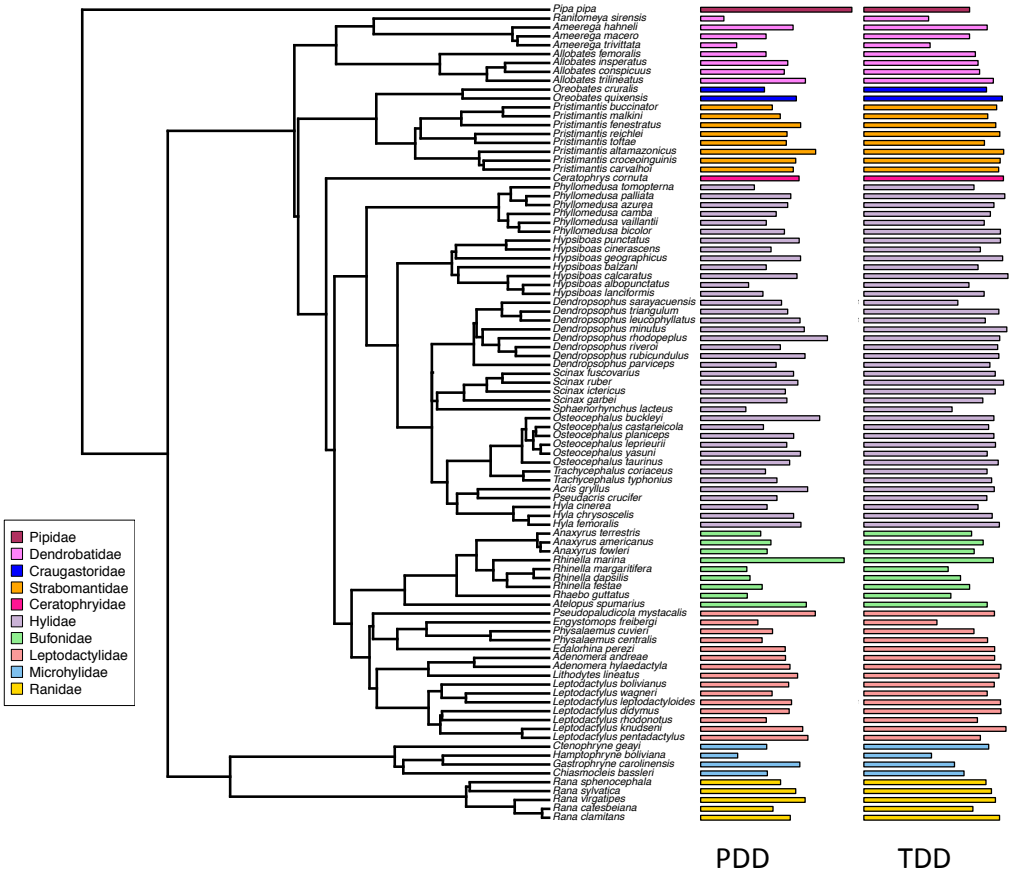

Figure S5.2: Relationships between interspecific frog phylogenetic distance and diet dissimilarity. Left: Diet dissimilarity calculated as the Bray-Curtis dissimilarity index with prey items identified to order level. Right: Diet dissimilarity computed as the mean pairwise phylogenetic distance between prey items of frog species.

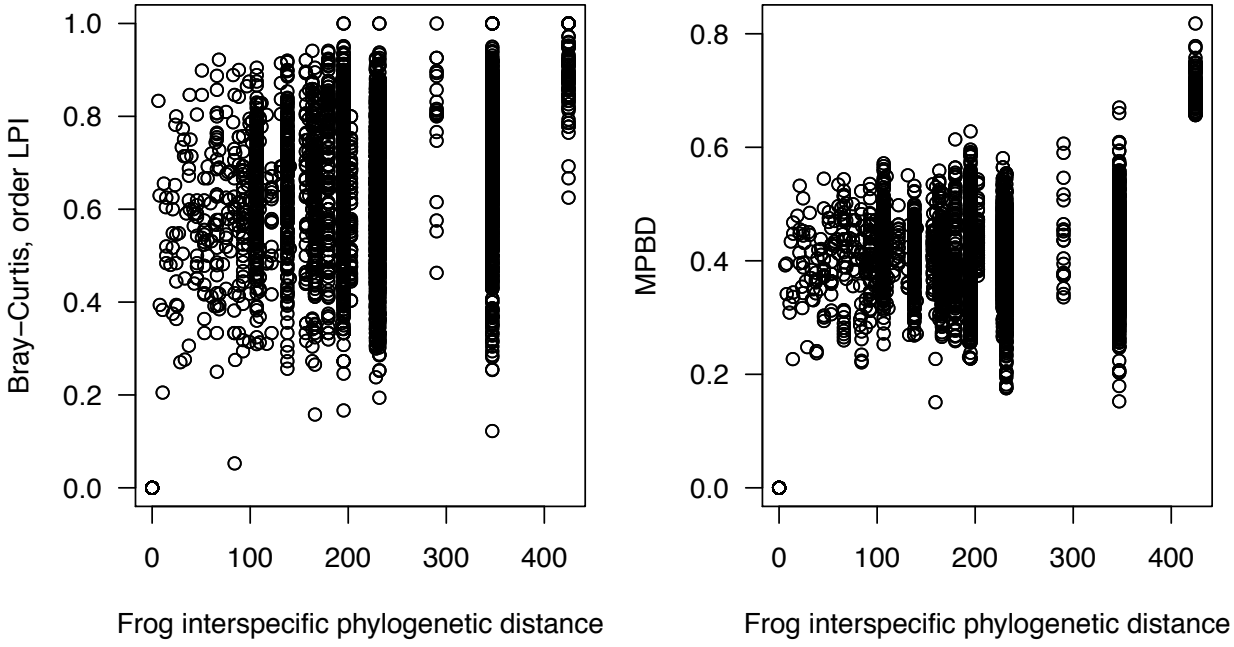

CHAPTER 6

Conclusion

In this dissertation, I presented work that quantifies and links spatial and phylogenetic patterns of frog trophic, morphological, and species diversity. To address these questions about frog diversity across multiple dimensions, I created large-scale morphological and dietary datasets using museum specimens, a cumulative year's worth of fieldwork, and high-throughput sequencing. These empirical datasets have great potential to be applied to other questions beyond the scope of this dissertation, as well as extensions of the research presented in these chapters.

In Chapter 2, we tested whether rates of morphological evolution and speciation rates in frogs were correlated. Our estimates of body size evolution and speciation showed high heterogeneity in rates across the 757 species in our study and we found a marginally significant positive correlation between these two rates. Utilizing an independent dataset of body size with triple the number of species did not resolve this ambiguous relationship between speciation and size evolutionary rates. Considering shape evolutionary rates, we again uncovered a positive, but not statistically significant, association with speciation rates. We also observed that evolutionary rates were positively correlated across phenotypic variables, so that a species with relatively fast evolutionary rates on one axis of body shape tended to have fast rates on all other phenotypic axes. Overall, rates of frog morphological evolution appear to be linked to speciation rates, but the strength and nature of this connection remain unclear.

The morphological measurements that we included in our study are informative of multiple important aspects of frog ecology, such as adult non-breeding habitat (Gomes et al. 2009; Moen et al. 2013; Moen et al. 2016), diet (Emerson 1985; Parmelee 1999; Duellman 2005; Moen and Wiens 2009), and locomotion (Zug 1972; Gomes et al. 2009; Lires et al. 2016), but are unlikely to have much power to infer evolution of other important areas of phenotype. In particular, measures of traits related to sexual signaling and reproductive mode were lacking and future research should examine the relationship between such traits and speciation. Sexual dichromatism has been linked to increased diversification within a radiation of frogs (Portik et al. 2019), which suggests that evolutionary rates of traits related to sexual selection could be coupled with speciation rates and warrant explicit study. Also, given the stunning array of reproductive strategies in frogs (Wells 2007), the evolutionary dynamics of traits related to reproduction warrant investigation, as well as how these relate to diversification.

In Chapter 3, we quantified how frog assemblages differ in the structure of multidimensional morphological space as species richness varies along the latitudinal diversity gradient. By examining 8,178 assemblages of frogs in the Western Hemisphere, we determined that the volume of morphospace increases with species richness, but that the maximum morphovolumes occupied by frogs does not correspond to the highest richness assemblages. This interesting anomaly presents an interesting avenue for further investigations into how frogs expand their use of morphovolume. We also found that frogs become more tightly packed within morphospace as richness increases. Our most intriguing result was that morphospace expansion rather than packing was the dominant pattern along species richness gradients, which is the opposite pattern seen in birds (Pigot et al. 2016; Pellissier and Kissling 2018; Schumm et al.

2019). Our result was consistent within and across biomes, so it appears unlikely to be driven by differences in phylogenetic structure of communities.

This chapter, like most other studies that address similar questions (Pigot et al. 2016; Pellissier and Kissling 2018; Schumm et al. 2019), uses spatial units that may not be informative about ecological processes that structure communities of interacting species. At these coarse spatial scales, each grouping of species that we refer to as an assemblage may include species that may be regionally sympatric, but not locally. A complementary study should quantify patterns of morphospace structure within communities of sympatric frogs to determine the ubiquity of our findings across spatial scales.

In Chapter 4, we evaluated approaches to quantifying frog dietary niche breadth and interspecific diet similarity in the age of molecular metabarcoding. We revisited the question of what the appropriate of level of prey identification is for dietary studies now that prey items can time and cost efficiently be identified to species level. We demonstrated that high numbers (40 - 70) of diet observations were insufficient to capture the full richness of prey species within a single frog species' diet or to even estimate this value. Since such sampling requirements would be prohibitive for most studies that are broader than a single focal species, it is critically valuable that our study determined that dietary diversity estimated with higher taxonomic categories of prey items or based on the phylogenetic diversity of prey items was ecologically informative at more moderate sampling depths.

Although there is strong correlation between measures of diet breadth and similarity using phylogenetic and taxonomic approaches, we find that there is meaningful variation in the results of the different approaches and each is capturing different dimensions of dietary diversity. In particular, we found that species can accumulate taxonomic dietary diversity while still being

phylogenetic dietary specialists. We recommend that computation of both can provide a more nuanced understanding of how frog species use dietary resources.

The focal community of this chapter is located in southeastern Peru in the lowland Amazonian rainforest that has a highly diverse resource base. A comparable study should be undertaken on sympatric frogs from community in a temperate location to assess whether large numbers of diet records are required to adequately enumerate dietary richness at the prey species level or whether our findings are applicable only to areas with high prey species diversity.

In Chapter 5, we test how evolutionary history has impacted present-day frog trophic ecology. We applied metabarcoding methods to identify prey items in the stomach contents of 1,266 frog individuals, representing 111 species from 10 families. We tested whether the Deep Time Hypothesis (Vitt and Pianka 2005) that ecological divergences early in the history of a clade are important determinants of extant ecology or the Adaptive Radiation Hypothesis that present-day variation reflects divergences in recent time better explains frog trophic ecology. We find that frogs have not significantly diverged in trophic strategy across their evolutionary history and diet composition is remarkably conserved across the radiation, thus making both hypotheses inapplicable. The one axis along which frogs appear to differ is the relative importance of ants to their diet and families that consumer higher proportions of ants generally have lower phylogenetic and taxonomic dietary diversity. We propose a novel paradigm, the Phylogenetically Widespread Hyper-Generalism Hypothesis, to explain present-day frog diets. This is characterized by generalized diets, high interspecific overlap, and limited specialization despite the amount of evolutionary time spanned by the clade and highlights how fundamentally different frog trophic ecology is in comparison to what is seen in all other vertebrate clades.

For this study, we do not distinguish between different life stages of prey items, which could be important given the marked difference between stages for many common prey items of frogs, such as dipterans and lepidopterans. Through visual inspection of the stomach contents, we are conscious of the fact that multiple life stages are present in our dataset of prey items. With the photographic documentation of each diet sample, we have the ability to account for these intraspecific differences between prey items in a future study. We could also use the photos to incorporate information about biomass and number of individuals per prey species.

With my dissertation research, I contribute large datasets on frog morphology and diet that can be leveraged to address additional questions on frog ecology and evolutionary biology. In particular, each frog diet sample is linked to a voucher specimen deposited in the University of Michigan Museum of Zoology or San Marcos Museum of Natural History (Lima, Peru), so the connection between diet and morphology can be explored at the individual consumer level. Furthermore, these voucher specimens have extensive ecological, parasite, and skin microbiome information. The multiple lines of data can be integrated to answer many outstanding questions about frog biodiversity and test hypotheses about the interactions between axes of variation.

Overall, my dissertation addresses some of the sizeable gaps in our knowledge about frog evolution and ecology. It presents novel frameworks for how to understand frog biodiversity and reveals that patterns of frog diversity differ from those seen in other clades. This indicates that paradigms designed on patterns observed in other vertebrate clades cannot necessarily be generalized to other groups and highlights the need to further study how patterns of frog diversity reflect their evolution and interaction with their environment.

REFERENCES

Colston, T. J., G. C. Costa, and L. J. Vitt. 2010. Snake diets and the deep history hypothesis. Biological Journal of the Linnean Society 101:476–486.

Duellman, W. E. 2005. Cusco Amazonico. Comstock Pub. Associates, Ithaca, NY.

Emerson, S. B. 1985. Skull Shape in Frogs : Correlations with Diet. Herpetologica 41:177–188.

Gomes, F. R., E. L. Rezende, M. B. Grizante, and C. A. Navas. 2009. The evolution of jumping performance in anurans : morphological correlates and ecological implications. European Society for Evolutionary Biology 22:1088–1097.

Lires, A. I., I. M. Soto, and R. O. Gómez. 2016. Walk before you jump : new insights on early frog locomotion from the oldest known salientian. Paleobiology 42:612–623.

Moen, D. S., D. J. Irschick, and J. Wiens. 2013. Evolutionary conservatism and convergence both lead to striking similarity in ecology, morphology and performance across continents in frogs. Proceedings of the Royal Society B: Biological Sciences 280:20132156.

Moen, D. S., H. Morlon, and J. J. Wiens. 2016. Testing convergence versus history: convergence dominates phenotypic evolution for over 150 million years in frogs. Systematic Biology 65:146–160.

Moen, D. S., and J. J. Wiens. 2009. Phylogenetic evidence for competitively driven divergence: Body-size evolution in caribbean treefrogs (Hylidae: Osteopilus). Evolution 63:195–214.

Parmelee, J. R. 1999. Trophic Ecology of a Tropical Anuran Assemblage. Scientific Papers Natural History Museum the University of Kansas 11:1–59.

Pellissier, V., and W. D. Kissling. 2018. Niche packing and expansion account for species richness – productivity relationships in global bird assemblages. Global Ecolog and Biogeography 27:604–615.

Pigot, A. L., C. H. Trisos, J. A. Tobias, and A. L. Pigot. 2016. Functional traits reveal the expansion and packing of ecological niche space underlying an elevational diversity gradient in passerine birds.

Portik, D. M., R. C. Bell, D. C. Blackburn, A. M. Bauer, C. D. Barratt, W. R. Branch, M. Burger, et al. 2019. Sexual Dichromatism Drives Diversification within a Major Radiation of African Amphibians. Systematic biology 68:859–875.

Schumm, M., A. E. White, K. Supriya, and T. D. Price. 2019. Ecological limits as the driver of bird species richness patterns along the east Himalayan elevational gradient. American Naturalist.

Vitt, L. J., and E. R. Pianka. 2005. Deep history impacts present-day ecology and biodiversity. Proceedings of the National Academy of Science 102:7877–7881.

Wells, K. D. 2007. The ecology and behavior of amphibians. University of Chicago Press, Chicago, IL.

Zug, G. R. 1972. Anuran Locomotion : Structure and Function . I . Preliminary Observations on Relation between Jumping and Osteometrics of Appendicular and Postaxial Skeleton. Copeia 1972:613–624.